

We are committed to providing [accessible customer service](#).  
If you need accessible formats or communications supports, please [contact us](#).

Nous tenons à améliorer [l'accessibilité des services à la clientèle](#).  
Si vous avez besoin de formats accessibles ou d'aide à la communication, veuillez [nous contacter](#).

**Report on the 2016 Geological Compilation and VTEM  
Survey  
Detour West Property, Cochrane District, Ontario**

**Porcupine Mining Division, Ontario**

**UTM NAD 83 (Zone 17) 562,400 mE, 5,538,000 mN**

**NTS 042I01 & 042H16**

FOR

**TRI ORIGIN EXPLORATION LTD.**

125 Don Hillock Dr., Unit 18  
Aurora, Ontario  
L4G 0H8

Meghan Hewton, MSc. & Robert Valliant, PhD

December 12, 2016

## Table of Contents

<b>1.0</b>	<b>INTRODUCTION AND PROPERTY DESCRIPTION</b> .....	<b>1</b>
<b>2.0</b>	<b>REGIONAL GEOLOGY</b> .....	<b>5</b>
2.1	PHYSIOGRAPHY AND VEGETATION.....	5
2.2	REGIONAL GEOLOGY AND ECONOMIC MINERALIZATION .....	5
<b>3.0</b>	<b>PROPERTY GEOLOGY</b> .....	<b>7</b>
<b>4.0</b>	<b>PREVIOUS WORK</b> .....	<b>7</b>
<b>5.0</b>	<b>GEOPHYSICAL &amp; GEOLOGICAL COMPILATIONS</b> .....	<b>10</b>
<b>6.0</b>	<b>PROPERTY VISITS AND ASSESSMENTS</b> .....	<b>18</b>
<b>7.0</b>	<b>VTEM SURVEY</b> .....	<b>20</b>
<b>8.0</b>	<b>IP SURVEY TEST LINE</b> .....	<b>20</b>
<b>9.0</b>	<b>RECOMMENDATIONS AND CONCLUSIONS</b> .....	<b>20</b>
<b>10.0</b>	<b>PERSONNEL</b> .....	<b>21</b>
<b>10.0</b>	<b>STATEMENT OF QUALIFICATIONS</b> .....	<b>22</b>
<b>11.0</b>	<b>REFERENCES</b> .....	<b>23</b>

## Figures

FIGURE 1. PROPERTY LOCATION .....	3
FIGURE 2. MINERAL TENURE MAP .....	4
FIGURE 3. REGIONAL GEOLOGY OF THE NORTHWEST PORTION OF THE ABITIBI GREENSTONE BELT AND THE LOCATION OF TRI ORIGIN'S DETOUR WEST PROJECT IN COMPARISON TO SELECT MINES IN ONTARIO AND QUEBEC. ....	6
FIGURE 4. FILED HISTORIC ASSESSMENT WORK. ....	9
FIGURE 5. TOTAL MAGNETIC INTENSITY, ONTARIO REGIONAL DATA (GDS 1036) AND DETOUR LAKE MINE AREA (GDS 1007/1008).....	11
FIGURE 6. TOTAL MAGNETIC INTENSITY, RE-PROCESSED BY BOB LO. IGRF TREND REMOVED. ....	12
FIGURE 7. TOTAL MAGNETIC INTENSITY, RE-PROCESSED BY BOB LO. IGRF TREND AND NORTH-SOUTH FEATURES REMOVED. ....	13
FIGURE 8. FIGURE 7, WITH PRELIMINARY BEDROCK GEOLOGY INTERPRETED FROM MAGNETICS AND DOME DIAMOND DRILLING.....	15
FIGURE 9. FINAL GEOLOGICAL INTERPRETATION MAP OF THE DETOUR WEST PROJECT. ...	17
FIGURE 10. PROPERTY ACCESS.....	19

## Tables

TABLE 1. LIST OF CLAIMS.....	2
TABLE 2. DETOUR WEST DIAMOND DRILL HOLE COMPILATION DATABASE. ....	16

## **1.0 INTRODUCTION AND PROPERTY DESCRIPTION**

The Detour West property is located approximately 120 km north-northeast of the Town of Cochrane, Ontario, and 20 km west of the Detour Lake Gold Mine (Figure 1), within the Marquis Lake and Newnham Creek Areas, Porcupine Mining Division. The property is located within NTS map sheets 042H16 and 042I01, at UTM NAD 83 coordinates 562,400 mE, 5, 538,000 mN. The property consists of 30 unpatented, contiguous claims totaling 480 units and covering an area of 76 km<sup>2</sup>. The claims are held 100% by Tri Origin Exploration Ltd., and all claims are in good standing until December 18, 2016. Table 1 lists the claims and current ownership, and Figure 2 shows the geographic boundaries of each claim. The property lies between 5 and 12 km north of the all-weather Detour Mine Road, and can be partially accessed by truck on forestry trails and further accessed by ATV, Argo, and on foot. A few all-terrain vehicle trails cross the property providing some access for exploration.

Detour West is a gold exploration project (with the potential for silver, copper, zinc, nickel, and PGEs) located 20 km west of the producing Detour Lake Gold Mine. The targeted deposit types are volcanic-hosted and/or iron formation-related lode gold deposits of high enough grade to be mined by underground methods or associated low grade-large tonnage open pit mineable deposits, similar to the past-producing Detour Lake underground mine, the currently producing Detour Lake open pit mine, and the 58N Zone high grade discovery currently being delineated by Detour Gold Corporation. The recent discovery by Balmoral Resources of the Grasset magmatic Ni-Cu-PGE deposit, just east of the Detour Lake Mine in Quebec, and Cu-Zn volcanic-hosted massive sulphide deposits (VHMS) further east as at Matagami, QC, demonstrates the potential for these types of deposits to be discovered as well.

The geological and geophysical compilation by Tri Origin Exploration was completed between January and September, 2016, and a site investigation was conducted in November 2016. The purpose of the compilation was to review historic geological, diamond drilling, and geophysical data to develop an understanding of the geology underlying the claim group, the thickness of the overburden, and to plan future work programs, including an airborne VTEM survey. The VTEM survey was flown between August 29 and September 15, 2016 by Geotech Ltd. of Aurora, ON.

**Table 1. List of Claims**

Claim Number	Township/Area	Recorded Holder	Due Date
4283131	MARQUIS LAKE AREA (G-1649)	TRI ORIGIN EXPLORATION LTD. (100%)	2016-DEC-18
4283132	MARQUIS LAKE AREA (G-1649)	TRI ORIGIN EXPLORATION LTD. (100%)	2016-DEC-18
4283133	MARQUIS LAKE AREA (G-1649)	TRI ORIGIN EXPLORATION LTD. (100%)	2016-DEC-18
4283134	MARQUIS LAKE AREA (G-1649)	TRI ORIGIN EXPLORATION LTD. (100%)	2016-DEC-18
4283135	MARQUIS LAKE AREA (G-1649)	TRI ORIGIN EXPLORATION LTD. (100%)	2016-DEC-18
4283136	MARQUIS LAKE AREA (G-1649)	TRI ORIGIN EXPLORATION LTD. (100%)	2016-DEC-18
4283137	MARQUIS LAKE AREA (G-1649)	TRI ORIGIN EXPLORATION LTD. (100%)	2016-DEC-18
4283138	MARQUIS LAKE AREA (G-1649)	TRI ORIGIN EXPLORATION LTD. (100%)	2016-DEC-18
4283139	MARQUIS LAKE AREA (G-1649)	TRI ORIGIN EXPLORATION LTD. (100%)	2016-DEC-18
4283140	MARQUIS LAKE AREA (G-1649)	TRI ORIGIN EXPLORATION LTD. (100%)	2016-DEC-18
4283141	MARQUIS LAKE AREA (G-1649)	TRI ORIGIN EXPLORATION LTD. (100%)	2016-DEC-18
4283142	MARQUIS LAKE AREA (G-1649)	TRI ORIGIN EXPLORATION LTD. (100%)	2016-DEC-18
4283143	MARQUIS LAKE AREA (G-1649)	TRI ORIGIN EXPLORATION LTD. (100%)	2016-DEC-18
4283144	MARQUIS LAKE AREA (G-1649)	TRI ORIGIN EXPLORATION LTD. (100%)	2016-DEC-18
4283145	MARQUIS LAKE AREA (G-1649)	TRI ORIGIN EXPLORATION LTD. (100%)	2016-DEC-18
4283146	MARQUIS LAKE AREA (G-1649)	TRI ORIGIN EXPLORATION LTD. (100%)	2016-DEC-18
4283147	MARQUIS LAKE AREA (G-1649)	TRI ORIGIN EXPLORATION LTD. (100%)	2016-DEC-18
4283148	MARQUIS LAKE AREA (G-1649)	TRI ORIGIN EXPLORATION LTD. (100%)	2016-DEC-18
4283149	MARQUIS LAKE AREA (G-1649)	TRI ORIGIN EXPLORATION LTD. (100%)	2016-DEC-18
4283150	MARQUIS LAKE AREA (G-1649)	TRI ORIGIN EXPLORATION LTD. (100%)	2016-DEC-18
4283121	NEWNHAM CREEK AREA (G-1658)	TRI ORIGIN EXPLORATION LTD. (100%)	2016-DEC-18
4283122	NEWNHAM CREEK AREA (G-1658)	TRI ORIGIN EXPLORATION LTD. (100%)	2016-DEC-18
4283123	NEWNHAM CREEK AREA (G-1658)	TRI ORIGIN EXPLORATION LTD. (100%)	2016-DEC-18
4283124	NEWNHAM CREEK AREA (G-1658)	TRI ORIGIN EXPLORATION LTD. (100%)	2016-DEC-18
4283125	NEWNHAM CREEK AREA (G-1658)	TRI ORIGIN EXPLORATION LTD. (100%)	2016-DEC-18
4283126	NEWNHAM CREEK AREA (G-1658)	TRI ORIGIN EXPLORATION LTD. (100%)	2016-DEC-18
4283127	NEWNHAM CREEK AREA (G-1658)	TRI ORIGIN EXPLORATION LTD. (100%)	2016-DEC-18
4283128	NEWNHAM CREEK AREA (G-1658)	TRI ORIGIN EXPLORATION LTD. (100%)	2016-DEC-18
4283129	NEWNHAM CREEK AREA (G-1658)	TRI ORIGIN EXPLORATION LTD. (100%)	2016-DEC-18
4283130	NEWNHAM CREEK AREA (G-1658)	TRI ORIGIN EXPLORATION LTD. (100%)	2016-DEC-18

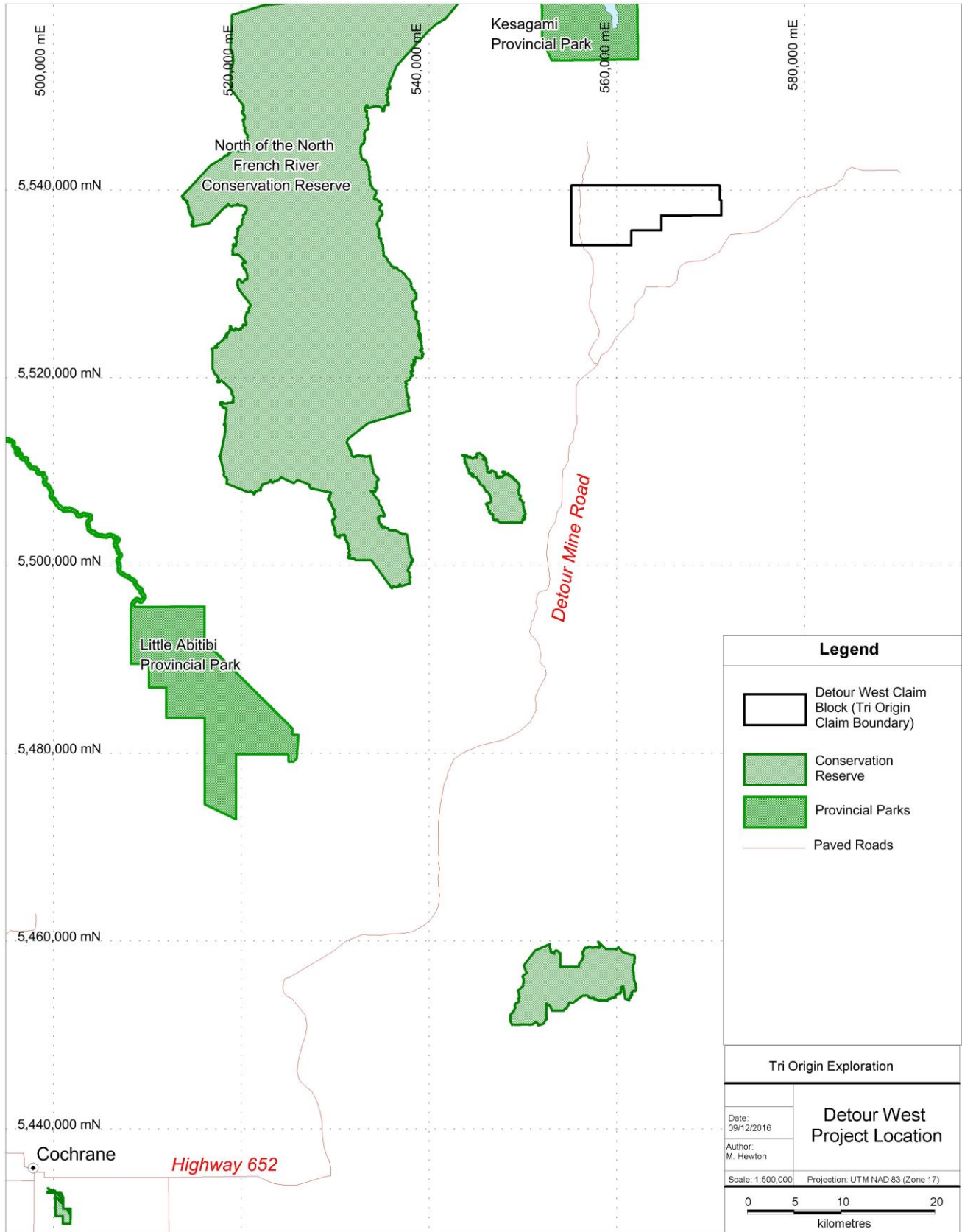


Figure 1. Property Location

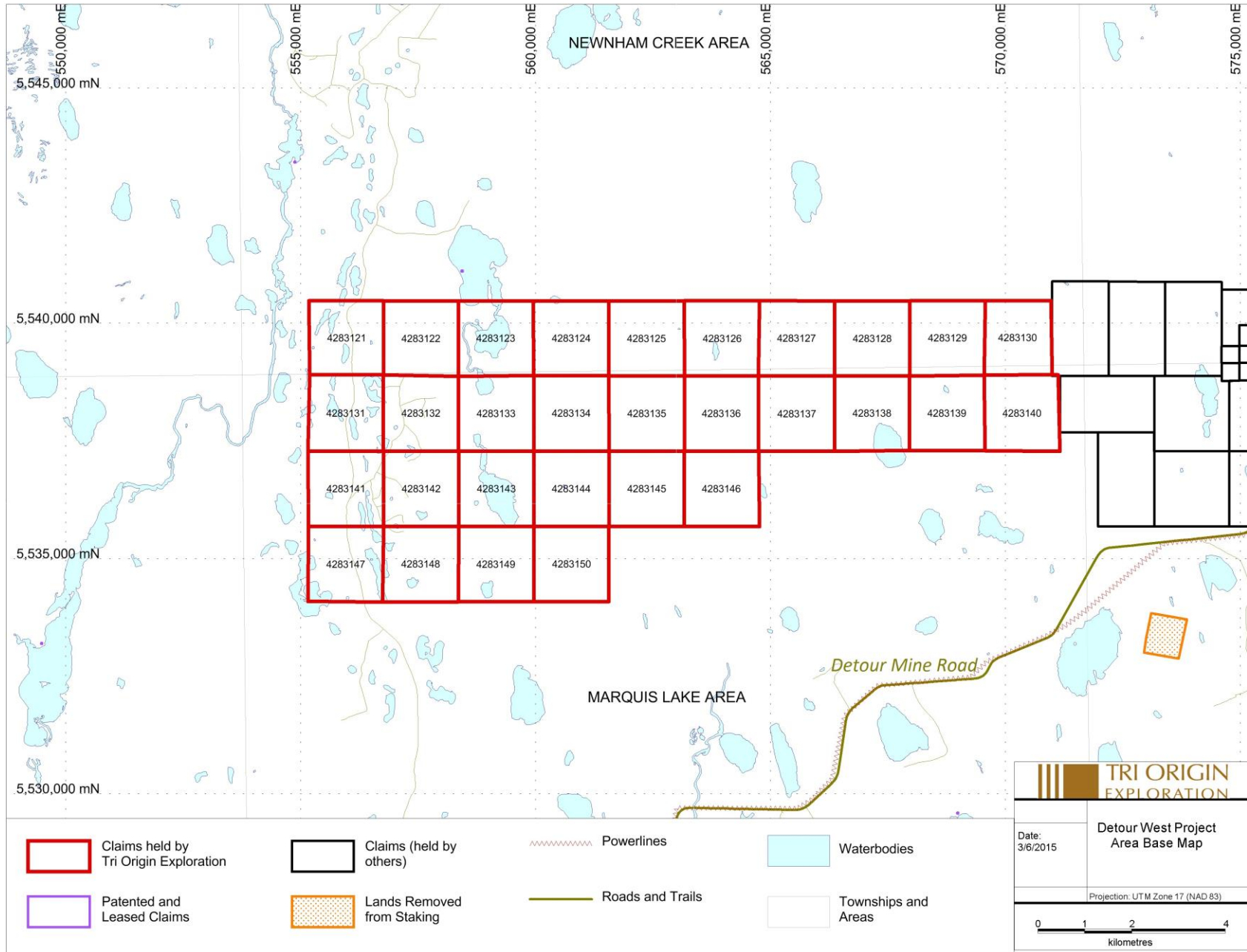


Figure 2. Mineral Tenure Map

## **2.0 REGIONAL GEOLOGY**

### **2.1 PHYSIOGRAPHY AND VEGETATION**

Drainage of the property area is northward via the Kattawagami River and Newnham Creek to Kesagami Lake and eventually to James Bay. Relief is low and there is no outcrop exposure as the overburden is extremely thick. A north-south esker covers the western-most end of the property, while the central and eastern portions of the property are covered by low-lying swamp and muskeg (Lee, 1979). The north-flowing Kattawagami River bisects the property in the central portion and is about 30 m wide, making access across the river limited to the winter months when frozen.

### **2.2 REGIONAL GEOLOGY AND ECONOMIC MINERALIZATION**

The Detour West project is located in the Detour Lake area at the northwestern-most extension of the east-west trending Abitibi Subprovince (Figure 3). The Detour segment of the Abitibi Subprovince extends for over 200 km east to west, and hosts the Detour Lake gold mine in Ontario and Matagami and Selbaie mining camps in Quebec. The geology of the Detour area consists of two distinct east-west trending volcanic-sedimentary assemblages, as well as mafic to ultramafic intrusive rocks and younger tonalitic to granodioritic intrusive rocks. The older Deloro assemblage can be sub-divided into the Lower part ( $\geq 2725$  Ma), comprised of a chert marker horizon and mafic to ultramafic flows, dykes, and sills, and the Upper part ( $< 2725$  Ma), comprised of basaltic flows, tuffs, and hyaloclastites. The younger Caopatina Assemblage ( $\sim 2700$  Ma) is comprised of greywackes and volcanoclastic rocks and makes up the central east-west trending core of the Detour area. These units are intruded by mafic to ultramafic plutons, dykes, and sills and younger tonalite to granodiorite plutons.



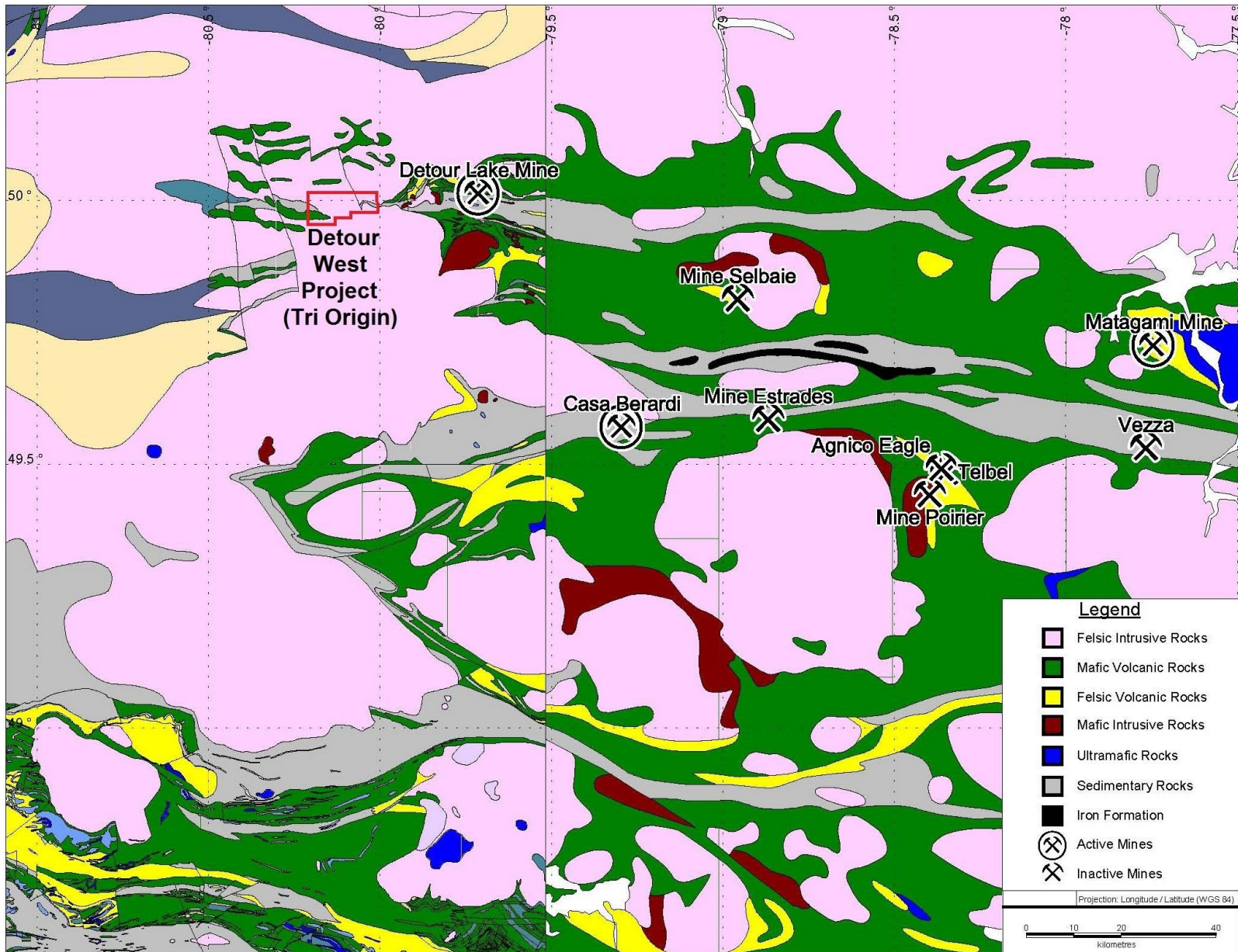


Figure 3. Regional geology of the northwest portion of the Abitibi greenstone belt and the location of Tri Origin's Detour West project in comparison to select mines in Ontario and Quebec.

### **3.0 PROPERTY GEOLOGY**

The entire Detour West area is covered by overburden (Holocene glacial tills and glaciolacustrine clay) ranging from a few tens of meters to over 100 m thick, and no geological mapping of the Detour West property exists. Geologic maps published by the Ontario Geological Survey have interpreted the geology at the Detour West property to be dominated by foliated to gneissic tonalite and granodiorite. Tri Origin has completed a detailed compilation of all available government and company data which has resulted in recognition of a westward extension and repetition of the same geology found at the Detour Lake Mine and Lower Detour discovery to the east. Interpretation of regional aeromagnetic survey data and historic drill core logs from holes drilled at the western margin of the property indicate that the property is underlain by east-west trending sedimentary rocks of the Caopatina Assemblage and bracketed to the north and south by volcanic rocks of the Deloro Assemblage. Iron formation is interpreted to occur within both the north and south volcanic-sedimentary contacts based on interpretation of OGS regional magnetic data, private company airborne magnetic data and airborne electromagnetic survey covering the western portion of the property, as well as on the intersection of massive magnetite and disseminated pyrrhotite in a diamond drill hole drilled by Dome Exploration (1982). Diamond drill core logs from holes drilled at and near the west end of the property refer mostly to slightly magnetic biotite-quartz-feldspar gneiss, but also include units logged as metasedimentary rocks, felsic intrusive or volcanic rocks, and felsic to intermediate volcanic rocks, all of which are strongly metamorphosed. Dome also drilled an additional twelve holes between 5 and 10 km along strike to the west of Tri Origin's claims. These holes intersected rocks logged as biotite-quartz-feldspar gneisses, chlorite-biotite-quartz-feldspar gneisses, and biotite schists interpreted as the metamorphosed equivalents of volcanic rocks, metasedimentary rocks, and komatiite.

### **4.0 PREVIOUS WORK**

There has been extensive and successful exploration across the length of the greenstone belt to the east of Tri Origin's Detour West property since 1974. The property's proximity to the Detour Lake Gold Mine makes it an attractive target for the discovery of a multi-million ounce, high-tonnage gold deposit of the lode gold type and an opportunity to open up a new exploration area in Ontario. On the Quebec side of the belt, Balmoral Resources is active at their Martiniere and Bug Lake gold zones as well as their Grasset nickel deposit; Midland Exploration is exploring a large property package with Soquem; Cogitore Resources is active at Selbaie West; and Adventure Gold is active at their Detour Quebec properties.

Exploration work over the Detour West property has been limited, and is summarized in Figure 4. The earliest reported exploration activity at the Detour West property was conducted by Dome Exploration Canada, who performed a ground geophysical survey over their project 159-G in October 1983 and March 1984 (Thompson, 1984). The ground survey was conducted as follow-up work to an airborne magnetic and EM survey, but there is no filed assessment work for such an airborne survey. The ground survey consisted of a horizontal loop Max-Min II EM survey, magnetic survey, and VLF survey over 78.1 line km at 100 m line spacing. Six other similar surveys were conducted west and north of the current claims between 1981 and 1985. Dome Exploration followed up these seven ground surveys with widely spaced diamond drilling programs in 1982 and 1985 on

most of their survey blocks and completed five diamond drill holes on the current Tri Origin claims in the southwestern corner of the property (drill holes 159G-1A to 159G-5). No sampling or assaying was reported for these holes in the government assessment files. Dome also drilled an additional twelve holes between 5 and 10 km along strike to the west.

In the fall of 1996, Eastmain Resources flew a GeoTEM electromagnetic and magnetic survey on the west side of the current Detour West project area. A total of 1,086 line km with a line spacing of 250 m was flown. No ground follow up to that airborne survey was reported, and no exploration work has been done on the Detour West project area since then.

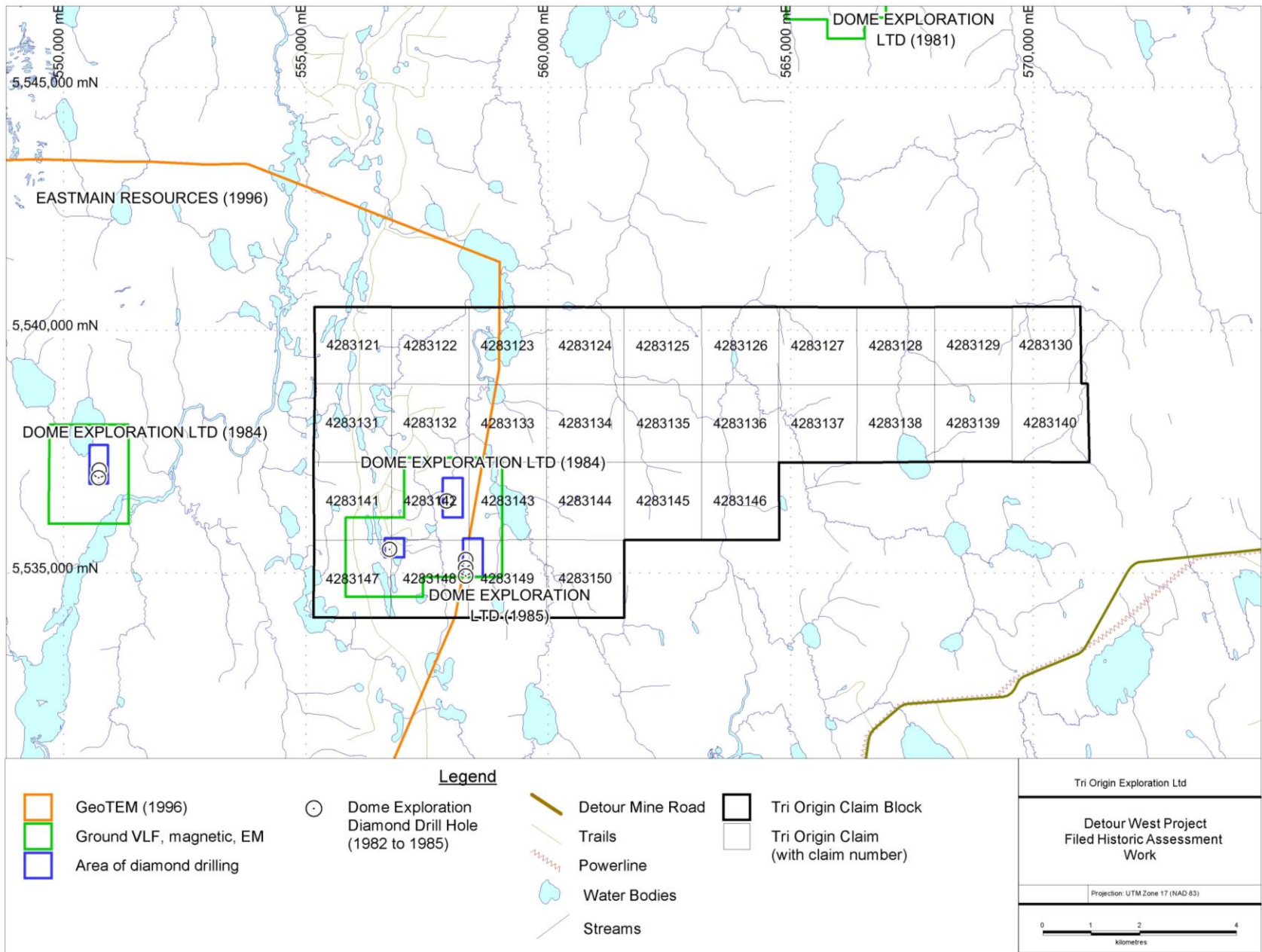


Figure 4. Filed historic assessment work.

## 5.0 GEOPHYSICAL & GEOLOGICAL COMPILATIONS

Between January and September, 2016, Tri Origin commenced a detailed geophysical and geological review and compilation of the Detour West property. This compilation incorporated the following publically-available data sets produced by government and exploration company surveys:

- 1) Ontario Geological Survey. 1999. Single Master Gravity and Aeromagnetic Data for Ontario - Geosoft® Format. Ontario Geological Survey, Geophysical Data Set 1036.
- 2) Ontario Geological Survey. 2003. Ontario airborne geophysical surveys, magnetic data, Detour-Burntbush-Abitibi area. Ontario Geological Survey, Geophysical Data Set 1007/1008.
- 3) Schacht, B. 1998. Logistics, Processing, and Interpretation Report of the Airborne Magnetics GEOTEM Electromagnetic Multicoil Survey in Northern Ontario, over the Abitibi Region. For Eastmain Resources (AFRI 32L05NE2001).
- 4) Ontario Geological Survey. 2011. 1:250,000 scale bedrock geology of Ontario; Ontario Geological Survey, Miscellaneous Release - Data 126-Revision 1.
- 5) Ayer, J.A., Chartrand, J.E., Duguet, M., Rainsford, D.R.B., and Trowell, N.F. 2009. Geological Compilation of the Burntbush-Detour lakes area, Abitibi greenstone belt; Ontario Geological Survey, Preliminary Map P.3609, scale 1: 100,000.
- 6) Johns, G.W. 1981. Burntbush-Detour Lakes; Ontario Geological Survey Map 2453, Precambrian Geology Series, Scale 1:100,000. Geology 1978.
- 7) Dome Exploration Canada Ltd. Diamond drill records for Projects 159A (1982; AFRI 42I01NE0003), 159B (1982; AFRI 42I01NE0001), 159D (1982; AFRI 42I01NE0001), 159F (1982; AFRI 42I01NW0004), 159G (1985; AFRI 42H15NE8014), 159H (1985; AFRI 42H16NW0005), 159J (1985; AFRI 42I01SW0001), 159K (1985; AFRI 42H16NW0020), and 159L (1985; 42H15NE8014).

Regional airborne magnetics were reviewed in February 2016 by consulting geophysicist Bob Lo at the request of Tri Origin Exploration. The review completed by Mr. Lo included re-gridding, re-processing, and filtering of publicly available OGS aeromagnetic survey data (OGS Geophysical Data Sets 1036 and 1007/1008). The known extent of the Detour Lake greenstone belt in the vicinity of the Detour Gold Mine (Geophysical Data Set 1007/1008, 2003) shows a strong east-west trend in the magnetic data which correlates with east-west trending volcanic and sedimentary stratigraphy and the Sunday Lake deformation zone which host the Detour Lake and Lower Detour gold deposits (Figure 5). To the west of the Detour Lake mine area, the regional OGS airborne magnetics data (OGS Geophysical Data Sets 1036, 1999), prior to re-gridding, re-processing, and filtering by Mr. Lo, faintly shows the east-west trend of the Detour Lake area volcanic and sedimentary stratigraphy continuing from the Detour Gold property, but this trend is obscured by abundant north-south trending structures (Figure 5). These north-south trending structures are interpreted to be Matachewan diabase dykes, and a north-south directional filter to extract the signature of the dykes was used in re-processing.

The images derived by Mr. Lo from re-gridding of government airborne mag surveys (GDS 1036 and 1007/1008) were processed to compile the two government surveys together into one image and remove the IGRF (International Geomagnetic Reference Field) from the image (Figure 6), and to subdue the signature of the north-south dykes which permeate the area and obscure the east-west volcanic-sedimentary stratigraphic trends (Figure 7). Once the trend and north-south features were removed by re-gridding, re-processing, and filtering, the east-west volcanic-sedimentary stratigraphy becomes more obvious and we were able to interpret geologic structures westward from the Detour Lake area.

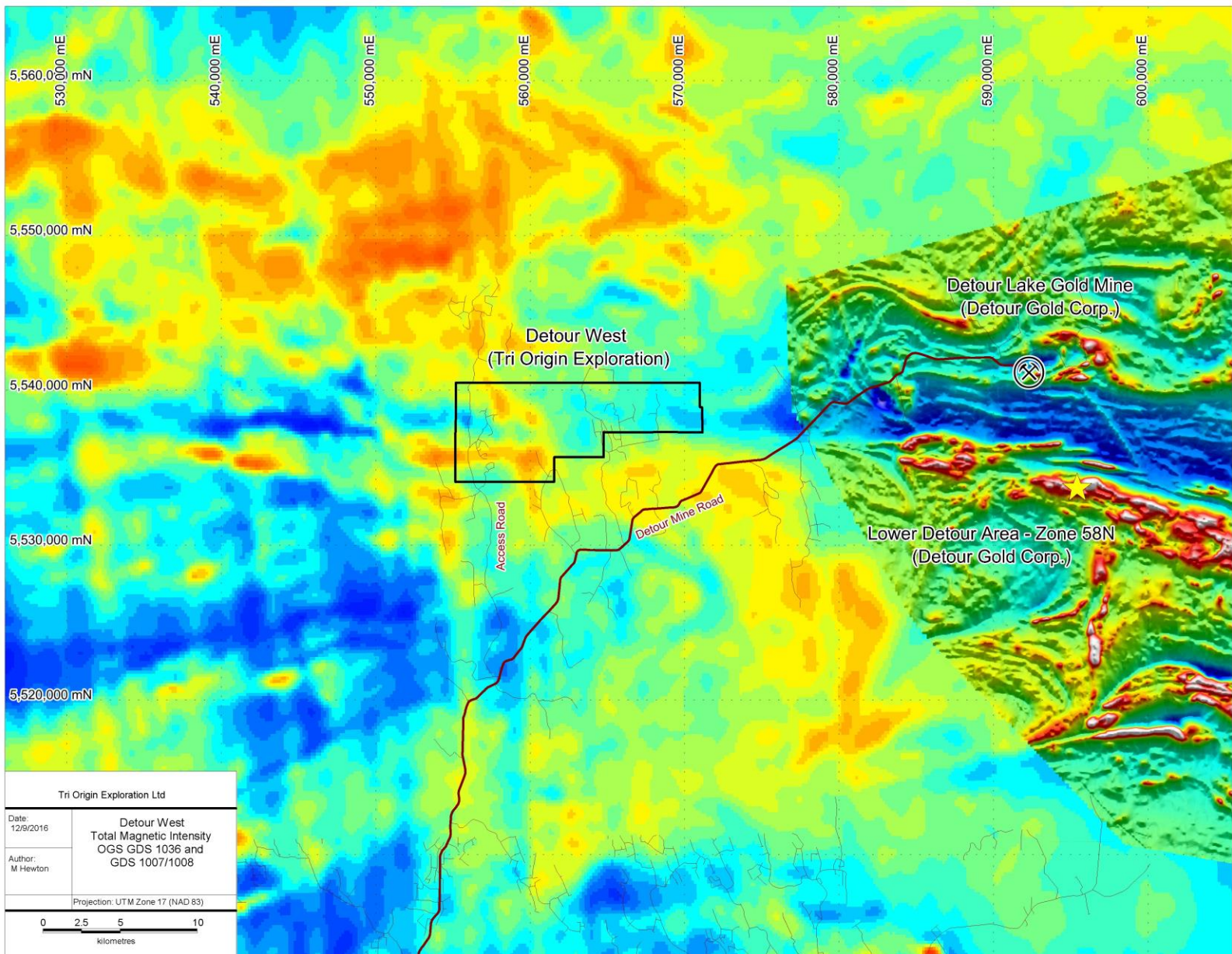


Figure 5. Total magnetic intensity, Ontario regional data (GDS 1036) and Detour Lake Mine Area (GDS 1007/1008)

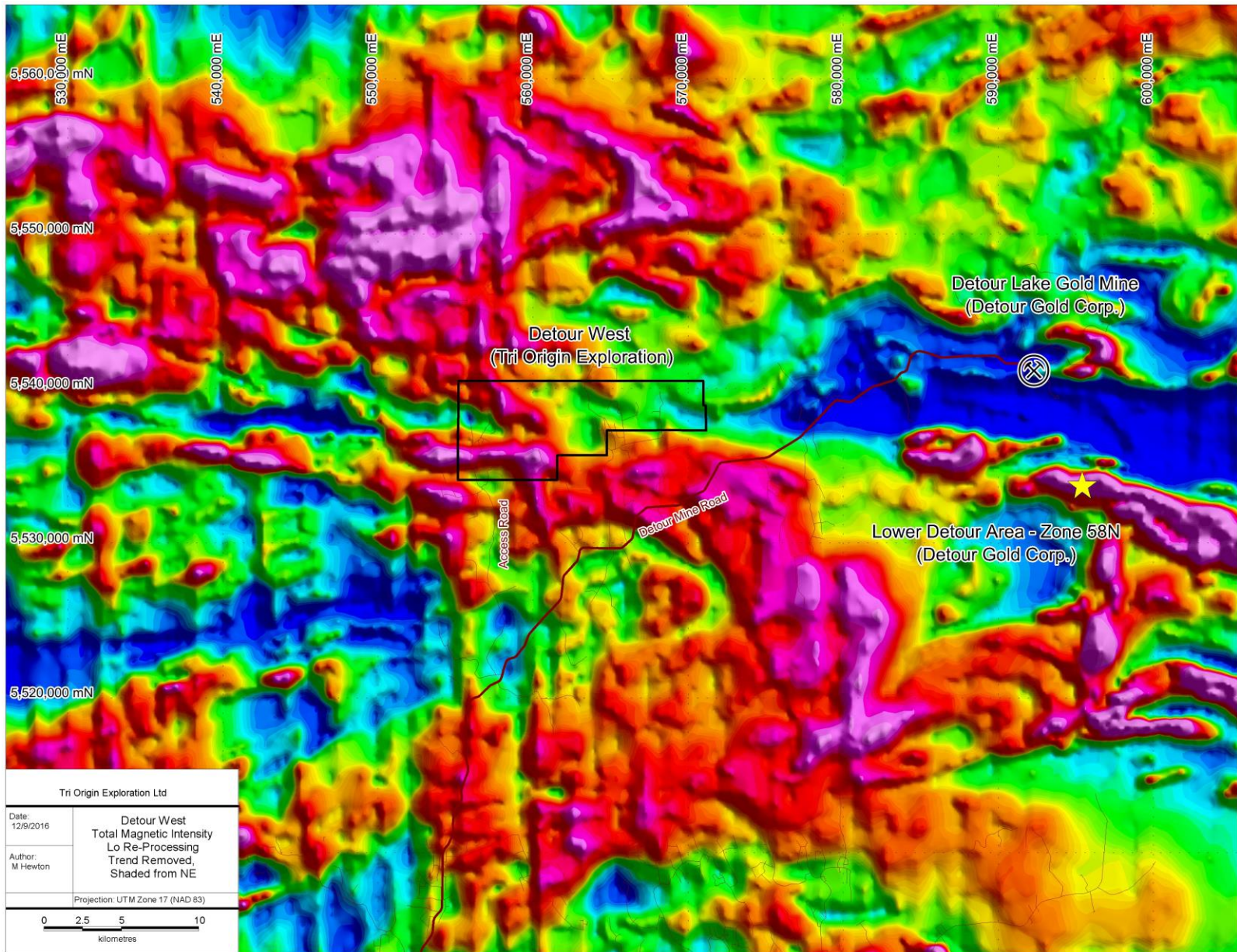


Figure 6. Total magnetic intensity, re-processed by Bob Lo. IGRF trend removed.

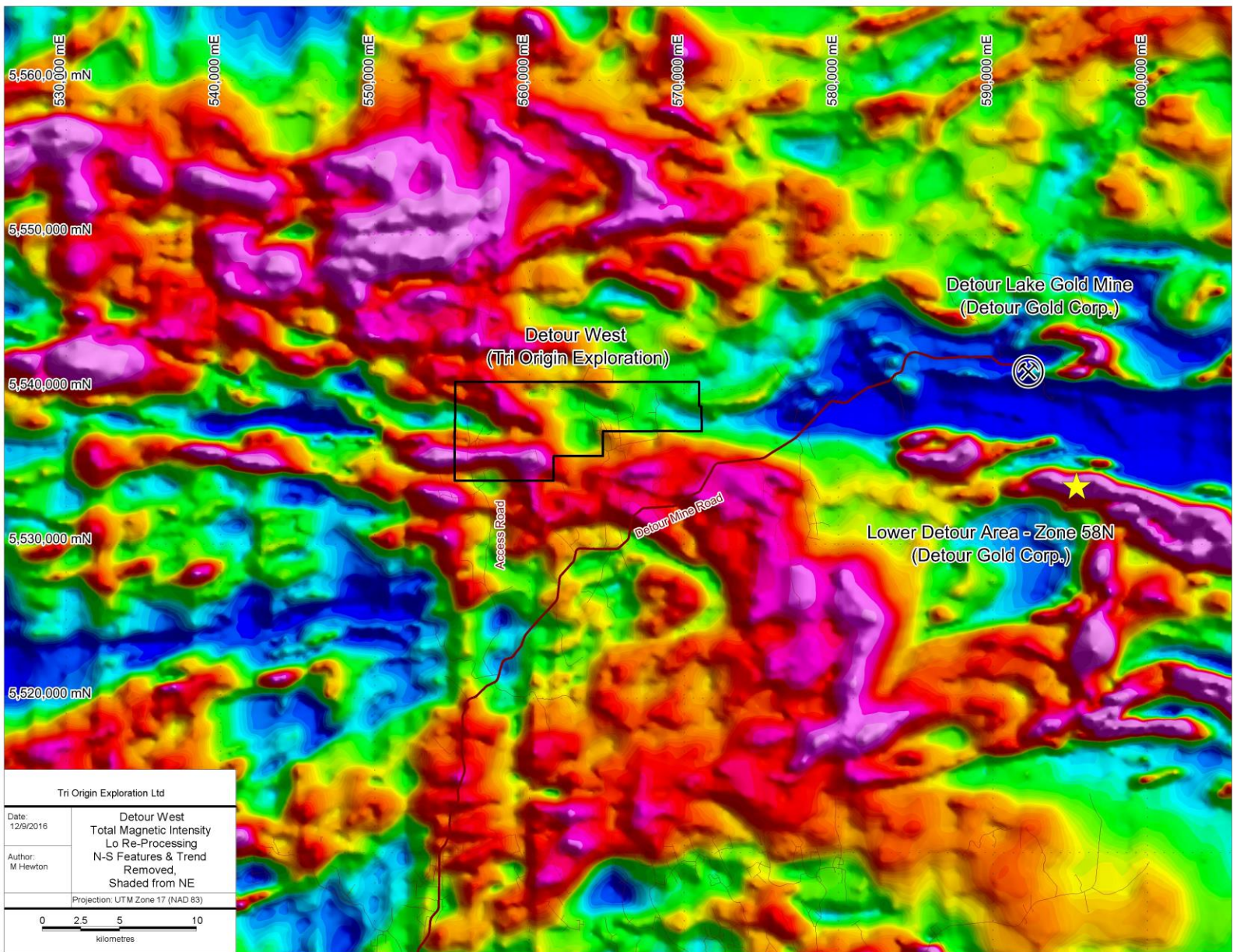


Figure 7. Total magnetic intensity, re-processed by Bob Lo. IGRF trend and north-south features removed.



Assuming that the magnetic lows (in blue) reflect sedimentary lithologies and magnetic highs (red and pink) reflect volcanic lithologies and iron formation, it appears that the stratigraphy from the Detour Lake Mine area continues westward (Figure 8), contrary to government mapping (Ayer et al., 2009). This interpretation is supported by diamond drilling conducted by Dome Exploration in 1982 and 1985 (Table 2), which reported in the drill core logs that described felsic, intermediate, and mafic tuffs and flows in addition to biotite-quartz-feldspar gneisses. In several cases, the gneisses were interpreted by the logging geologist as metavolcanics and metatuffs (Dome, 1982, 1985). Specifically, drill holes completed on the Tri Origin Detour West claims (drill hole series 159G) intersected biotite-quartz-feldspar gneiss, metasedimentary rocks, and felsic to intermediate volcanics with frequent fault gouge and minor chlorite-magnetite-epidote alteration. The results of the Dome Canada drilling program demonstrate that the area is currently incorrectly interpreted by the Ontario Geological Survey as felsic to intermediate intrusive rocks with lesser, small and narrow belts of mafic volcanic rocks. Figure 9 shows the final geologic interpretation of the Detour West project.

Overburden in the drill holes ranged from 15 m (hole 159B-1) to 133 m (hole 159G-1A) thick in the area west of Tri Origin's Detour West property. The hole with the deepest overburden (hole 159G-1A) was drilled on the esker in the western part of the property, but 4 other holes drilled on the current Detour West property (159G-2, 159G-3, 159G-4, and 159G-5) by Dome showed that overburden is generally between 40 and 62 m thick.

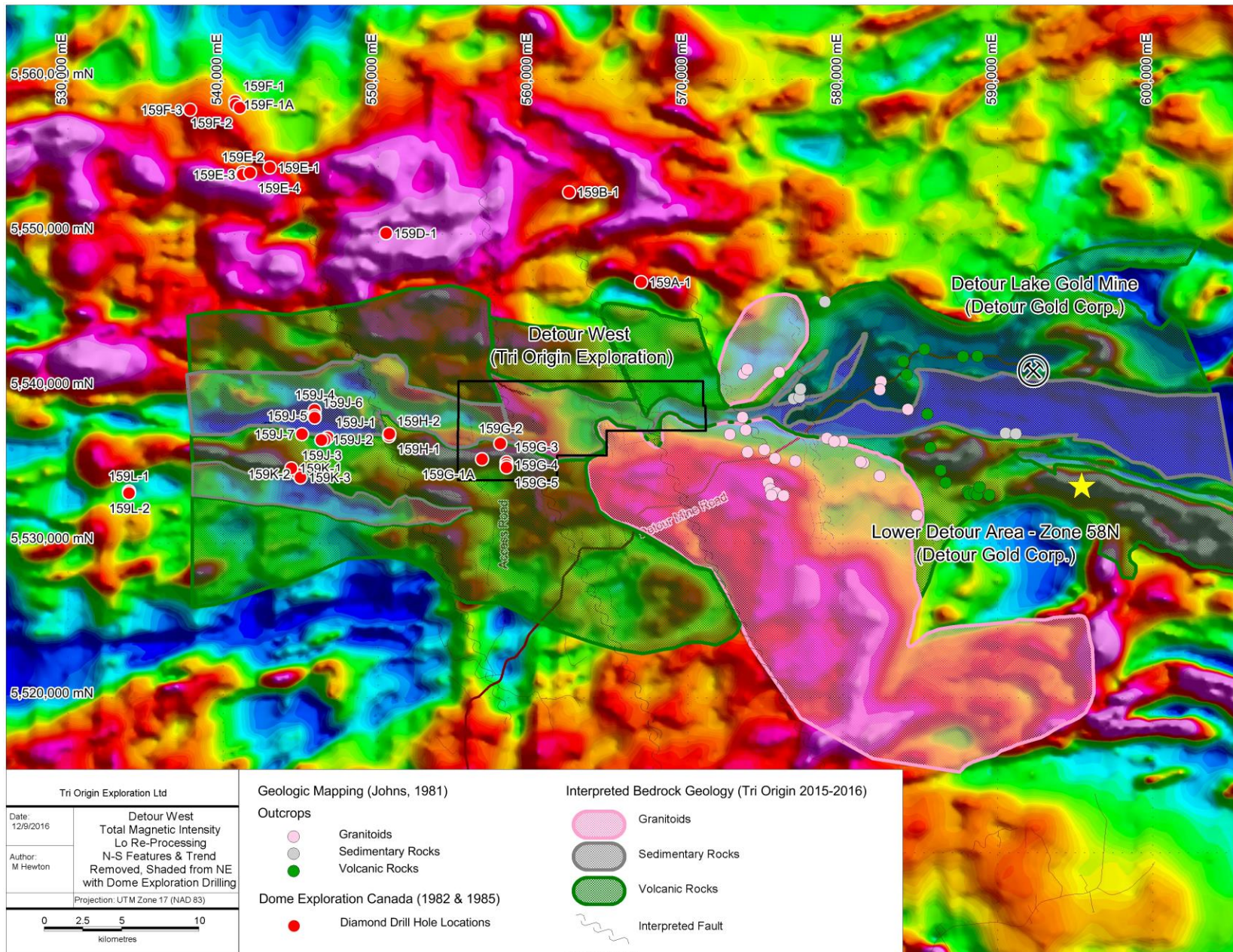


Figure 8. Figure 7, with preliminary bedrock geology interpreted from magnetics and Dome diamond drilling.

Table 2. Detour West Diamond Drill Hole Compilation Database.

Dome Canada Hole ID	Year	Lithology	Sulphides	Gold Assay Results	Base Metal Assay Results	AFRI
159F-1, 159F-1A, 159F-2, 159F-3	1982	mostly acid tuff, flows, gneiss; acid agglomerate tuff w semi-mass po-py; intermediate to basic tuff, flows, gneiss	tr-10% py-po; locally 40-90% po>py, esp in felsic agglomerate tuff, tr sph vns, tr graph	0.1 to 0.31 g/t	0.1 to 0.3% Zn, 0.1% Cu	42I01NW0004
159E-1, 159E-2, 159E-3, 159E-4	1982	mostly acid to int gneiss (met'd volc tuffs, flows, local grt), some basic gneiss, gneissic granite	1-10% py-po; local 40-70% po>py w/ tr cpy, tr grph, rare mo	0.1 to 0.31g/t	0.1-0.2% Cu, 0.2% Zn	42I01NW0835
159D-1	1982	basic gneiss, peg, acid gneiss	tr to 2% py-po, mostly as stringers, tr cpy	nil	ns	42I01SW0002
159B-1	1982	alternating basic & acid gneiss (metavolcs, metatuffs; local grt), minor int gneiss, pegmatite	tr to 5% po-py strings, tr cpy; local 15-20% po>py, and 70-90% po>py>>cpy	0.1-0.622 g/t	0.1% Cu, 0.1 oz/t Ag	42I01NE0001
159A-1	1982	alternating basic & acid gneiss (metavolcs, metatuffs; local grt), pegmatite	tr po-py, local 2-10% po-py, rare cpy	0.31 g/t	nil	42I01NE0003
159J-4, 159J-5, 159J-6	1985	bt-qz-fsp gneiss with minor chl-ep+/-hem alteration, mag blebs; metasediments in 159J-6		Not sampled	Not sampled	42I01SW0001
159J-7	1985	bt-qz-fsp gneiss; targeted EM conductor, but no evidence of it		Not sampled	Not sampled	42I01SW0001
159J-1, 159J-2, 159J-3	1985	bt-qz-fsp gneiss, faulted, minor ep-qz alteration	5% py in minor quartz veins, local 15% py in gneiss is rare in 159J-3	Not sampled	Not sampled	42I01SW0001
159K-1, 159K-2, 159K-3	1985	biotite-quartz-feldspar gneiss, hematite alteration		Not sampled	Not sampled	42H16NW0020
159H-1, 159H-2	1985	chl-bt-qz-fsp gneiss (komatiitic/ultramafic basalt?), w/ minor srct alt		Not sampled	Not sampled	42H16NW0005
159G-1A, 159G-2, 159G-3, 159G-4, 159G-5	1985	bt-qz-fsp gneiss w/ lots of fault gouge, minor chl-mag-ep alt; metaseds; felsic-int volcs (4,5)		Not sampled	Not sampled	42H16NE0001

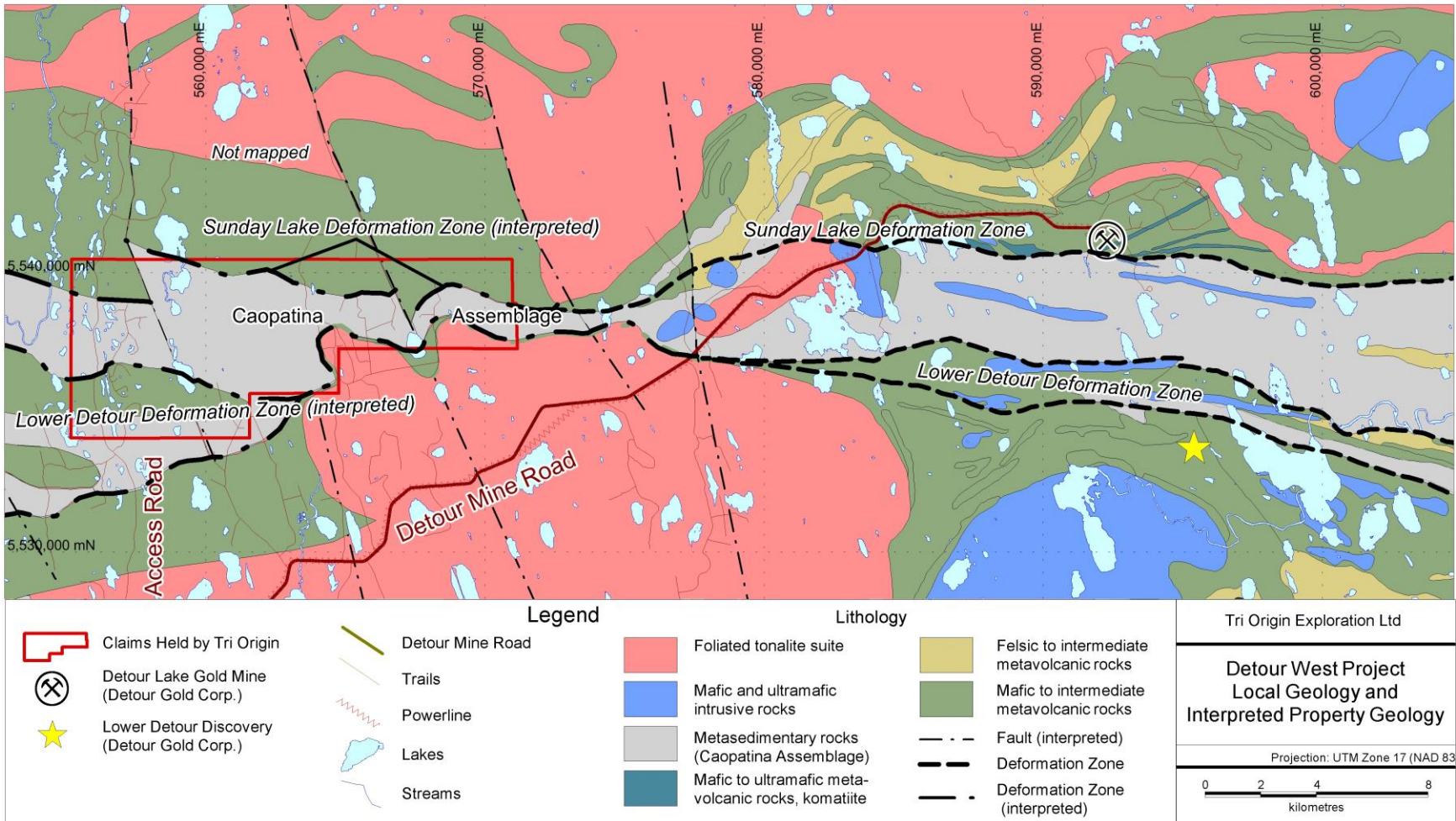


Figure 9. Final geological interpretation map of the Detour West project.

## **6.0 PROPERTY VISITS AND ASSESSMENTS**

The Detour West property was visited on November 3 and November 21 by Tri Origin geologists (Gregg Morris and Frank Kendle) to assess property access and logistics for future program planning, particularly to assess the property for the potential of conducting an overburden drilling program, and to assess the geology and geography of the property. No outcrop was observed during the property visits. Figure 10 shows access roads and trails across the property. The south side of the property can be accessed by winter roads only from the paved Detour Lake Mine Road. Two winter roads going north from the mine road cannot be accessed in the warmer months as they are flooded. Access Road along the west side of the property can be driven by truck year round.

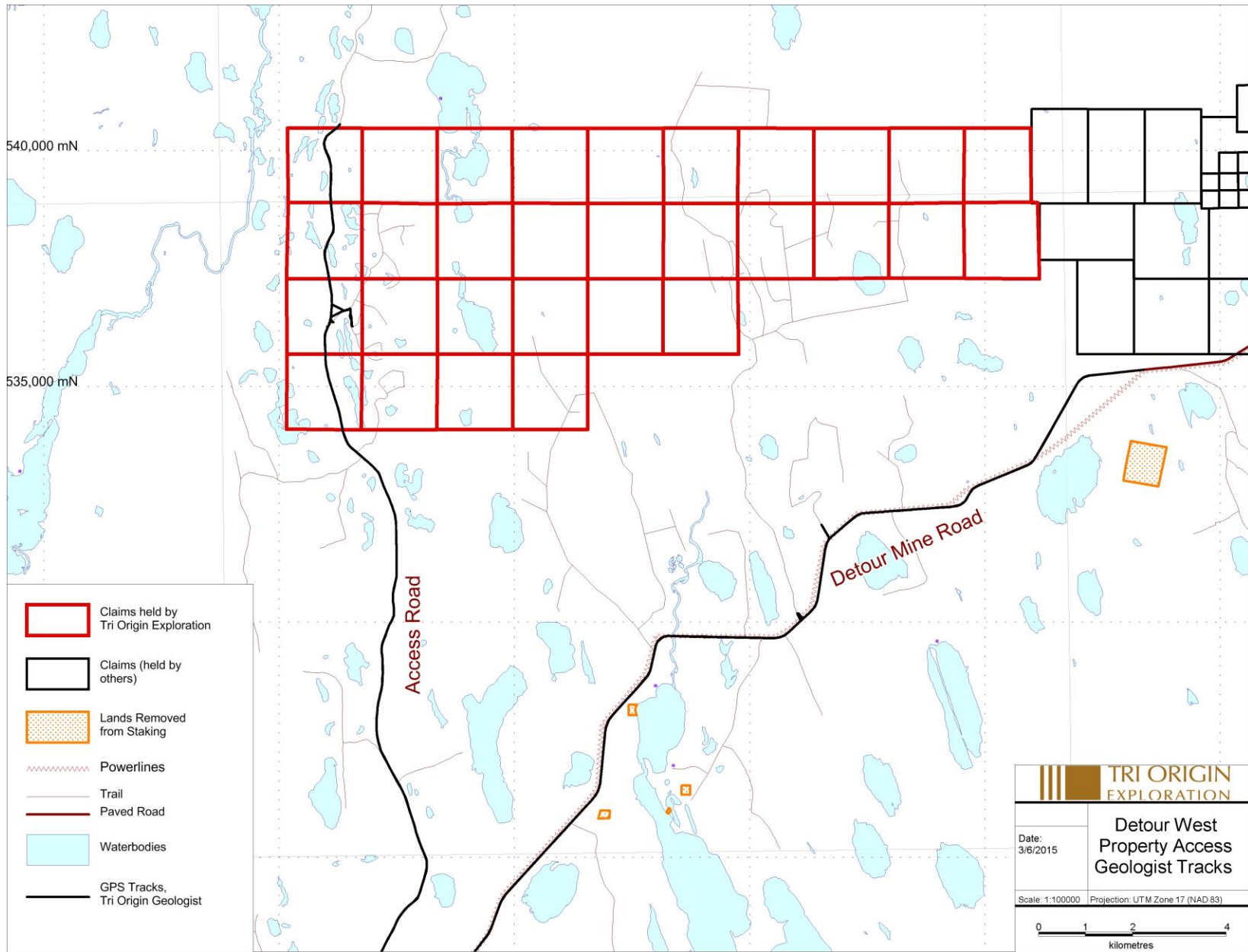


Figure 10. Property access.

## **7.0 VTEM SURVEY**

Tri Origin Exploration contracted Geotech Ltd of Aurora, ON, to fly a helicopter-borne geophysical survey over the Detour West project between August 29<sup>th</sup> and September 15<sup>th</sup>, 2016. The geophysical and geological compilation resulted in several significant findings that were used in the planning of the VTEM survey over the Detour West property. The interpreted east-west magnetic trend of the Archean bedrock in the Detour mine area continues to the Detour West property necessitated that the VTEM survey lines be flown in a north-south direction. Traverse line spacing was 100 m, and tie lines were flown at a spacing of 2,000 m. A total of 1,235 line-kilometers of geophysical data was collected by the survey, covering a total area of 117 km<sup>2</sup>. Survey details and results are presented in Appendix A in a report written by Geotech Ltd.

Magnetic results from VTEM confirm Tri Origin's interpretations of the western extension of rock units and structures hosting the nearby Detour Lake gold mine. The EM response is subdued and certainly hindered by conductive overburden, especially in the central and western parts of the property. Weak west and west-northwest trending electromagnetic responses occur through the central part of the property. These responses are masked by conductive overburden to the west and northwest. These responses flank the north and south boundaries of a west-northwest trending magnetic low interpreted to represent the westward extension of the Caopatina Assemblage, which is a similar setting at the Detour Lake and Lower Detour gold deposits.

## **8.0 IP SURVEY TEST LINE**

A test IP (induced polarization) survey line was conducted by Dias Geophysics November 28, 29, and 30, 2016. This test line was conducted along the Access Road leading north across the western-most extent of the property. The test line was conducted to see if the IP technique could penetrate through the thick overburden to the Archean bedrock below. Stations were taken every 50 m. Results from the survey are pending.

## **9.0 RECOMMENDATIONS AND CONCLUSIONS**

Considering the favourable location of the property only 20 km west of the Detour Lake gold mine, follow-up is strongly recommended. Several areas identified by this compilation and VTEM survey warrant further geological investigation. Detailed treatment of both the magnetic and EM data will further refine our geological interpretation. Geochemical exploration programs would probably be limited to overburden drilling and sampling down-ice from selected magnetic and EM trends. IP surveying should also be conducted at selected targets. Finally, exploring the sediment-volcanic contacts through the property with a diamond drilling programme will be conducted once targets are generated from the aforementioned surveys.

Overall this compilation was very useful in leading to a better understanding of the geology on the Detour West property and identifying areas for further work.

## 10.0 PERSONNEL

Meghan Hewton	Geologist Tri Origin Exploration Ltd	Goodwood, Ontario
Frank Kendle	Contract Geologist Tri Origin Exploration Ltd.	Queensville, Ontario
Gregg Morris	Contract Geologist Tower Resources	Halifax, Nova Scotia

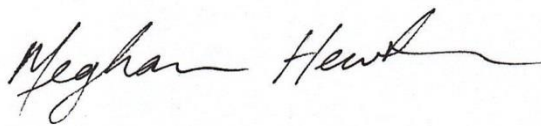


## 10.0 STATEMENT OF QUALIFICATIONS

I, Meghan Hewton, of 17 Tindall Lane, Goodwood, Ontario, L0C 1A0, do hereby certify that:

1. I am employed as a geologist by Tri Origin Exploration Ltd.
2. I graduated with a Master's of Science (Geology) from Simon Fraser University in 2012, and a Bachelor of Science (Honours Environmental Geosciences) from the University of Western Ontario in 2010.
3. Hold a GIT (Geoscientist-in-Training) membership with the Association of Professional Geoscientists of Ontario (membership number 10384).
4. I have worked as a geologist for a total of four years.
5. I am responsible for the technical report titled "Report on the 2016 Geological Compilation and VTEM Survey, Detour West Property, Cochrane District, Ontario".
6. My knowledge of the property as described herein was obtained by literature review.
7. I have no direct interest, nor do I expect to receive any interest in the mining claims that comprise the Detour West Property within the Marquis Lake and Newnham Creek Areas, Porcupine Mining Division.
8. I am not aware of any material fact or material change with respect to the subject matter of the Technical Report that is not reflected in the Technical Report, the omission to disclose which makes the Technical Report misleading.
9. I consent to the filing of the Technical Report with any stock exchange and other regulatory authority and any publication by them for regulatory purposes, including electronic publication in the public company files on their websites accessible by the public, of the Technical Report.

Dated this 12<sup>th</sup> day of December, 2016.

A handwritten signature in black ink that reads "Meghan Hewton". The signature is fluid and cursive, with a long horizontal flourish extending to the right.

Meghan Hewton, MSc, GIT

## **11.0 REFERENCES**

- Ayer, J.A., Chartrand, J.E., Duguet, M., Rainsford, D.R.B., and Trowell, N.F. 2009. Geological Compilation of the Burntbush-Detour lakes area, Abitibi greenstone belt; Ontario Geological Survey, Preliminary Map P.3609, scale 1: 100,000.
- Johns, G. W. 1981: Burntbush - Detour Lakes; Ontario Geological Survey Map 2453, Precambrian Geology Series, Scale 1:100,000.
- Lee, Hulbert A. 1979. Northern Ontario Engineering Geology Terrain Study, Data Base Map, Montreuil Lake. Ontario Geological Survey. Map 5034, Scale 1:100,000.
- Thompson, W.H. 1984. Electromagnetic, VLF, and Magnetic Surveys for Dome Exploration (Canada) Limited on Project 159G, Detour Lake Area, Ontario. Geosearch Consultants Limited. (AFRI 42H15NE0002)
- Schacht, B. 1998. Logistics, Processing, and Interpretation Report of the Airborne Magnetics GEOTEM Electromagnetic Multicoil Survey in Northern Ontario, over the Abitibi Region. For Eastmain Resources (AFRI 32L05NE2001).

**Appendix A**

---

**REPORT ON A HELICOPTER-BORNE VERSATILE TIME DOMAIN  
ELECTROMAGNETIC (VTEM™ Plus) AND HORIZONTAL MAGNETIC  
GRADIOMETER GEOPHYSICAL SURVEY**

**Geotech Ltd.  
245 Industrial Parkway North  
Aurora, ON Canada L4G 4C4**



# VTEM™ Plus

---

REPORT ON A HELICOPTER-BORNE VERSATILE TIME DOMAIN  
ELECTROMAGNETIC (VTEM™ Plus) AND HORIZONTAL MAGNETIC  
GRADIOMETER GEOPHYSICAL SURVEY

PROJECT:	DETOUR WEST
LOCATION:	LITTLE ABITIBI LAKE, ONTARIO
FOR:	TRI ORIGIN EXPLORATION
SURVEY FLOWN:	AUGUST - SEPTEMBER 2016
PROJECT:	GL160157

Geotech Ltd.  
245 Industrial Parkway North  
Aurora, ON Canada L4G 4C4

Tel: +1 905 841 5004  
Web: [www.geotech.ca](http://www.geotech.ca)  
Email: [info@geotech.ca](mailto:info@geotech.ca)



# TABLE OF CONTENTS

EXECUTIVE SUMMARY.....	III
1. INTRODUCTION.....	1
1.1 General Considerations.....	1
1.2 Survey and System Specifications.....	2
1.3 Topographic Relief and Cultural Features.....	3
2. DATA ACQUISITION.....	4
2.1 Survey Area.....	4
2.2 Survey Operations.....	4
2.3 Flight Specifications.....	5
2.4 Aircraft and Equipment.....	5
2.4.1 Survey Aircraft.....	5
2.4.2 Electromagnetic System.....	5
2.4.3 Full waveform vtem™ sensor calibration.....	9
2.4.4 Horizontal Magnetic Gradiometer.....	9
2.4.5 Radar Altimeter.....	9
2.4.6 GPS Navigation System.....	9
2.4.7 Digital Acquisition System.....	9
2.5 Base Station.....	10
3. PERSONNEL.....	11
4. DATA PROCESSING AND PRESENTATION.....	12
4.1 Flight Path.....	12
4.2 Electromagnetic Data.....	12
4.3 Horizontal Magnetic Gradiometer Data.....	14
5. DELIVERABLES.....	15
5.1 Survey Report.....	15
5.2 Maps.....	15
5.3 Digital Data.....	16
6. CONCLUSIONS AND RECOMMENDATIONS.....	20

## LIST OF FIGURES

Figure 1: Survey location.....	1
Figure 2: Survey area location on Google Earth.....	2
Figure 3: Flight path over a Google Earth Image.....	3
Figure 4: VTEM™ Transmitter Current Waveform.....	6
Figure 5: VTEM™Plus System Configuration.....	8
Figure 6: Z, X and Fraser filtered X (FFx) components for "thin" target.....	13

## LIST OF TABLES

Table 1: Survey Specifications.....	4
Table 2: Survey schedule.....	4
Table 3: Off-Time Decay Sampling Scheme.....	6
Table 4: Acquisition Sampling Rates.....	9
Table 5: Geosoft GDB Data Format.....	16
Table 6: Geosoft Resistivity Depth Image GDB Data Format.....	18
Table 7: Geosoft database for the VTEM waveform.....	18

## APPENDICES

A.	Survey location maps .....
B.	Survey Survey area Coordinates .....
C.	Geophysical Maps .....
D.	Generalized Modelling Results of the VTEM System.....
E.	TAU Analysis .....
F.	TEM Resistivity Depth Imaging (RDI) .....

## EXECUTIVE SUMMARY

### DETOUR WEST - LITTLE ABITIBI LAKE, ONTARIO

During August 29<sup>th</sup> to September 15<sup>th</sup> 2016 Geotech Ltd. carried out a helicopter-borne geophysical survey over Detour West Project situated near Little Abitibi, Ontario.

Principal geophysical sensors included a versatile time domain electromagnetic (VTEMplus) system and horizontal magnetic gradiometer with two caesium sensors. Ancillary equipment included a GPS navigation system and a radar altimeter. A total of 1235 line-kilometres of geophysical data were acquired during the survey.

In-field data quality assurance and preliminary processing were carried out on a daily basis during the acquisition phase. Preliminary and final data processing, including generation of final digital data and map products were undertaken from the office of Geotech Ltd. in Aurora, Ontario.

The processed survey results are presented as the following maps:

- Electromagnetic stacked profiles of the B-field Z Component,
- Electromagnetic stacked profiles of dB/dt Z Component,
- B-Field Z Component Channel grids,
- Total Magnetic Intensity (TMI),
- Magnetic Total Horizontal Gradient,
- Magnetic Tilt-Angle Derivative of TMI,
- Calculated Time Constant (Tau) with Calculated Vertical Derivative contours and
- Resistivity Depth Images (RDI) sections are presented.

Digital data includes all electromagnetic and magnetic products, plus ancillary data including the waveform.

The survey report describes the procedures for data acquisition, processing, final image presentation and the specifications for the digital data set.

# 1. INTRODUCTION

## 1.1 GENERAL CONSIDERATIONS

Geotech Ltd. performed a helicopter-borne geophysical survey over Detour West Project situated near Little Abitibi, Ontario (Figure 1 & Figure 2).

Robert Valliant represented Tri Origin Exploration during the data acquisition and data processing phases of this project.

The geophysical surveys consisted of helicopter borne EM using the versatile time-domain electromagnetic (VTEMplus) system with Full-Waveform processing. Measurements consisted of Vertical (Z) and In-line Horizontal (X) components of the EM fields using induction coils and the aeromagnetic total field using a magnetic gradiometer. A total of 1235 line-km of geophysical data were acquired during the survey.

The crew was based out of Little Abitibi Lake (Figure 2) in Ontario for the acquisition phase of the survey. Survey flying started on August 29<sup>th</sup> and was completed on September 15<sup>th</sup>, 2016.

Data quality control and quality assurance, and preliminary data processing were carried out on a daily basis during the acquisition phase of the project. Final data processing followed immediately after the end of the survey. Final reporting, data presentation and archiving were completed from the Aurora office of Geotech Ltd. in November, 2016.

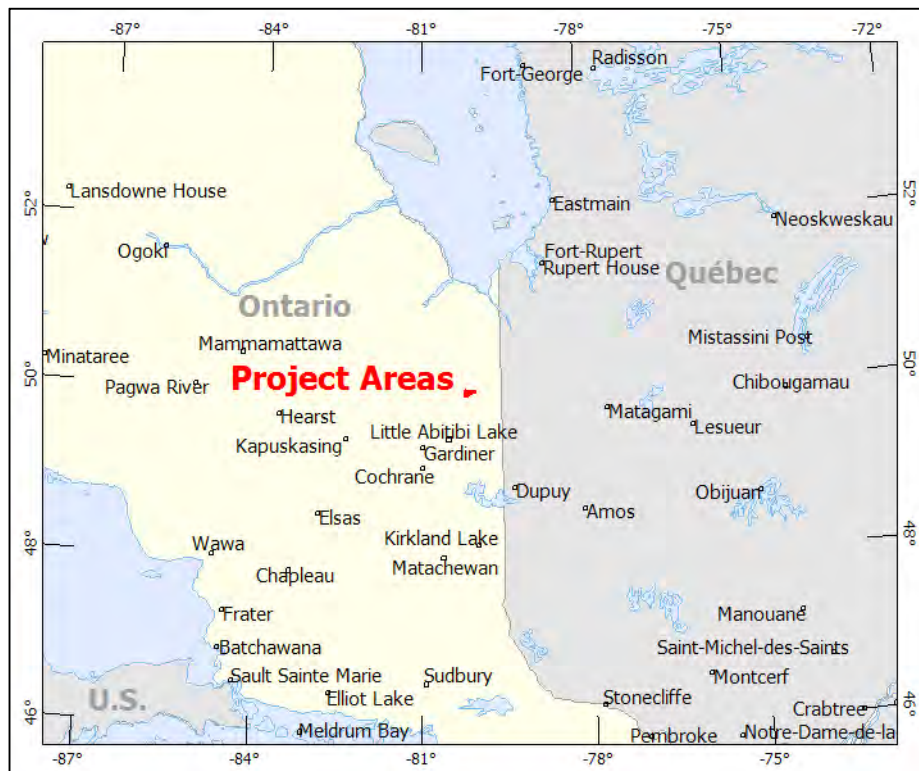


Figure 1: Survey location



## 1.2 SURVEY AND SYSTEM SPECIFICATIONS

The survey area was located approximately 63 kilometres northeast of Little Abitibi Lake, Ontario (Figure 2).

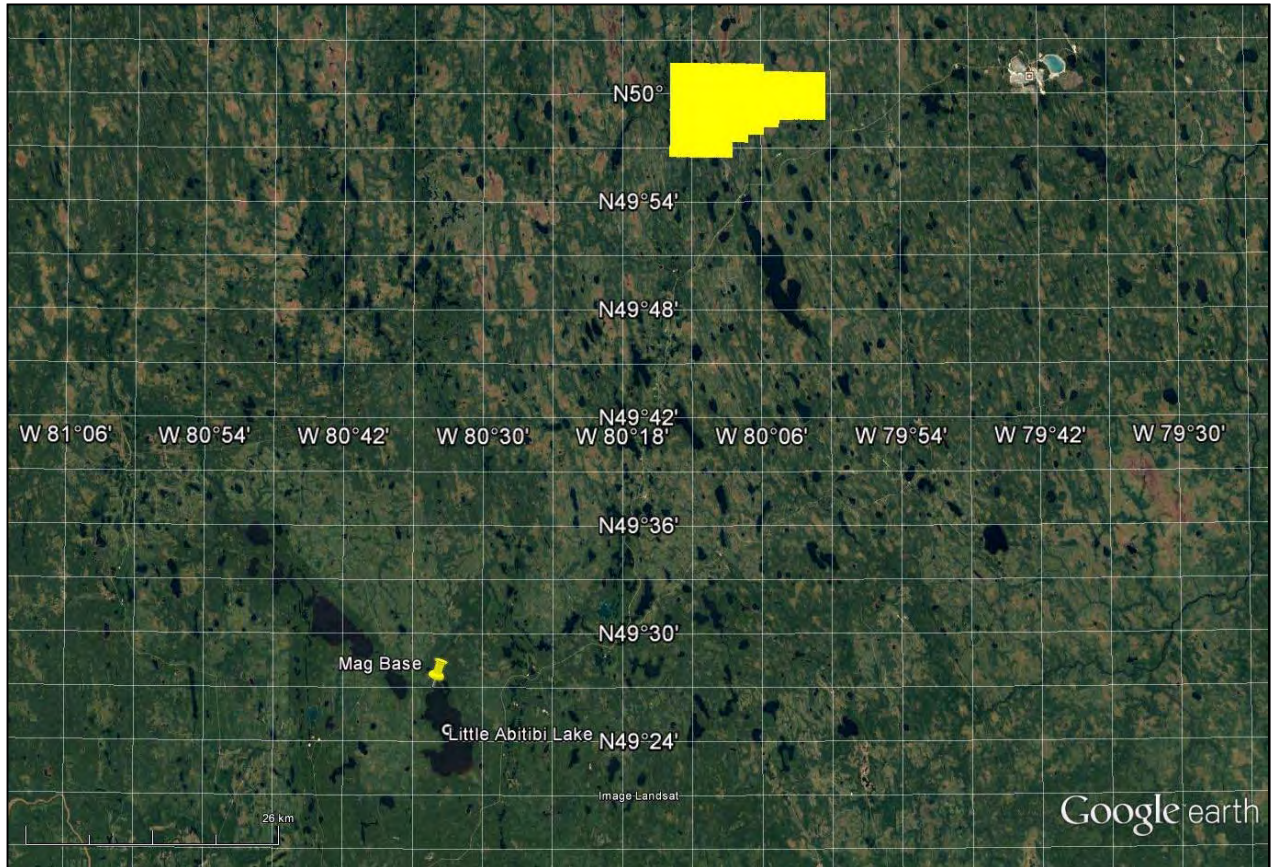


Figure 2: Survey area location on Google Earth.

The block was flown in a north to south ( $N 0^{\circ} E$  azimuth) direction with traverse line spacing of 100 metres as depicted in Figure 3. Tie lines were flown perpendicular to the traverse lines at a spacing of 2000 metres. For more detailed information on the flight spacing and direction see Table 1.

### 1.3 TOPOGRAPHIC RELIEF AND CULTURAL FEATURES

Topographically, the survey area exhibits a level relief with an elevation ranging from 277 to 338 metres above mean sea level over an area of 46 square kilometres (Figure 3).

There are various rivers and streams running through the survey area. There are no visible signs of culture located in the survey areas (Figure 3).

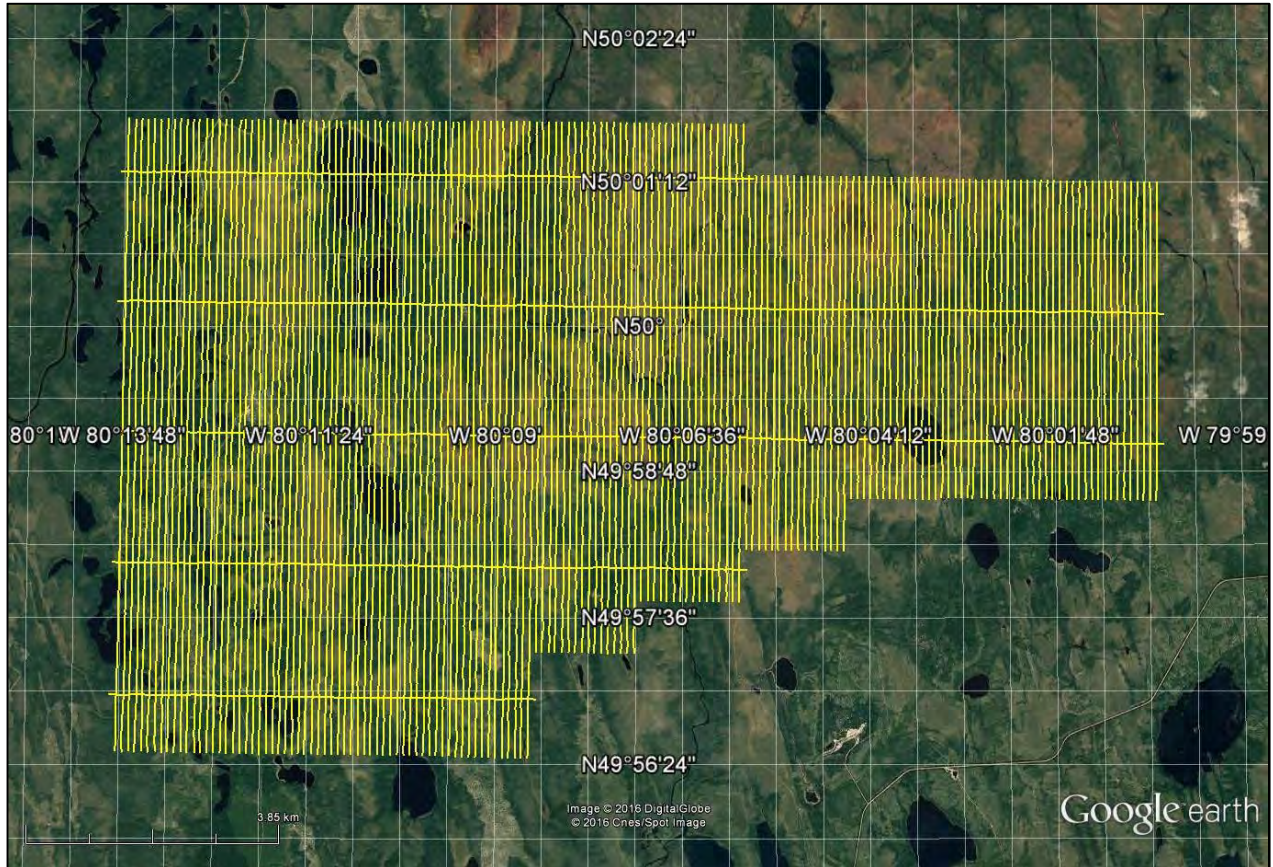


Figure 3: Flight path over a Google Earth Image.

## 2. DATA ACQUISITION

### 2.1 SURVEY AREA

The survey areas (see Figure 3 and Appendix A) and general flight specifications are as follows:

**Table 1:** Survey Specifications

Survey block	Line spacing (m)	Area (Km <sup>2</sup> )	Planned <sup>1</sup> Line-km	Actual Line-km	Flight direction	Line numbers
Detour West	Traverse: 100	117	1235	1198	N 0° E / N 180° E	L1000 - L2590
	Tie: 2000			58.4	N 90° E / N 270° E	T3000 - T3040
<b>TOTAL</b>		117	1235	1256.4		

Survey area boundaries co-ordinates are provided in Appendix B.

### 2.2 SURVEY OPERATIONS

Survey operations were based out of Little Abitibi Lake in Ontario from August 19<sup>th</sup> until September 15<sup>th</sup> 2016. The following table shows the timing of the flying.

**Table 2:** Survey schedule

Date	Flight #	Flown km	Block	Crew location	Comments
19-Aug-2016				Little Abitibi Lake, ON	Mobilization
20-Aug-2016				Little Abitibi Lake, ON	Mobilization
21-Aug-2016				Little Abitibi Lake, ON	Mobilization
22-Aug-2016				Little Abitibi Lake, ON	Set up and test flight
23-Aug-2016				Little Abitibi Lake, ON	No testing due to weather
24-Aug-2016				Little Abitibi Lake, ON	No testing due to weather
25-Aug-2016				Little Abitibi Lake, ON	No testing due to weather
26-Aug-2016				Little Abitibi Lake, ON	Test flight aborted due to weather
27-Aug-2016				Little Abitibi Lake, ON	Test flight
28-Aug-2016				Little Abitibi Lake, ON	Test flight
29-Aug-2016	1	106	Detour West	Little Abitibi Lake, ON	106km flown
30-Aug-2016	2	163	Detour West	Little Abitibi Lake, ON	163km flown
31-Aug-2016				Little Abitibi Lake, ON	No production due to weather
1-Sep-2016				Little Abitibi Lake, ON	No production due to weather
2-Sep-2016	3,4	192	Detour West	Little Abitibi Lake, ON	192km flown
3-Sep-2016	5,6	192	Detour West	Little Abitibi Lake, ON	192km flown
4-Sep-2016				Little Abitibi Lake, ON	No production due to weather
5-Sep-2016				Little Abitibi Lake, ON	No production due to weather
6-Sep-2016	7,8	124	Detour West	Little Abitibi Lake, ON	124km flown

<sup>1</sup> Note: Actual Line kilometres represent the total line kilometres in the final database. These line-km normally exceed the Planned Line-km, as indicated in the survey NAV files.

Date	Flight #	Flown km	Block	Crew location	Comments
7-Sep-2016				Little Abitibi Lake, ON	No production due to weather
8-Sep-2016				Little Abitibi Lake, ON	No production due to weather
9-Sep-2016				Little Abitibi Lake, ON	No production due to weather
10-Sep-2016				Little Abitibi Lake, ON	No production due to weather
11-Sep-2016	9,10,11	218	Detour West	Little Abitibi Lake, ON	218km flown
12-Sep-2016	12,13,14	143	Detour West	Little Abitibi Lake, ON	143km flown
13-Sep-2016				Little Abitibi Lake, ON	No production due to weather
14-Sep-2016				Little Abitibi Lake, ON	No production due to helicopter maintenance
15-Sep-2016	15	97	Detour West	Little Abitibi Lake, ON	Remaining kms were flown- flying complete

## 2.3 FLIGHT SPECIFICATIONS

During the survey the helicopter was maintained at a mean altitude of 78 metres above the ground with an average survey speed of 80 km/hour. This allowed for an actual average Transmitter-receiver loop terrain clearance of 38 metres and a magnetic sensor clearance of 48 metres.

The on board operator was responsible for monitoring the system integrity. He also maintained a detailed flight log during the survey, tracking the times of the flight as well as any unusual geophysical or topographic features.

On return of the aircrew to the base camp the survey data was transferred from a compact flash card (PCMCIA) to the data processing computer. The data were then uploaded via ftp to the Geotech office in Aurora for daily quality assurance and quality control by qualified personnel.

## 2.4 AIRCRAFT AND EQUIPMENT

### 2.4.1 SURVEY AIRCRAFT

The survey was flown using a Eurocopter Aerospatiale (Astar) 350 B3 helicopter, registration C-FBZN. The helicopter is owned and operated by Geotech Aviation. Installation of the geophysical and ancillary equipment was carried out by a Geotech Ltd crew.

### 2.4.2 ELECTROMAGNETIC SYSTEM

The electromagnetic system was a Geotech Time Domain EM (VTEM™Plus) full receiver-waveform streamed data recorded system. The “full waveform VTEM system” uses the streamed half-cycle recording of transmitter and receiver waveforms to obtain a complete system response calibration throughout the entire survey flight. The VTEM™ transmitter current waveform is shown diagrammatically in Figure 4. VTEM with the Serial number 19 had been used for the survey.

The VTEM™ Receiver and transmitter coils were in concentric-coplanar and Z-direction oriented configuration. The receiver system for the project also included a coincident-coaxial X-direction coil to measure the in-line dB/dt and calculate B-Field responses. The Transmitter-receiver loop was towed at a mean distance of 31 metres below the aircraft as shown in Figure 5.

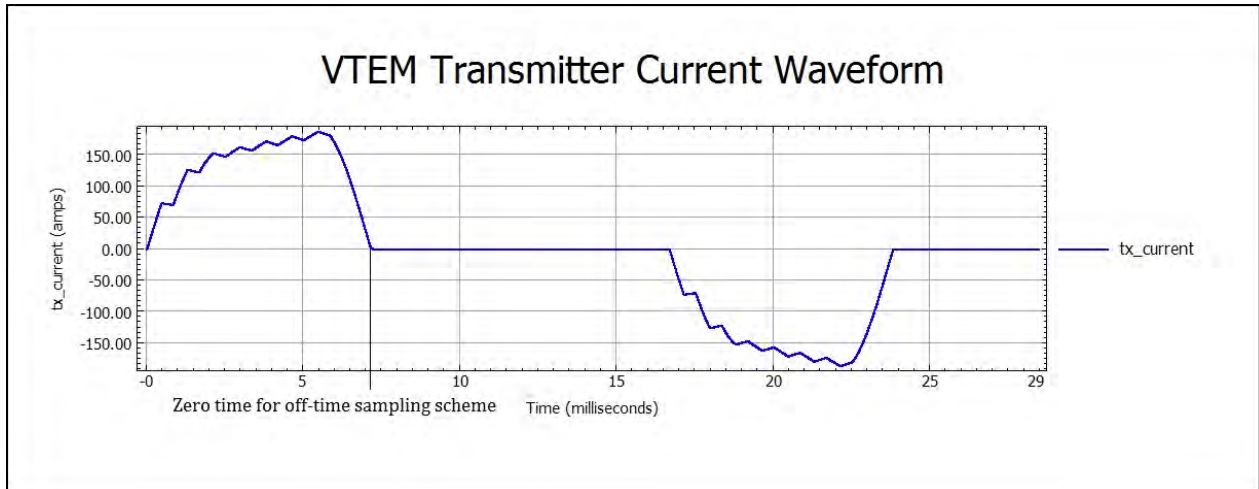


Figure 4: VTEM™ Transmitter Current Waveform

The VTEM™ decay sampling scheme is shown in Table 3 below. Forty-three time measurement gates were used for the final data processing in the range from 0.021 to 8.083 msec. Zero time for the off-time sampling scheme is equal to the current pulse width and is defined as the time near the end of the turn-off ramp where the  $di/dt$  waveform falls to 1/2 of its peak value.

Table 3: Off-Time Decay Sampling Scheme

VTEM™ Decay Sampling Scheme				
Index	Start	End	Middle	Width
Milliseconds				
4	0.018	0.023	0.021	0.005
5	0.023	0.029	0.026	0.005
6	0.029	0.034	0.031	0.005
7	0.034	0.039	0.036	0.005
8	0.039	0.045	0.042	0.006
9	0.045	0.051	0.048	0.007
10	0.051	0.059	0.055	0.008
11	0.059	0.068	0.063	0.009
12	0.068	0.078	0.073	0.010
13	0.078	0.090	0.083	0.012
14	0.090	0.103	0.096	0.013
15	0.103	0.118	0.110	0.015
16	0.118	0.136	0.126	0.018
17	0.136	0.156	0.145	0.020
18	0.156	0.179	0.167	0.023
19	0.179	0.206	0.192	0.027
20	0.206	0.236	0.220	0.030
21	0.236	0.271	0.253	0.035
22	0.271	0.312	0.290	0.040
23	0.312	0.358	0.333	0.046

VTEM™ Decay Sampling Scheme				
Index	Start	End	Middle	Width
Milliseconds				
24	0.358	0.411	0.383	0.053
25	0.411	0.472	0.440	0.061
26	0.472	0.543	0.505	0.070
27	0.543	0.623	0.580	0.081
28	0.623	0.716	0.667	0.093
29	0.716	0.823	0.766	0.107
30	0.823	0.945	0.880	0.122
31	0.945	1.086	1.010	0.141
32	1.086	1.247	1.161	0.161
33	1.247	1.432	1.333	0.185
34	1.432	1.646	1.531	0.214
35	1.646	1.891	1.760	0.245
36	1.891	2.172	2.021	0.281
37	2.172	2.495	2.323	0.323
38	2.495	2.865	2.667	0.370
39	2.865	3.292	3.063	0.427
40	3.292	3.781	3.521	0.490
41	3.781	4.341	4.042	0.560
42	4.341	4.987	4.641	0.646
43	4.987	5.729	5.333	0.742
44	5.729	6.581	6.125	0.852
45	6.581	7.560	7.036	0.979
46	7.560	8.685	8.083	1.125

Z Component: 4 - 46 time gates  
X Component: 20 - 46 time gates

VTEM™ system specifications:

Transmitter	Receiver
<ul style="list-style-type: none"> <li>• Transmitter loop diameter: 26 m</li> <li>• Number of turns: 4</li> <li>• Effective Transmitter loop area: 2123.7 m<sup>2</sup></li> <li>• Transmitter base frequency: 30 Hz</li> <li>• Peak current: 187 A</li> <li>• Pulse width: 7.16 ms</li> <li>• Waveform shape: Bi-polar trapezoid</li> <li>• Peak dipole moment: 397,135 nIA</li> <li>• Actual average Transmitter-receiver loop terrain clearance: 38 metres above the ground</li> </ul>	<ul style="list-style-type: none"> <li>• X Coil diameter: 0.32 m</li> <li>• Number of turns: 245</li> <li>• Effective coil area: 19.69 m<sup>2</sup></li> <li>• Z-Coil diameter: 1.2 m</li> <li>• Number of turns: 100</li> <li>• Effective coil area: 113.04 m<sup>2</sup></li> </ul>

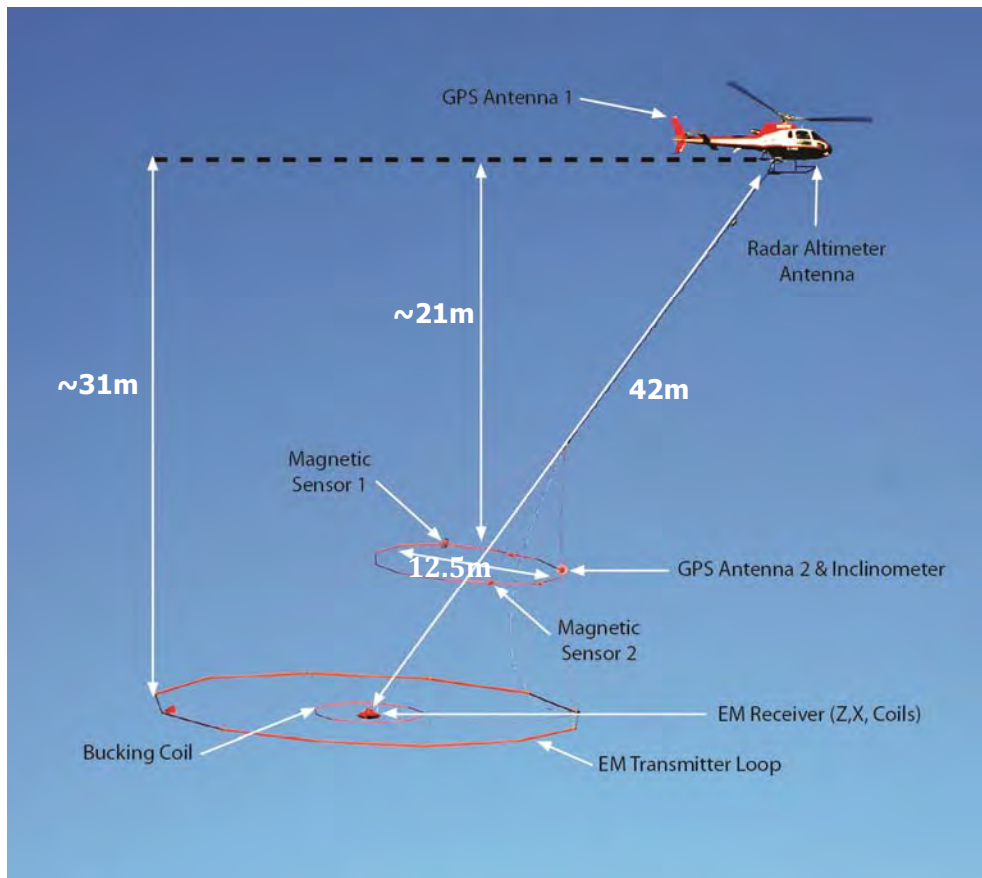


Figure 5: VTEM™ Plus System Configuration.

### 2.4.3 FULL WAVEFORM VTEM™ SENSOR CALIBRATION

The calibration is performed on the complete VTEM™ system installed in and connected to the helicopter, using special calibration equipment.

The procedure takes half-cycle files acquired and calculates a calibration file consisting of a single stacked half-cycle waveform. The purpose of the stacking is to attenuate natural and man-made magnetic signals, leaving only the response to the calibration signal.

### 2.4.4 HORIZONTAL MAGNETIC GRADIOMETER

The horizontal magnetic gradiometer consists of two Geometrics split-beam field magnetic sensors with a sampling interval of 0.1 seconds. These sensors are mounted 12.5 metres apart on a separate loop, 10 metres above the Transmitter-receiver loop. A GPS antenna and Gyro Inclinometer is installed on the separate loop to accurately record the tilt and position of the magnetic gradiometer.

### 2.4.5 RADAR ALTIMETER

A Terra TRA 3000/TRI 40 radar altimeter was used to record terrain clearance. The antenna was mounted beneath the bubble of the helicopter cockpit (Figure 5).

### 2.4.6 GPS NAVIGATION SYSTEM

The navigation system used was a Geotech PC104 based navigation system utilizing a NovAtel's WAAS (Wide Area Augmentation System) enabled GPS receiver, Geotech navigate software, a full screen display with controls in front of the pilot to direct the flight and a NovAtel GPS antenna mounted on the helicopter tail (Figure 5). As many as 11 GPS and two WAAS satellites may be monitored at any one time. The positional accuracy or circular error probability (CEP) is 1.8 m, with WAAS active, it is 1.0 m. The co-ordinates of the survey area were set-up prior to the survey and the information was fed into the airborne navigation system. The second GPS antenna is installed on the additional magnetic loop together with Gyro Inclinometer.

### 2.4.7 DIGITAL ACQUISITION SYSTEM

A Geotech data acquisition system recorded the digital survey data on an internal compact flash card. Data is displayed on an LCD screen as traces to allow the operator to monitor the integrity of the system. The data type and sampling interval as provided in Table 4.

Table 4: Acquisition Sampling Rates

Data Type	Sampling
TDEM	0.1 sec
Magnetometer	0.1 sec
GPS Position	0.2 sec
Radar Altimeter	0.2 sec
Inclinometer	0.1 sec



## 2.5 BASE STATION

A combined magnetometer/GPS base station was utilized on this project. A Geometrics Caesium vapour magnetometer was used as a magnetic sensor with a sensitivity of 0.001 nT. The base station was recording the magnetic field together with the GPS time at 1 Hz on a base station computer.

The base station magnetometer sensor was installed at 80°34'18.18"W, 49°26'58.86"N; away from electric transmission lines and moving ferrous objects such as motor vehicles. The base station data were backed-up to the data processing computer at the end of each survey day.

### 3. PERSONNEL

The following Geotech Ltd. personnel were involved in the project.

#### FIELD:

Project Manager:	Darren Tuck (Office)
Data QC:	Thomas Wade (Office)
	Neil Fiset (Office)
	Nick Venter (Office)
Crew chief:	Terry Lacey
	Paul Taylor
Operator:	Scott Taylor

The survey pilot and the mechanical engineer were employed directly by the helicopter operator – Geotech Aviation

Pilot:	Robert Girard
	Greg Heuring
	Bill Hofstede
Mechanical Engineer:	Clayton Whitney
	Christine McArthur

#### OFFICE:

Preliminary Data Processing:	Thomas Wade/ Neil Fiset/ Nick Venter
Final Data Processing:	ZiHao Han
Final Data QA/QC:	Geoffrey Plastow
Reporting/Mapping:	Liz Mathew

Data acquisition phase was carried out under the supervision of Andrei Bagrianski, P. Geo, and Chief Operating Officer. Processing phase was carried out under the supervision of Geoffrey Plastow, P. Geo, Data Processing Manager. The customer relations were looked after by David Hitz.

## 4. DATA PROCESSING AND PRESENTATION

Data compilation and processing were carried out by the application of Geosoft OASIS Montaj and programs proprietary to Geotech Ltd.

### 4.1 FLIGHT PATH

The flight path, recorded by the acquisition program as WGS 84 latitude/longitude, was converted into the NAD83 Datum, UTM Zone 17 North coordinate system in Oasis Montaj.

The flight path was drawn using linear interpolation between x, y positions from the navigation system. Positions are updated every second and expressed as UTM easting's (x) and UTM northing's (y).

### 4.2 ELECTROMAGNETIC DATA

The Full Waveform EM specific data processing operations included:

- Half cycle stacking (performed at time of acquisition);
- System response correction;
- Parasitic and drift removal by deconvolution.

A three stage digital filtering process was used to reject major spheric events and to reduce noise levels. Local spheric activity can produce sharp, large amplitude events that cannot be removed by conventional filtering procedures. Smoothing or stacking will reduce their amplitude but leave a broader residual response that can be confused with geological phenomena. To avoid this possibility, a computer algorithm searches out and rejects the major spheric events.

The signal to noise ratio was further improved by the application of a low pass linear digital filter. This filter has zero phase shift which prevents any lag or peak displacement from occurring, and it suppresses only variations with a wavelength less than about 1 second or 15 metres. This filter is a symmetrical 1 sec linear filter.

The results are presented as stacked profiles of EM voltages for the time gates, in linear - logarithmic scale for the B-field Z component and dB/dt responses in the Z and X components. B-field Z component time channel recorded at 0.110 milliseconds after the termination of the impulse is also presented as a colour image. Calculated Time Constant (TAU) with Calculated Vertical Derivative contours is presented in Appendix C and E. Resistivity Depth Image (RDI) is also presented in Appendix F

VTEM has two receiver coil orientations. Z-axis coil is oriented parallel to the transmitter coil axis and both are horizontal to the ground. The X-axis coil is oriented parallel to the ground and along the line-of-flight. This combined two coil configuration provides information on the position, depth, dip and thickness of a conductor. Generalized modeling results of VTEM max data are shown in Appendix D.

In general X-component data produce cross-over type anomalies: from “+ to -” in flight direction of flight for “thin” sub vertical targets and from “- to +” in direction of flight for “thick” targets. Z component data produce double peak type anomalies for “thin” sub vertical targets and single peak for “thick” targets.

The limits and change-over of “thin-thick” depends on dimensions of a TEM system (Appendix D, Figure D-16).

Because of X component polarity is under line-of-flight, convolution Fraser Filter (Figure 6) is applied to X component data to represent axes of conductors in the form of grid map. In this case positive FF anomalies always correspond to “plus-to-minus” X data crossovers independent of the flight direction.

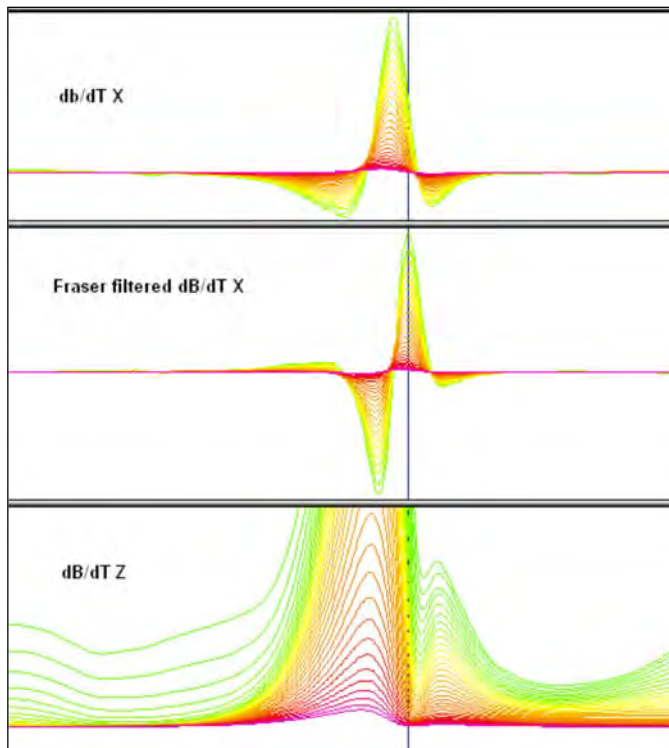


Figure 6: Z, X and Fraser filtered X (FFx) components for “thin” target.

### 4.3 HORIZONTAL MAGNETIC GRADIOMETER DATA

The horizontal gradients data from the VTEM™Plus are measured by two magnetometers 12.5 m apart on an independent bird mounted 10m above the VTEM™ loop. A GPS and a Gyro Inclinometer help to determine the positions and orientations of the magnetometers. The data from the two magnetometers are corrected for position and orientation variations, as well as for the diurnal variations using the base station data.

The position of the centre of the horizontal magnetic gradiometer bird is calculated from the GPS utilizing in-house processing tool in Geosoft. Following that total magnetic intensity is calculated at the center of the bird by calculating the mean values from both sensors. In addition to the total intensity advanced processing is done to calculate the in-line and cross-line (or lateral) horizontal gradient which enhance the understanding of magnetic targets. The in-line (longitudinal) horizontal gradient is calculated from the difference of two consecutive total magnetic field readings divided by the distance along the flight line direction, while the cross-line (lateral) horizontal magnetic gradient is calculated from the difference in the magnetic readings from both magnetic sensors divided by their horizontal separation.

Two advanced magnetic derivative products, the total horizontal derivative (THDR), and tilt angle derivative and are also created. The total horizontal derivative or gradient is defined as:

$THDR = \sqrt{H_x^2 + H_y^2}$ , where  $H_x$  and  $H_y$  are cross-line and in-line horizontal gradients.

The tilt angle derivative (TDR) is defined as:

$TDR = \arctan(V_z/THDR)$ , where THDR is the total horizontal derivative, and  $V_z$  is the vertical derivative.

Measured cross-line gradients can help to enhance cross-line linear features during gridding.

## 5. DELIVERABLES

### 5.1 SURVEY REPORT

The survey report describes the data acquisition, processing, and final presentation of the survey results. The survey report is provided in two paper copies and digitally in PDF format.

### 5.2 MAPS

Final maps were produced at scale of 1:10,000 for best representation of the survey size and line spacing. The coordinate/projection system used was NAD83 Datum, UTM Zone 17 North. All maps show the flight path trace and topographic data; latitude and longitude are also noted on maps.

The preliminary and final results of the survey are presented as EM profiles, a late-time gate gridded EM channel, and a colour magnetic TMI contour map.

- Maps at 1:10,000 in Geosoft MAP format, as follows:

GL160157_10k_dBdtz:	dB/dt profiles Z Component, Time Gates 0.220 – 7.036 ms in linear – logarithmic scale.
GL160157_10k_Bfieldz:	B-field profiles Z Component, Time Gates 0.220 – 7.036 ms in linear – logarithmic scale.
GL160157_10k_BFz15:	B-field Z Component Channel 15, Time Gate 0.110 ms colour image.
GL160157_10k_TMI:	Total magnetic intensity (TMI) colour image and contours.
GL160157_10k_TauSF:	dB/dt Calculated Time Constant (Tau) with Calculated Vertical Derivative contours
GL160157_10k_TotHGrad:	Magnetic Total Horizontal Gradient colour image.
GL160157_10k_TiltDrv:	Magnetic Tilt-Angle Derivative colour image.

- Maps are also presented in PDF format.
- The topographic data base was derived from 1:50,000 NRC (Natural Resources Canada) NTDB data, [www.geogratis.ca](http://www.geogratis.ca).
- A Google Earth file *GL160157\_FP.kml* showing the flight path of the block is included. Free versions of Google Earth software from: <http://earth.google.com/download-earth.html>

### 5.3 DIGITAL DATA

Two copies of the data and maps on DVD were prepared to accompany the report. Each DVD contains a digital file of the line data in GDB Geosoft Montaj format as well as the maps in Geosoft Montaj Map and PDF format.

- DVD structure.

**Data** contains databases, grids and maps, as described below.  
**Report** contains a copy of the report and appendices in PDF format.

Databases in Geosoft GDB format, containing the channels listed in Table 5.

**Table 5:** Geosoft GDB Data Format

Channel name	Units	Description
X:	metres	UTM Easting NAD83 Zone 17 North
Y:	metres	UTM Northing NAD83 Zone 17 North
Longitude:	Decimal Degrees	WGS 84 Longitude data
Latitude:	Decimal Degrees	WGS 84 Latitude data
Z:	metres	GPS antenna elevation (above Geoid)
Zb:	metres	EM bird elevation (above Geoid)
Radar:	metres	helicopter terrain clearance from radar altimeter
Radarb:	metres	Calculated EM transmitter-receiver loop terrain clearance from radar altimeter
DEM:	metres	Digital Elevation Model
Gtime:	Seconds of the day	GPS time
Mag1L:	nT	Measured Total Magnetic field data (left sensor)
Mag1R:	nT	Measured Total Magnetic field data (right sensor)
Basemag:	nT	Magnetic diurnal variation data
Mag2LZ:	nT	Z corrected (w.r.t. loop center) and diurnal corrected magnetic field left mag
Mag2RZ:	nT	Z corrected (w.r.t. loop center) and diurnal corrected magnetic field right mag
TMI2:	nT	Calculated from diurnal corrected total magnetic field intensity of the centre of the loop
TMI3:	nT	Microleveled total magnetic field intensity of the centre of the loop
Hginline:		Calculated in-line gradient
Hgcxline:		measured cross-line gradient
CVG:	nT/m	Calculated Magnetic Vertical Gradient
SFz[4]:	pV/(A*m <sup>4</sup> )	Z dB/dt 0.021 millisecond time channel
SFz[5]:	pV/(A*m <sup>4</sup> )	Z dB/dt 0.026 millisecond time channel
SFz[6]:	pV/(A*m <sup>4</sup> )	Z dB/dt 0.031 millisecond time channel
SFz[7]:	pV/(A*m <sup>4</sup> )	Z dB/dt 0.036 millisecond time channel
SFz[8]:	pV/(A*m <sup>4</sup> )	Z dB/dt 0.042 millisecond time channel
SFz[9]:	pV/(A*m <sup>4</sup> )	Z dB/dt 0.048 millisecond time channel
SFz[10]:	pV/(A*m <sup>4</sup> )	Z dB/dt 0.055 millisecond time channel
SFz[11]:	pV/(A*m <sup>4</sup> )	Z dB/dt 0.063 millisecond time channel
SFz[12]:	pV/(A*m <sup>4</sup> )	Z dB/dt 0.073 millisecond time channel
SFz[13]:	pV/(A*m <sup>4</sup> )	Z dB/dt 0.083 millisecond time channel
SFz[14]:	pV/(A*m <sup>4</sup> )	Z dB/dt 0.096 millisecond time channel

Channel name	Units	Description
SFz[15]:	pV/(A*m <sup>4</sup> )	Z dB/dt 0.110 millisecond time channel
SFz[16]:	pV/(A*m <sup>4</sup> )	Z dB/dt 0.126 millisecond time channel
SFz[17]:	pV/(A*m <sup>4</sup> )	Z dB/dt 0.145 millisecond time channel
SFz[18]:	pV/(A*m <sup>4</sup> )	Z dB/dt 0.167 millisecond time channel
SFz[19]:	pV/(A*m <sup>4</sup> )	Z dB/dt 0.192 millisecond time channel
SFz[20]:	pV/(A*m <sup>4</sup> )	Z dB/dt 0.220 millisecond time channel
SFz[21]:	pV/(A*m <sup>4</sup> )	Z dB/dt 0.253 millisecond time channel
SFz[22]:	pV/(A*m <sup>4</sup> )	Z dB/dt 0.290 millisecond time channel
SFz[23]:	pV/(A*m <sup>4</sup> )	Z dB/dt 0.333 millisecond time channel
SFz[24]:	pV/(A*m <sup>4</sup> )	Z dB/dt 0.383 millisecond time channel
SFz[25]:	pV/(A*m <sup>4</sup> )	Z dB/dt 0.440 millisecond time channel
SFz[26]:	pV/(A*m <sup>4</sup> )	Z dB/dt 0.505 millisecond time channel
SFz[27]:	pV/(A*m <sup>4</sup> )	Z dB/dt 0.580 millisecond time channel
SFz[28]:	pV/(A*m <sup>4</sup> )	Z dB/dt 0.667 millisecond time channel
SFz[29]:	pV/(A*m <sup>4</sup> )	Z dB/dt 0.766 millisecond time channel
SFz[30]:	pV/(A*m <sup>4</sup> )	Z dB/dt 0.880 millisecond time channel
SFz[31]:	pV/(A*m <sup>4</sup> )	Z dB/dt 1.010 millisecond time channel
SFz[32]:	pV/(A*m <sup>4</sup> )	Z dB/dt 1.161 millisecond time channel
SFz[33]:	pV/(A*m <sup>4</sup> )	Z dB/dt 1.333 millisecond time channel
SFz[34]:	pV/(A*m <sup>4</sup> )	Z dB/dt 1.531 millisecond time channel
SFz[35]:	pV/(A*m <sup>4</sup> )	Z dB/dt 1.760 millisecond time channel
SFz[36]:	pV/(A*m <sup>4</sup> )	Z dB/dt 2.021 millisecond time channel
SFz[37]:	pV/(A*m <sup>4</sup> )	Z dB/dt 2.323 millisecond time channel
SFz[38]:	pV/(A*m <sup>4</sup> )	Z dB/dt 2.667 millisecond time channel
SFz[39]:	pV/(A*m <sup>4</sup> )	Z dB/dt 3.063 millisecond time channel
SFz[40]:	pV/(A*m <sup>4</sup> )	Z dB/dt 3.521 millisecond time channel
SFz[41]:	pV/(A*m <sup>4</sup> )	Z dB/dt 4.042 millisecond time channel
SFz[42]:	pV/(A*m <sup>4</sup> )	Z dB/dt 4.641 millisecond time channel
SFz[43]:	pV/(A*m <sup>4</sup> )	Z dB/dt 5.333 millisecond time channel
SFz[44]:	pV/(A*m <sup>4</sup> )	Z dB/dt 6.125 millisecond time channel
SFz[45]:	pV/(A*m <sup>4</sup> )	Z dB/dt 7.036 millisecond time channel
SFz[46]:	pV/(A*m <sup>4</sup> )	Z dB/dt 8.083 millisecond time channel
SFx[20]:	pV/(A*m <sup>4</sup> )	X dB/dt 0.220 millisecond time channel
SFx[21]:	pV/(A*m <sup>4</sup> )	X dB/dt 0.253 millisecond time channel
SFx[22]:	pV/(A*m <sup>4</sup> )	X dB/dt 0.290 millisecond time channel
SFx[23]:	pV/(A*m <sup>4</sup> )	X dB/dt 0.333 millisecond time channel
SFx[24]:	pV/(A*m <sup>4</sup> )	X dB/dt 0.383 millisecond time channel
SFx[25]:	pV/(A*m <sup>4</sup> )	X dB/dt 0.440 millisecond time channel
SFx[26]:	pV/(A*m <sup>4</sup> )	X dB/dt 0.505 millisecond time channel
SFx[27]:	pV/(A*m <sup>4</sup> )	X dB/dt 0.580 millisecond time channel
SFx[28]:	pV/(A*m <sup>4</sup> )	X dB/dt 0.667 millisecond time channel
SFx[29]:	pV/(A*m <sup>4</sup> )	X dB/dt 0.766 millisecond time channel
SFx[30]:	pV/(A*m <sup>4</sup> )	X dB/dt 0.880 millisecond time channel
SFx[31]:	pV/(A*m <sup>4</sup> )	X dB/dt 1.010 millisecond time channel
SFx[32]:	pV/(A*m <sup>4</sup> )	X dB/dt 1.161 millisecond time channel
SFx[33]:	pV/(A*m <sup>4</sup> )	X dB/dt 1.333 millisecond time channel
SFx[34]:	pV/(A*m <sup>4</sup> )	X dB/dt 1.531 millisecond time channel
SFx[35]:	pV/(A*m <sup>4</sup> )	X dB/dt 1.760 millisecond time channel
SFx[36]:	pV/(A*m <sup>4</sup> )	X dB/dt 2.021 millisecond time channel
SFx[37]:	pV/(A*m <sup>4</sup> )	X dB/dt 2.323 millisecond time channel



Channel name	Units	Description
SFx[38]:	pV/(A*m <sup>4</sup> )	X dB/dt 2.667 millisecond time channel
SFx[39]:	pV/(A*m <sup>4</sup> )	X dB/dt 3.063 millisecond time channel
SFx[40]:	pV/(A*m <sup>4</sup> )	X dB/dt 3.521 millisecond time channel
SFx[41]:	pV/(A*m <sup>4</sup> )	X dB/dt 4.042 millisecond time channel
SFx[42]:	pV/(A*m <sup>4</sup> )	X dB/dt 4.641 millisecond time channel
SFx[43]:	pV/(A*m <sup>4</sup> )	X dB/dt 5.333 millisecond time channel
SFx[44]:	pV/(A*m <sup>4</sup> )	X dB/dt 6.125 millisecond time channel
SFx[45]:	pV/(A*m <sup>4</sup> )	X dB/dt 7.036 millisecond time channel
SFx[46]:	pV/(A*m <sup>4</sup> )	X dB/dt 8.083 millisecond time channel
BFz	(pV*ms)/(A*m <sup>4</sup> )	Z B-Field data for time channels 4 to 46
BFx	(pV*ms)/(A*m <sup>4</sup> )	X B-Field data for time channels 20 to 46
SFxFF:	pV/(A*m <sup>4</sup> )	Fraser Filtered X dB/dt
NchanBF:		Latest time channels of TAU calculation
TauBF:	ms	Time constant B-Field
NchanSF:		Latest time channels of TAU calculation
TauSF:	ms	Time constant dB/dt
PLM:		60 Hz power line monitor

Electromagnetic B-field and dB/dt Z component data is found in array channel format between indexes 4 – 46, and X component data from 20 – 46, as described above.

- Database of the Resistivity Depth Images in Geosoft GDB format, containing the following channels:

**Table 6:** Geosoft Resistivity Depth Image GDB Data Format

Channel name	Units	Description
Xg:	metres	UTM Easting NAD83 Zone 17 North
Yg:	metres	UTM Northing NAD83 Zone 17 North
Dist:	meters	Distance from the beginning of the line
Depth:	meters	array channel, depth from the surface
Z:	meters	array channel, depth from sea level
AppRes:	Ohm-m	array channel, Apparent Resistivity
TR:	meters	EM system height from sea level
Topo:	meters	digital elevation model
Radarb:	metres	Calculated EM transmitter-receiver loop terrain clearance from radar altimeter
SF:	pV/(A*m <sup>4</sup> )	array channel, dB/dT
MAG:	nT	TMI data
CVG:	nT/m	CVG data
DOI:	metres	Depth of Investigation: a measure of VTEM depth effectiveness
PLM:		60Hz Power Line Monitor

- Database of the VTEM Waveform “GL160157\_waveform\_final.gdb” in Geosoft GDB format, containing the following channels:

**Table 7:** Geosoft database for the VTEM waveform

Channel name	Units	Description
Time:	milliseconds	Sampling rate interval, 5.2083 microseconds
Tx_Current:	amps	Output current of the transmitter

- Grids in Geosoft GRD and GeoTIFF format, as follows:

BFz15:	B-Field Z Component Channel 15 (Time Gate 0.110 ms)
CVG:	Calculated Vertical Derivative (nT/m)
DEM:	Digital Elevation Model (metres)
Hgcxline:	Measured Cross-Line Gradient (nT/m)
Hginline:	Measured In-Line Gradient (nT/m)
PLM:	Power Line Monitor (60Hz)
SFxFF20:	Fraser Filtered dB/dt X Component Channel 20 (Time Gate 0.220ms)
SFz10:	dB/dt Z Component Channel 10 (Time Gate 0.055 ms)
SFz15:	dB/dt Z Component Channel 15 (Time Gate 0.110 ms)
SFz25:	dB/dt Z Component Channel 25 (Time Gate 0.440 ms)
TauBF:	B-Field Z Component, Calculated Time Constant (ms)
TauSF:	dB/dt Z Component, Calculated Time Constant (ms)
TiltDrv:	Magnetic Tilt derivative (radians)
TMI3:	Total Magnetic Intensity (nT)
TotalHgrad:	Magnetic Total Horizontal Gradient (nT/m)

A Geosoft .GRD file has a .GI metadata file associated with it, containing grid projection information. A grid cell size of 25 metres was used.

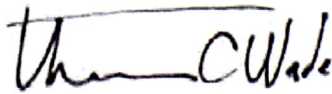
## 6. CONCLUSIONS AND RECOMMENDATIONS

A helicopter-borne versatile time domain electromagnetic (VTEMplus) and horizontal magnetic gradiometer geophysical survey has been completed over Detour West Project situated near Little Abitibi Lake, Ontario.

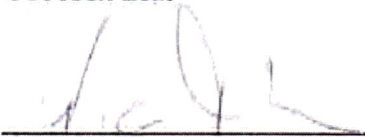
The total area coverage is 117 km<sup>2</sup>. Total survey line coverage 1235 line kilometres. The principal sensors included a Time Domain EM system and a horizontal magnetic gradiometer using two caesium magnetometers. Results have been presented as stacked profiles, and contour colour images at a scale of 1:10,000. A formal Interpretation has not been included or requested.

Based on the geophysical results obtained, a number of EM anomalies were identified across the properties. According to calculated TAU values, they correspond to very weak conductive targets. Most of these conductors have contacts with high magnetic gradient zones. According to the RDI sections, the conductive zones seem to be overburned layers. The top depths of these conductors are estimated to be from near surface to less than 100 meters.

Respectfully submitted<sup>2</sup>,



Thomas Wade  
**Geotech Ltd.**



Nick Venter  
**Geotech Ltd.**



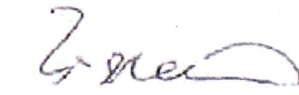
Geoffrey Plastow, P. Geo.  
Data Processing Manager  
**Geotech Ltd.**



November, 2016



Neil Fiset  
**Geotech Ltd.**

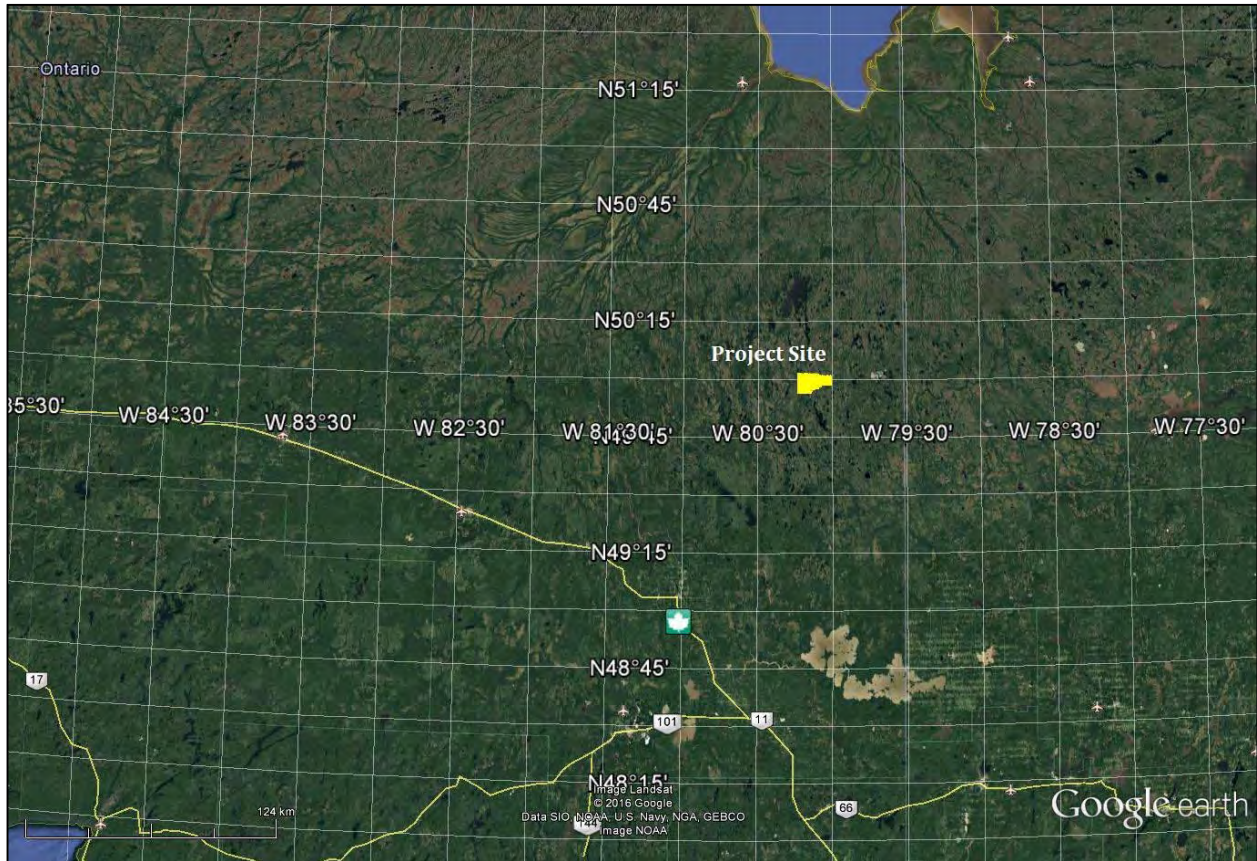


ZiHao Han  
**Geotech Ltd.**

<sup>2</sup> Final data processing of the EM and magnetic data were carried out by ZiHao Han, from the office of Geotech Ltd. in Aurora, Ontario, under the supervision of Geoffrey Plastow, P. Geo. Data Processing Manager.

# APPENDIX A

## SURVEY AREA LOCATION MAP



Overview of the Survey Area

## APPENDIX B

### SURVEY AREA COORDINATES

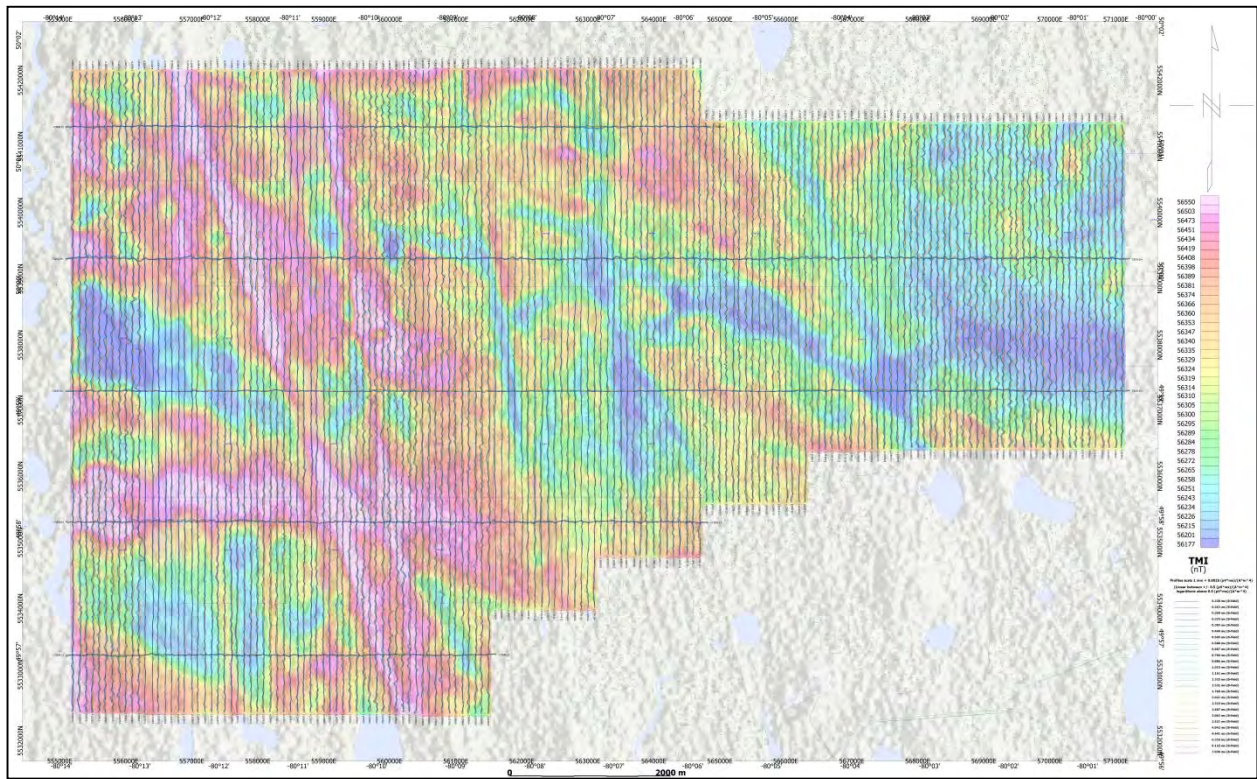
(WGS 84, UTM Zone 17 North)

#### Detour West

X	Y
555200	5542077
555200	5532485
561500	5532485
561564	5534085
563163	5534085
563200	5534880
564700	5534880
564800	5535680
566300	5535680
566400	5536481
571100	5536481
571100	5541285
564800	5541285
564700	5542077
555200	5542077

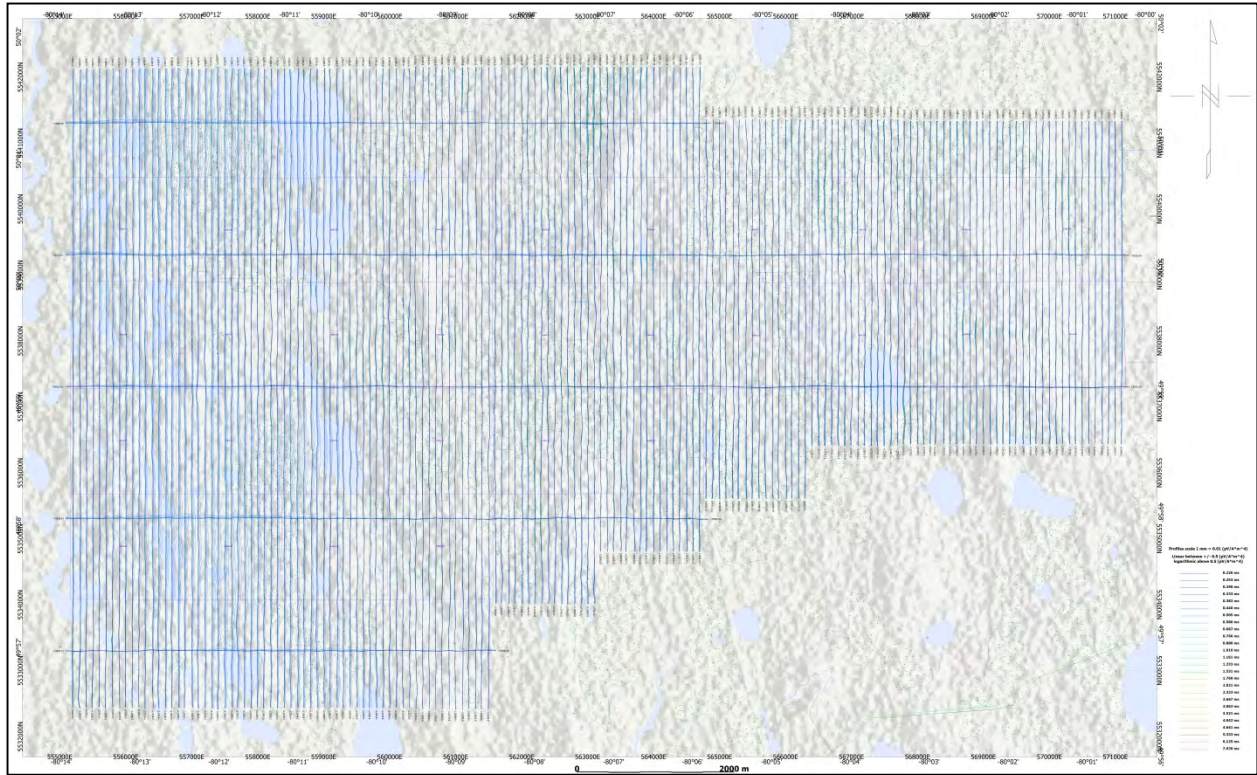
# APPENDIX C

## GEOPHYSICAL MAPS<sup>1</sup>

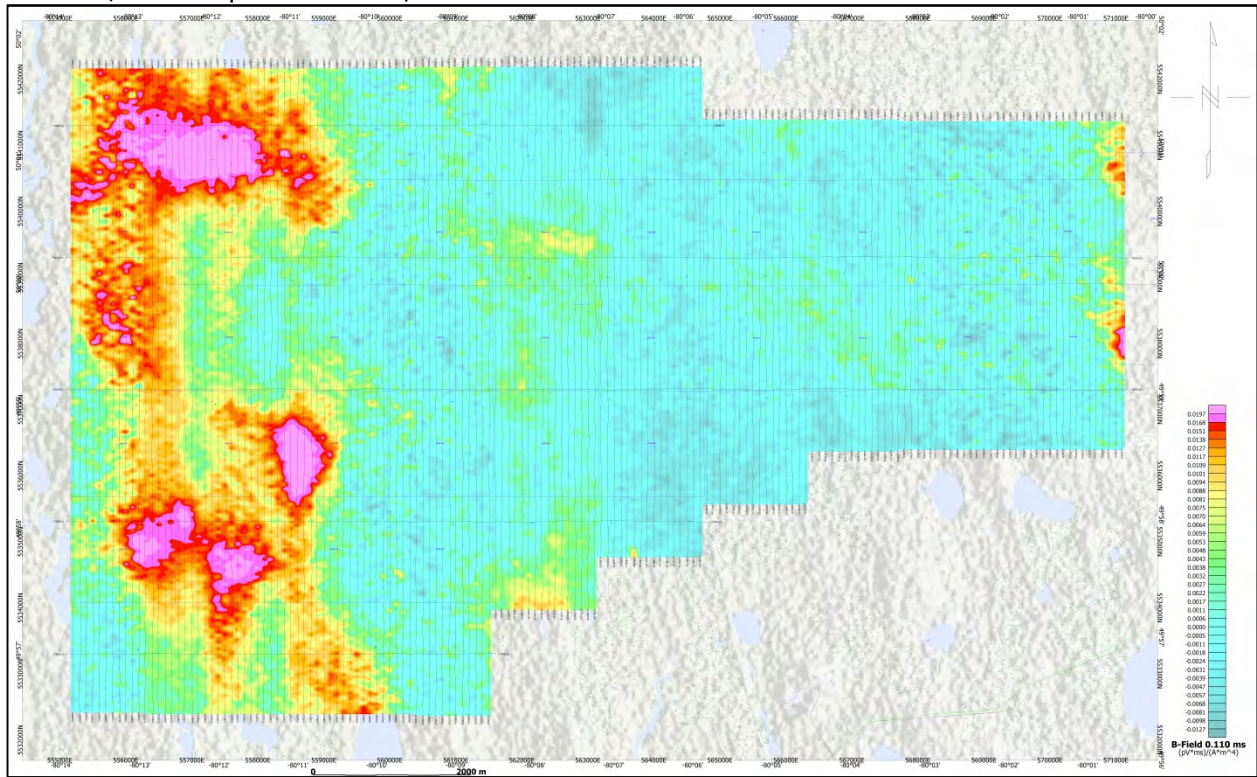


VTEM B-Field Z Component Profiles, Time Gates 0.220 to 7.036 ms

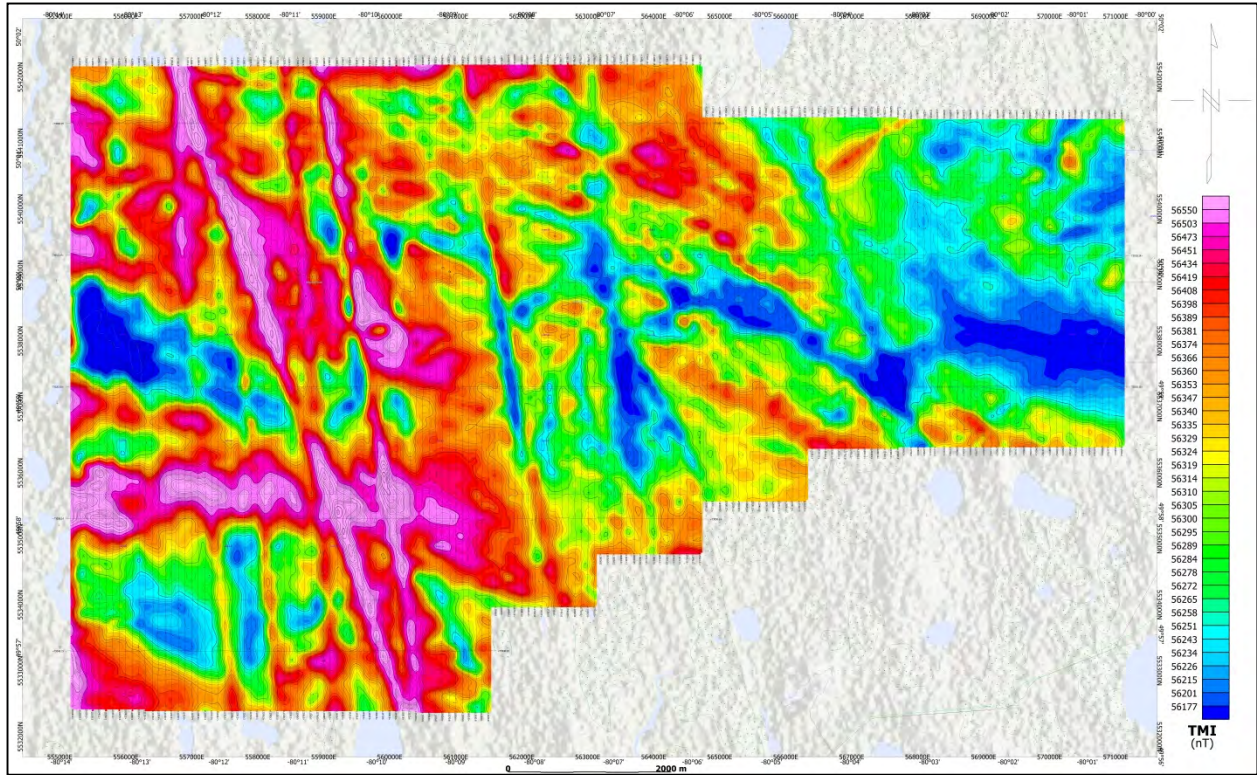
<sup>1</sup> Full size geophysical maps are also available in PDF format on the final DVD



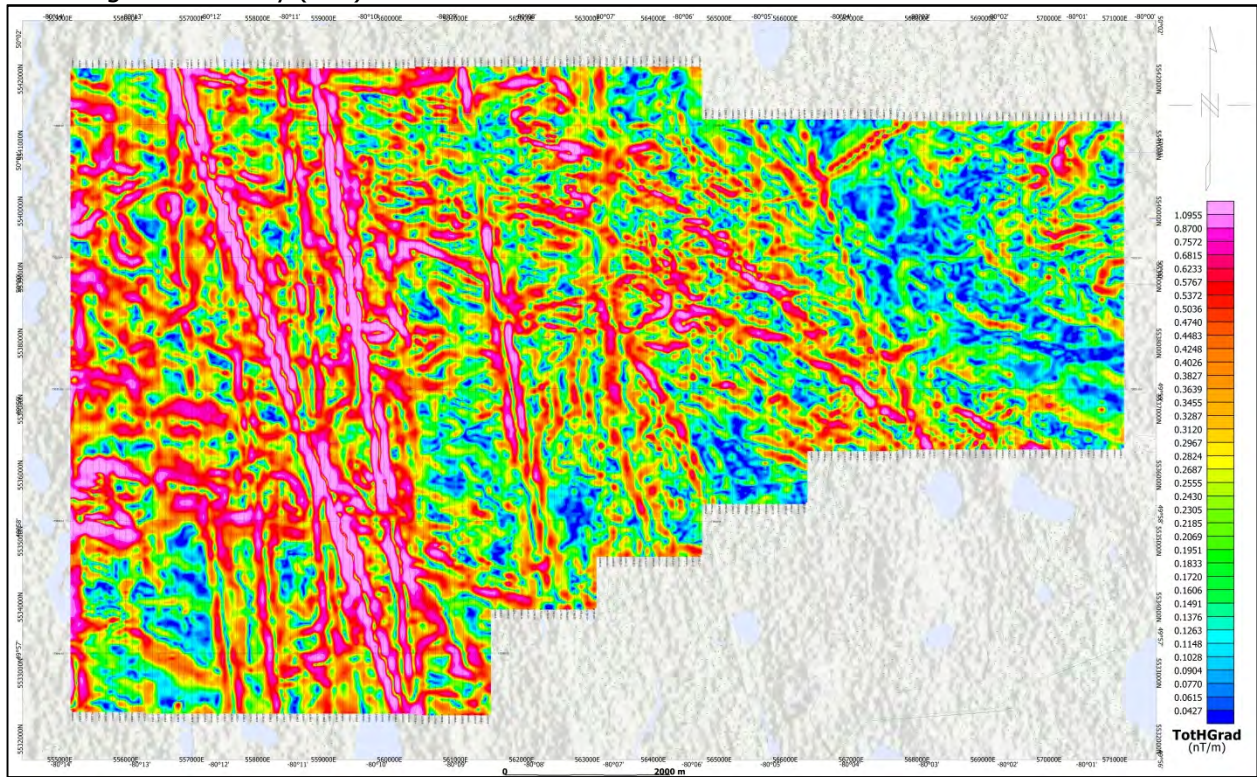
VTEM dB/dt Z Component Profiles, Time Gates 0.220 to 7.036 ms



VTEM B-Field Z Component Channel 15, Time Gate 0.110 ms

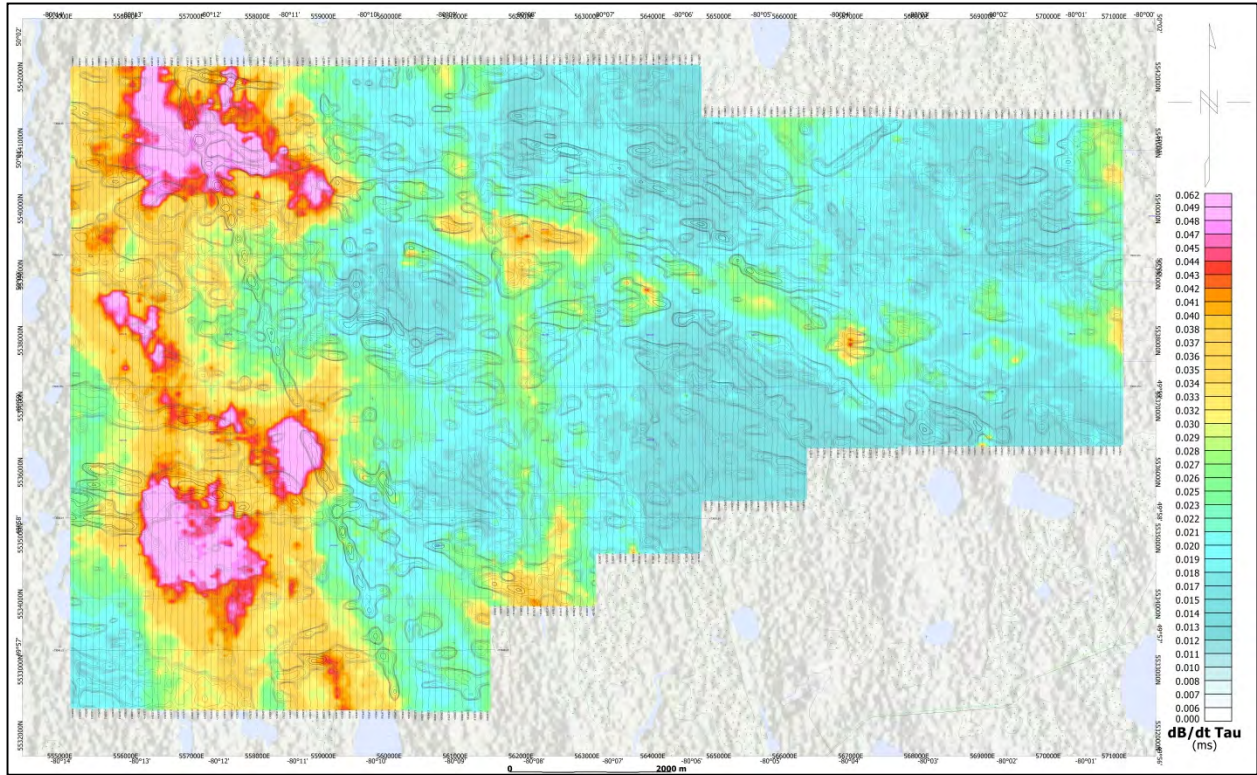


Total Magnetic Intensity (TMI)

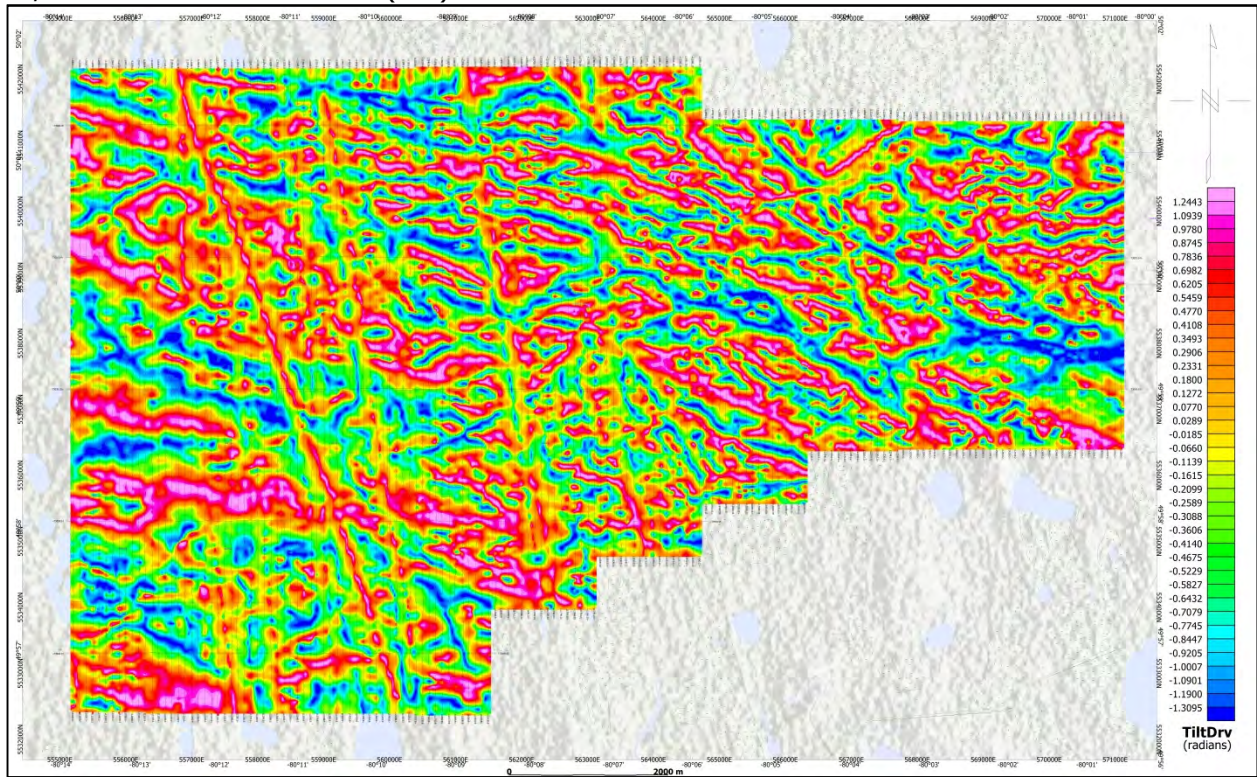


Magnetic Total Horizontal Gradient





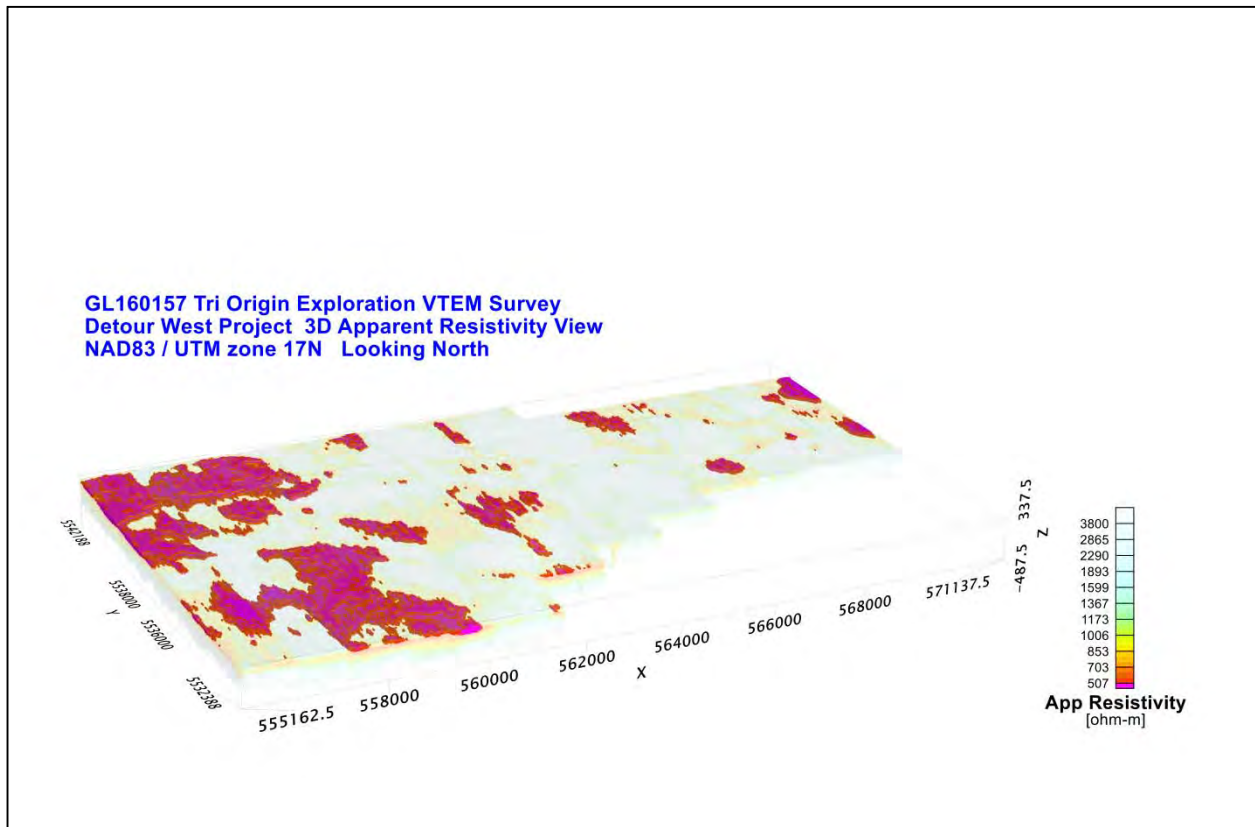
dB/dt Calculated Time Constant (Tau) with Calculated Vertical Derivative contours



Magnetic Tilt - Angle Derivative

## RESISTIVITY DEPTH IMAGE (RDI) MAPS

### 3D Resistivity-Depth Image (RDI)



## APPENDIX D

### GENERALIZED MODELING RESULTS OF THE VTEM SYSTEM INTRODUCTION

The VTEM system is based on a concentric or central loop design, whereby, the receiver is positioned at the centre of a transmitter loop that produces a primary field. The wave form is a bipolar, modified square wave with a turn-on and turn-off at each end.

During turn-on and turn-off, a time varying field is produced (dB/dt) and an electro-motive force (emf) is created as a finite impulse response. A current ring around the transmitter loop moves outward and downward as time progresses. When conductive rocks and mineralization are encountered, a secondary field is created by mutual induction and measured by the receiver at the centre of the transmitter loop.

Efficient modeling of the results can be carried out on regularly shaped geometries, thus yielding close approximations to the parameters of the measured targets. The following is a description of a series of common models made for the purpose of promoting a general understanding of the measured results.

A set of models has been produced for the Geotech VTEM® system dB/dT Z and X components (see models D1 to D15). The Maxwell™ modeling program (EMIT Technology Pty. Ltd. Midland, WA, AU) used to generate the following responses assumes a resistive half-space. The reader is encouraged to review these models, so as to get a general understanding of the responses as they apply to survey results. While these models do not begin to cover all possibilities, they give a general perspective on the simple and most commonly encountered anomalies.

As the plate dips and departs from the vertical position, the peaks become asymmetrical.

As the dip increases, the aspect ratio (Min/Max) decreases and this aspect ratio can be used as an empirical guide to dip angles from near 90° to about 30°. The method is not sensitive enough where dips are less than about 30°.

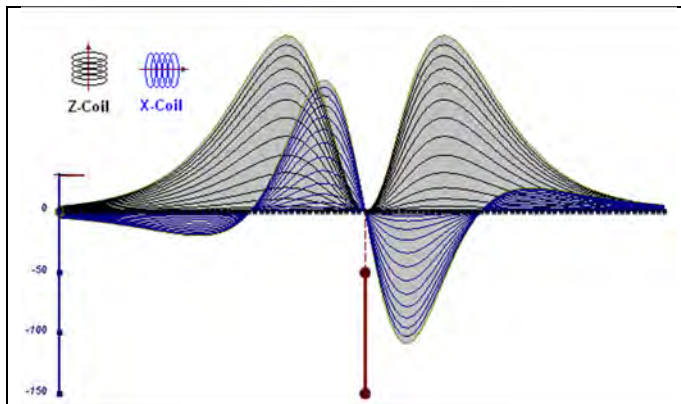


**Figure D-1:** vertical thin plate

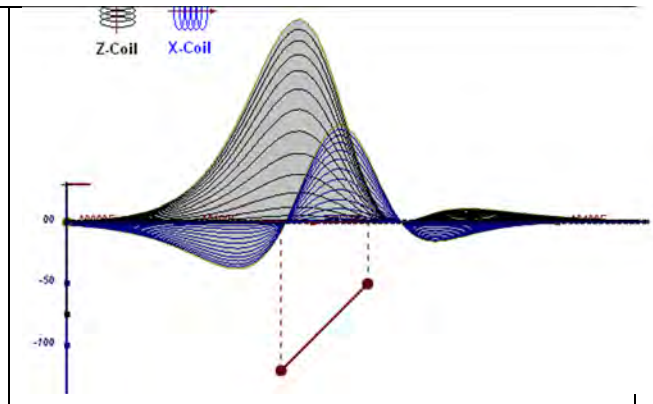


**Figure D-2:** inclined thin plate

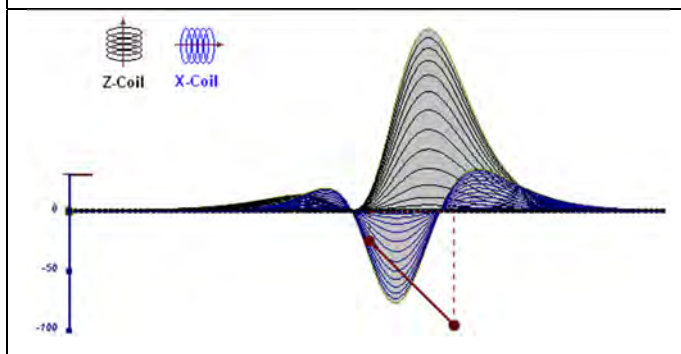


**Figure D-3:** inclined thin plate

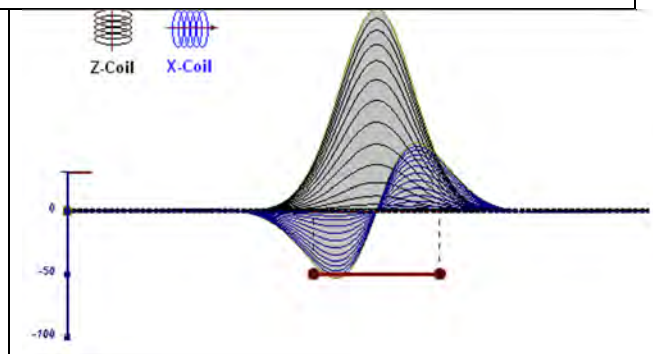


**Figure D-4:** horizontal thin plate

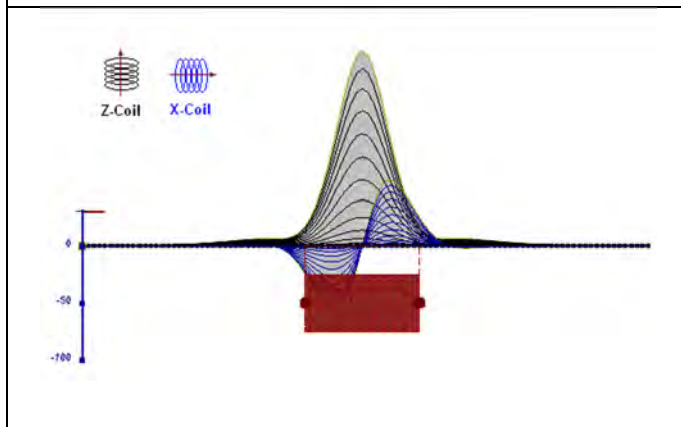


**Figure D-5:** horizontal thick plate (linear scale of the response)

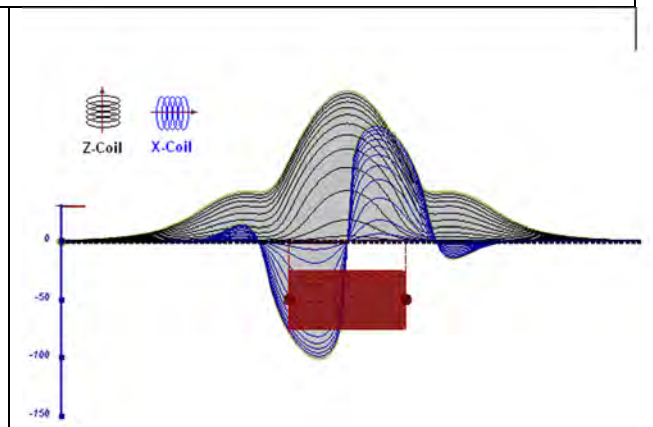


**Figure D-6:** horizontal thick plate (log scale of the response)

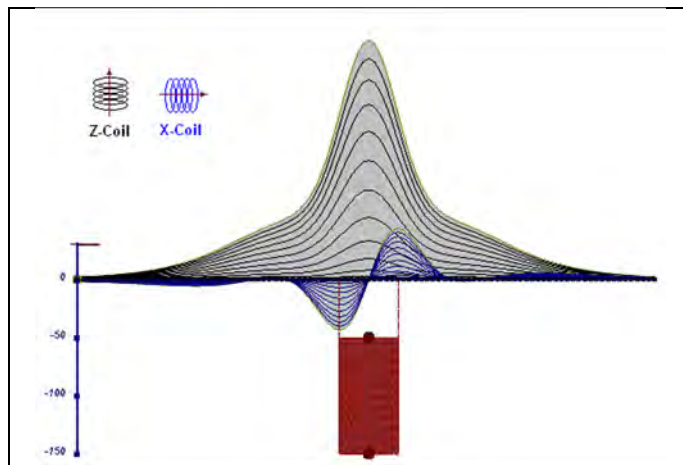


**Figure D-7:** vertical thick plate (linear scale of the response). 50 m depth

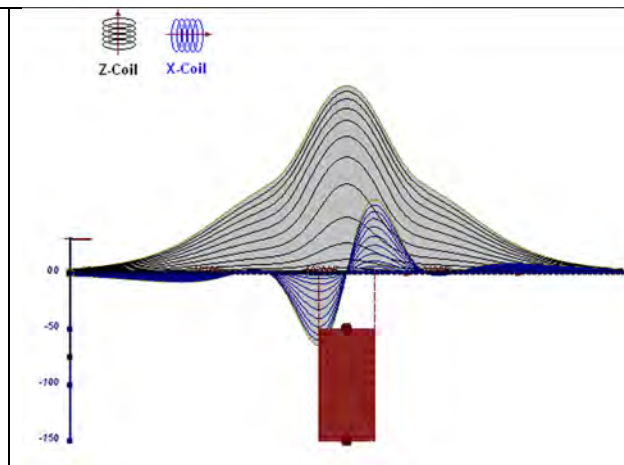


**Figure D-8:** vertical thick plate (log scale of the response). 50 m depth

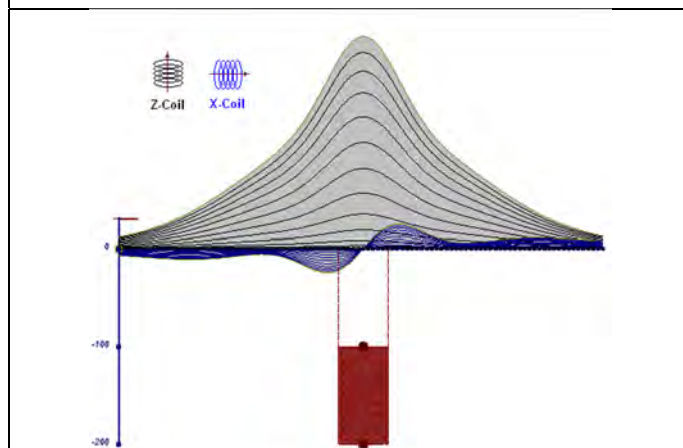


**Figure D-9:** vertical thick plate (linear scale of the response). 100 m depth

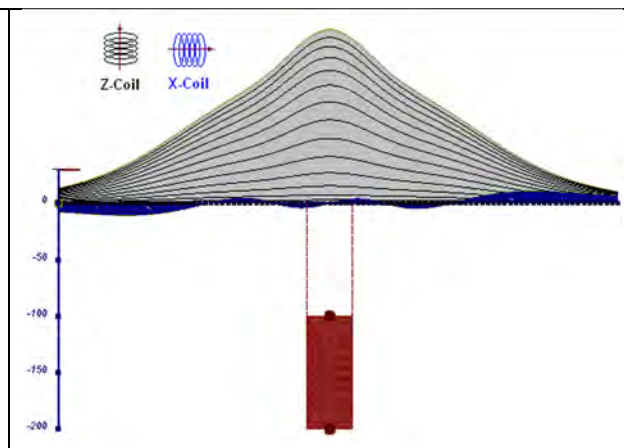


**Figure D-10:** vertical thick plate (linear scale of the response). Depth / horizontal thickness=2.5

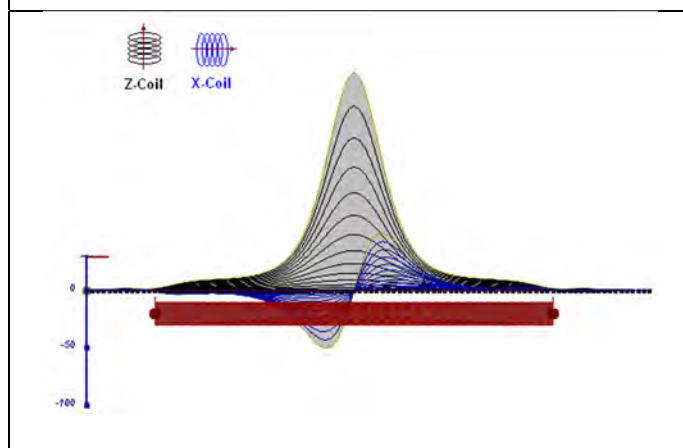


**Figure D-11:** horizontal thick plate (linear scale of the response)

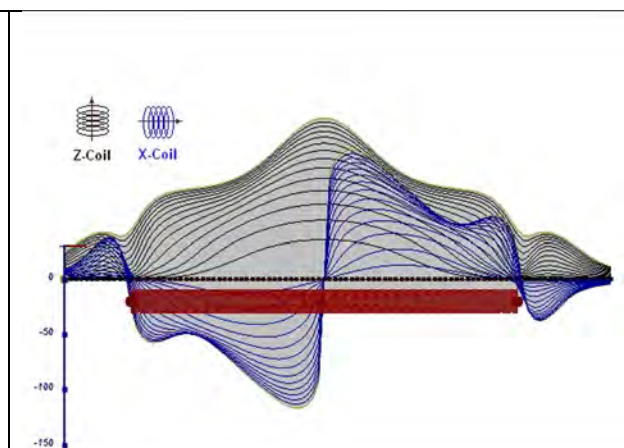


**Figure D-12:** horizontal thick plate (log scale of the response)

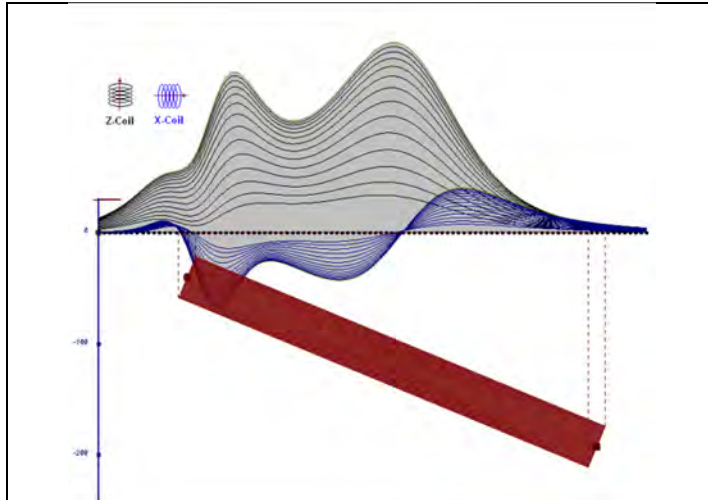


**Figure D-13:** inclined long thick plate

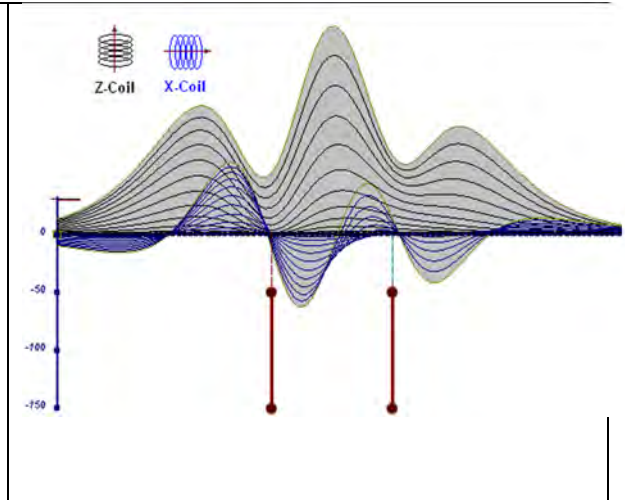


**Figure D-14:** two vertical thin plates

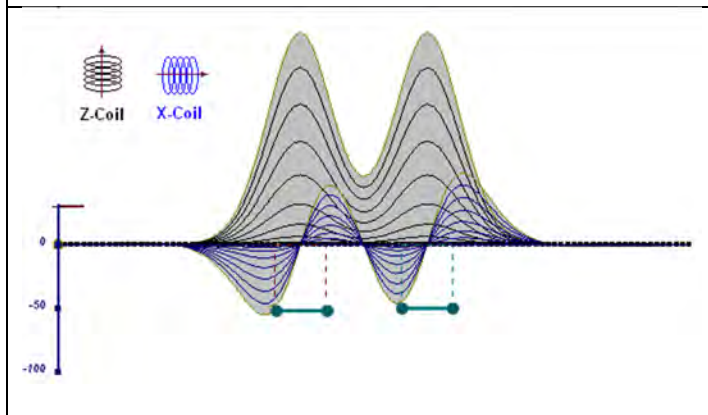


**Figure D-15:** two horizontal thin plates

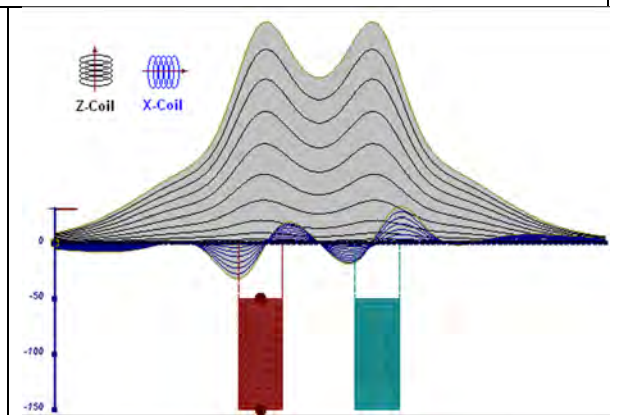


**Figure D-16:** two vertical thick plates

The same type of target but with different thickness, for example, creates different form of the response:

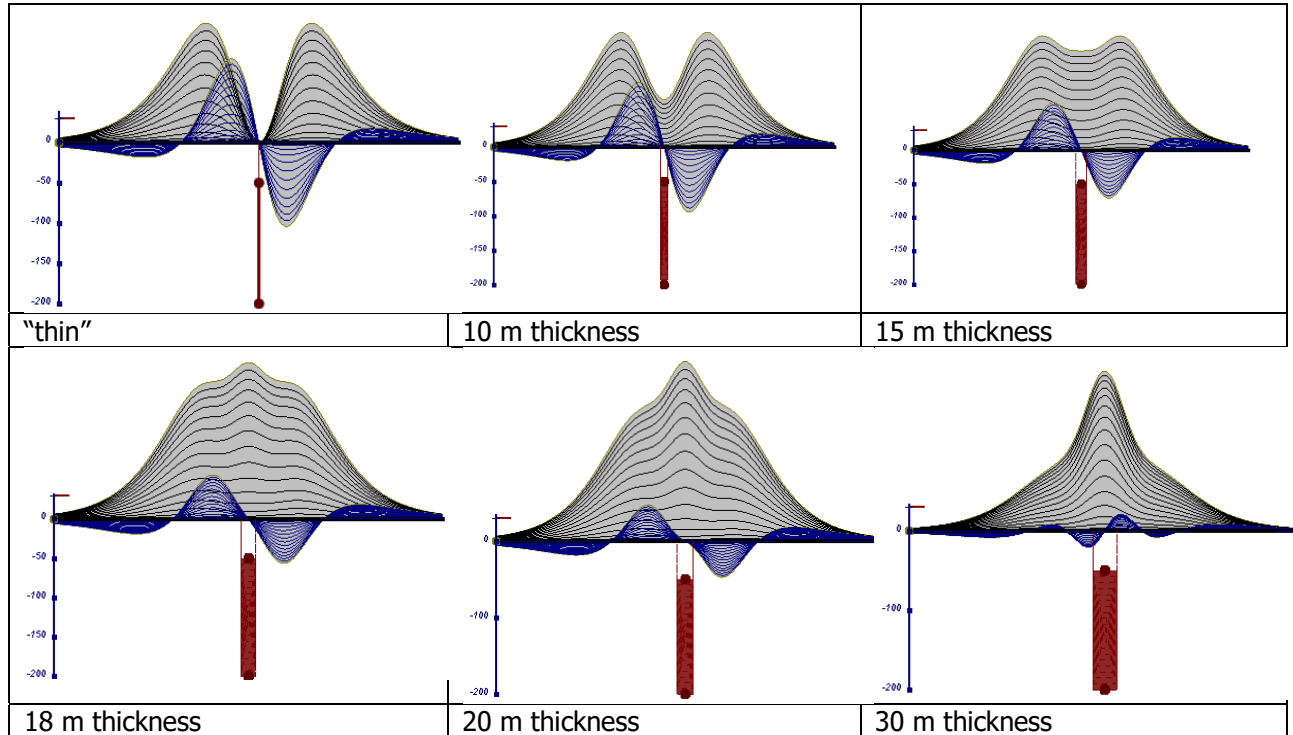


**Figure D-17:** Conductive vertical plate, depth 50 m, strike length 200 m, depth extends 150 m.

Alexander Prikhodko, PhD, P.Ge  
**Geotech Ltd.**

September 2010

## APPENDIX E

### EM TIME CONSTANT (TAU) ANALYSIS

Estimation of time constant parameter<sup>1</sup> in transient electromagnetic method is one of the steps toward the extraction of the information about conductances beneath the surface from TEM measurements.

The most reliable method to discriminate or rank conductors from overburden, background or one and other is by calculating the EM field decay time constant (TAU parameter), which directly depends on conductance despite their depth and accordingly amplitude of the response.

### THEORY

As established in electromagnetic theory, the magnitude of the electro-motive force (emf) induced is proportional to the time rate of change of primary magnetic field at the conductor. This emf causes eddy currents to flow in the conductor with a characteristic transient decay, whose Time Constant (Tau) is a function of the conductance of the survey target or conductivity and geometry (including dimensions) of the target. The decaying currents generate a proportional secondary magnetic field, the time rate of change of which is measured by the receiver coil as induced voltage during the Off time.

The receiver coil output voltage ( $e_0$ ) is proportional to the time rate of change of the secondary magnetic field and has the form,

$$e_0 \propto (1 / \tau) e^{-(t/\tau)}$$

Where,

$\tau = L/R$  is the characteristic time constant of the target (TAU)

R = resistance

L = inductance

From the expression, conductive targets that have small value of resistance and hence large value of  $\tau$  yield signals with small initial amplitude that decays relatively slowly with progress of time. Conversely, signals from poorly conducting targets that have large resistance value and small  $\tau$ , have high initial amplitude but decay rapidly with time<sup>1</sup> (Fig. E1).

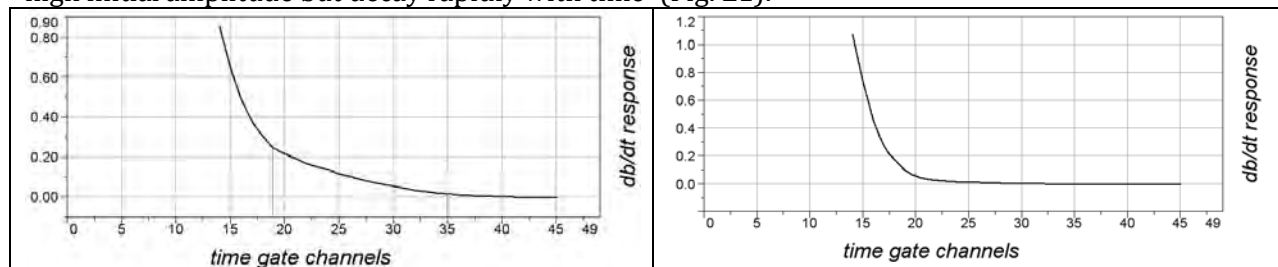


Figure E-1: Left – presence of good conductor, right – poor conductor.

<sup>1</sup> McNeill, JD, 1980, "Applications of Transient Electromagnetic Techniques", Technical Note TN-7 page 5, Geonics Limited, Mississauga, Ontario.



## EM Time Constant (Tau) Calculation

The EM Time-Constant (TAU) is a general measure of the speed of decay of the electromagnetic response and indicates the presence of eddy currents in conductive sources as well as reflecting the “conductance quality” of a source. Although TAU can be calculated using either the measured dB/dt decay or the calculated B-field decay, dB/dt is commonly preferred due to better stability (S/N) relating to signal noise. Generally, TAU calculated on base of early time response reflects both near surface overburden and poor conductors whereas, in the late ranges of time, deep and more conductive sources, respectively. For example early time TAU distribution in an area that indicates conductive overburden is shown in Figure 2.

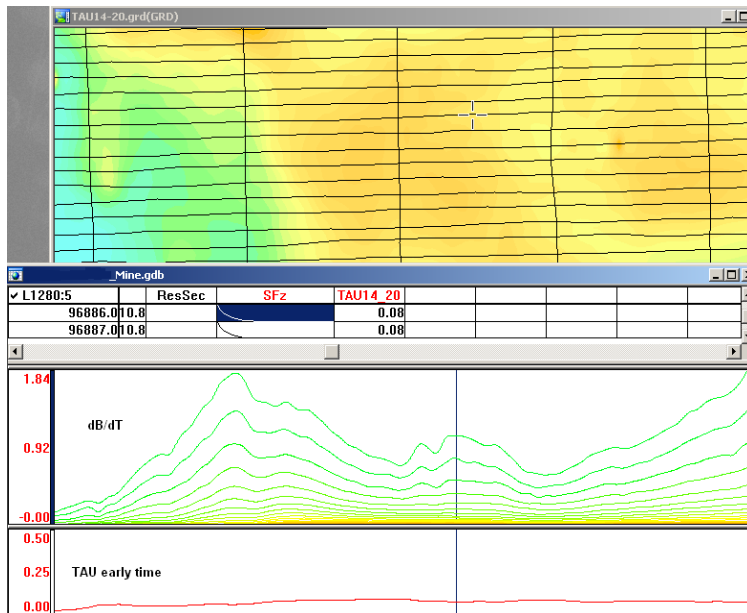


Figure E-2: Map of early time TAU. Area with overburden conductive layer and local sources.

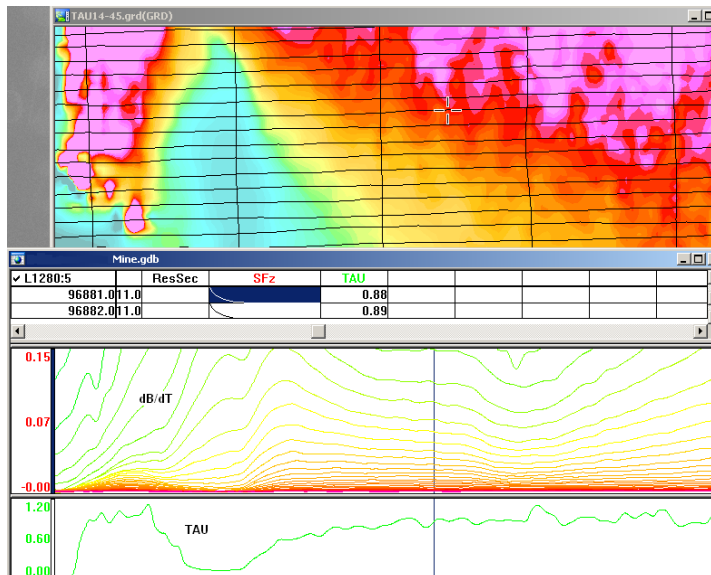


Figure E-3: Map of full time range TAU with EM anomaly due to deep highly conductive target.

There are many advantages of TAU maps:

- TAU depends only on one parameter (conductance) in contrast to response magnitude;
- TAU is integral parameter, which covers time range and all conductive zones and targets are displayed independently of their depth and conductivity on a single map.
- Very good differential resolution in complex conductive places with many sources with different conductivity.
- Signs of the presence of good conductive targets are amplified and emphasized independently of their depth and level of response accordingly.

In the example shown in Figure 4 and 5, three local targets are defined, each of them with a different depth of burial, as indicated on the resistivity depth image (RDI). All are very good conductors but the deeper target (number 2) has a relatively weak dB/dt signal yet also features the strongest total TAU (Figure 4). This example highlights the benefit of TAU analysis in terms of an additional target discrimination tool.

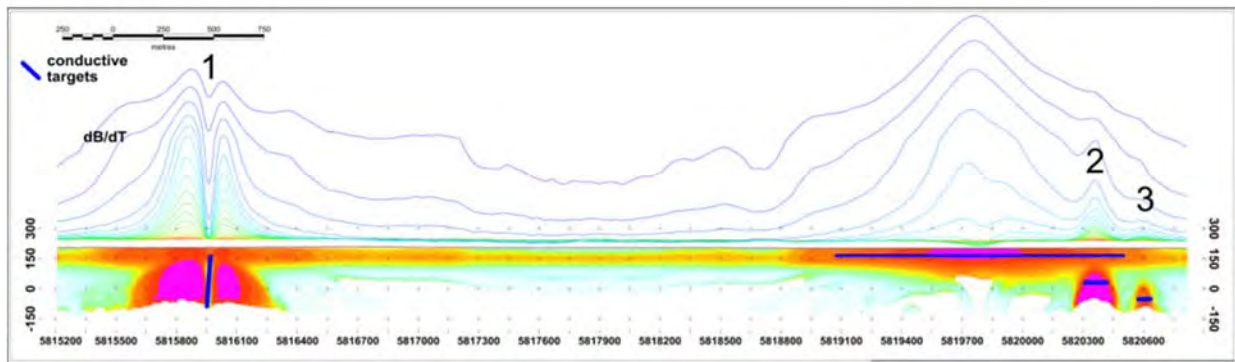


Figure E-4: dB/dt profile and RDI with different depths of targets.

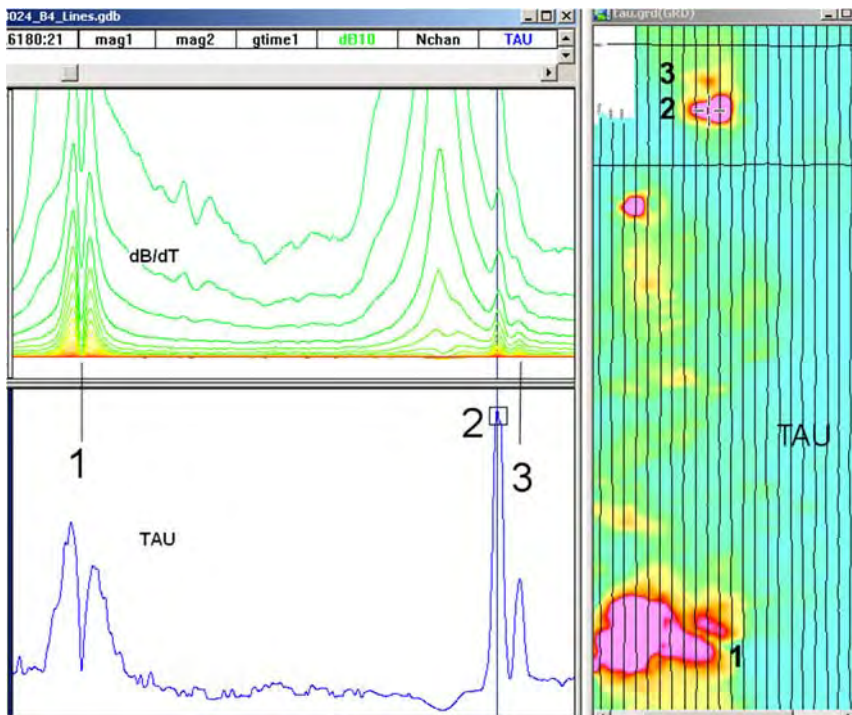


Figure E-5: Map of total TAU and dB/dt profile.

The EM Time Constants for dB/dt and B-field were calculated using the “sliding Tau” in-house program developed at Geotech2. The principle of the calculation is based on using of time window (4 time channels) which is sliding along the curve decay and looking for latest time channels which have a response above the level of noise and decay. The EM decays are obtained from all available decay channels, starting at the latest channel. Time constants are taken from a least square fit of a straight-line (log/linear space) over the last 4 gates above a pre-set signal threshold level (Figure F6). Threshold settings are pointed in the “label” property of TAU database channels. The sliding Tau method determines that, as the amplitudes increase, the time-constant is taken at progressively later times in the EM decay. Conversely, as the amplitudes decrease, Tau is taken at progressively earlier times in the decay. If the maximum signal amplitude falls below the threshold, or becomes negative for any of the 4 time gates, then Tau is not calculated and is assigned a value of “dummy” by default.

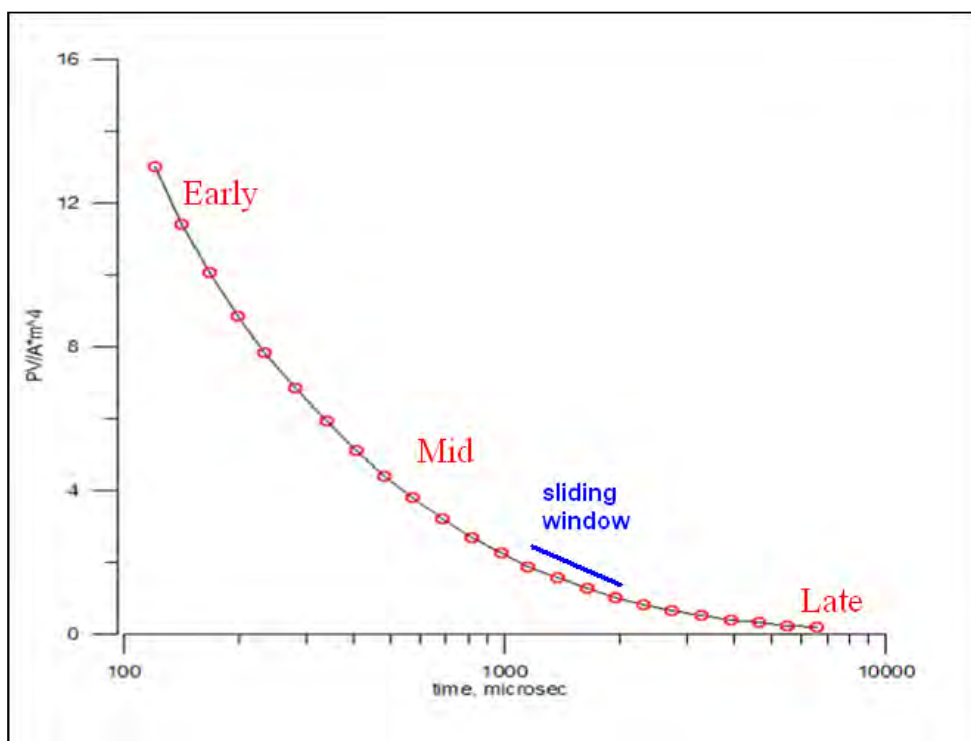


Figure E-6: Typical dB/dt decays of Vtem data

Alexander Prikhodko, PhD, P.Ge  
**Geotech Ltd.**

September 2010

<sup>2</sup> by A.Prikhodko

## APPENDIX F

### TEM RESISTIVITY DEPTH IMAGING (RDI)

Resistivity depth imaging (RDI) is a technique used to rapidly convert EM profile decay data into an equivalent resistivity versus depth cross-section, by deconvolving the measured TEM data. The used RDI algorithm of Resistivity-Depth transformation is based on the scheme of the apparent resistivity transform of Maxwell A. Meju (1998)<sup>1</sup> and TEM response from a conductive half-space. The program is developed by Alexander Prikhodko and is depth-calibrated based on forward plate modeling for VTEM system configuration (Fig. 1-10).

RDIs provide reasonable indications of conductor relative depth and vertical extent, as well as accurate 1D layered-earth apparent conductivity/resistivity structure across VTEM flight lines. Approximate depth of investigation of a TEM system, image of secondary field distribution in half-space, effective resistivity, initial geometry and position of conductive targets is the information obtained on the basis of the RDIs.

Maxwell forward modeling with RDI sections from the synthetic responses (VTEM system).

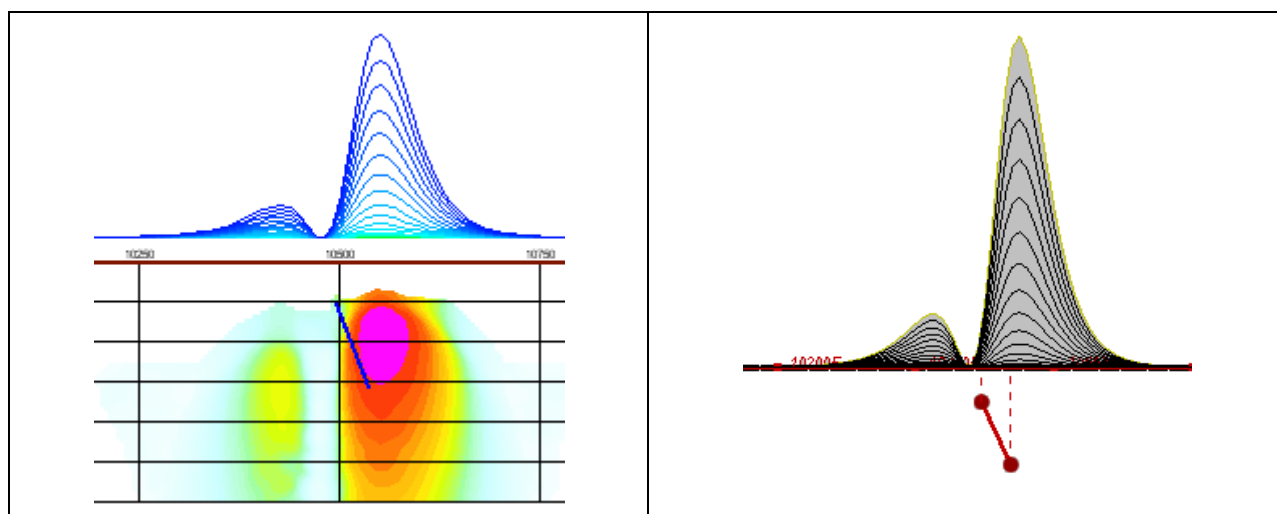


**Figure F-1:** Maxwell plate model and RDI from the calculated response for a conductive “thin” plate (depth 50 m, dip 65 degree, depth extend 100 m).

<sup>1</sup> Maxwell A. Meju, 1998, Short Note: A simple method of transient electromagnetic data analysis, *Geophysics*, **63**, 405–410.

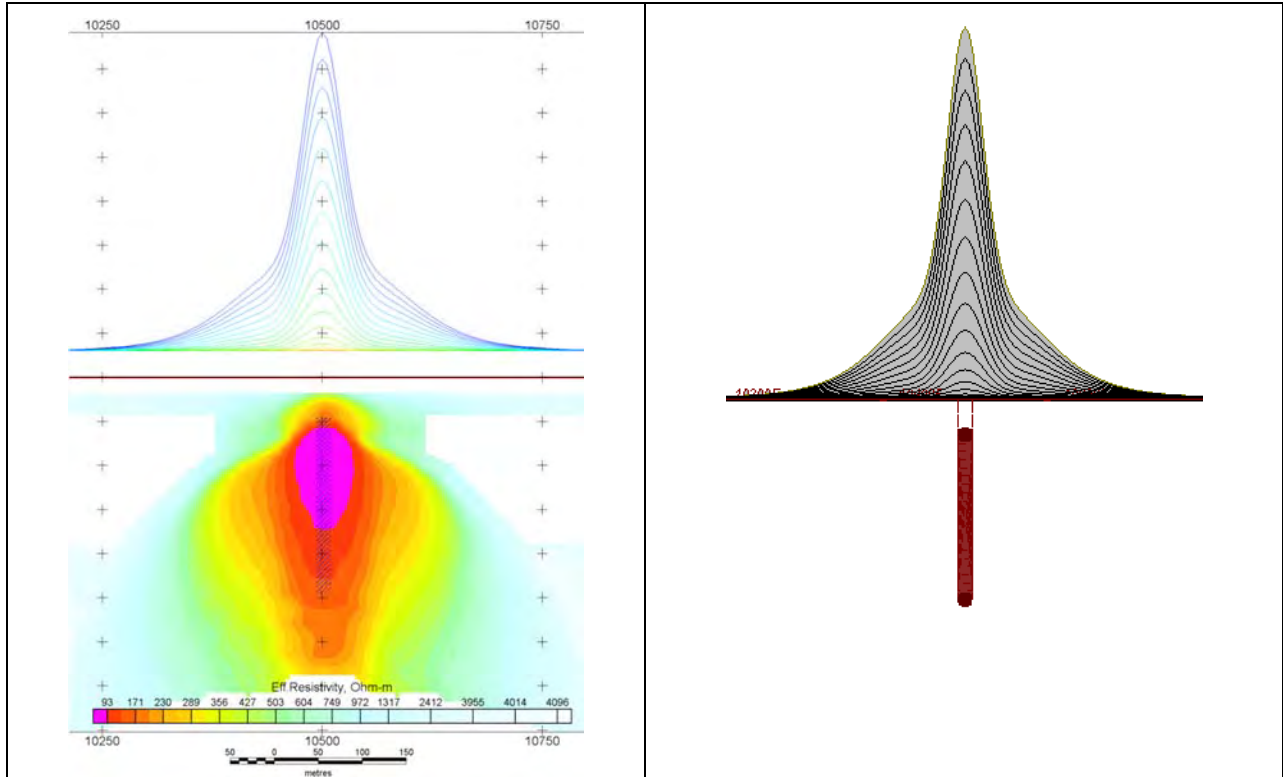


Figure F-2: Maxwell plate model and RDI from the calculated response for "thick" plate 18 m thickness, depth 50 m, depth extend 200 m).

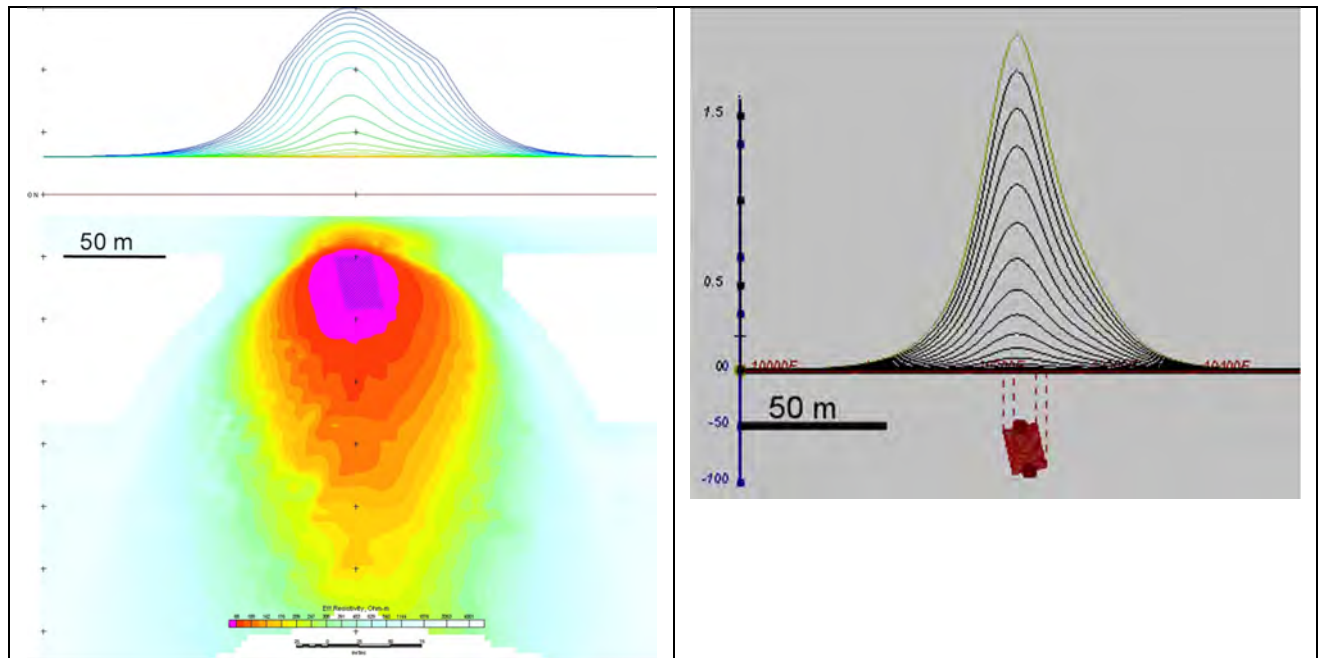


Figure F-3: Maxwell plate model and RDI from the calculated response for bulk ("thick") 100 m length, 40 m depth extend, 30 m thickness

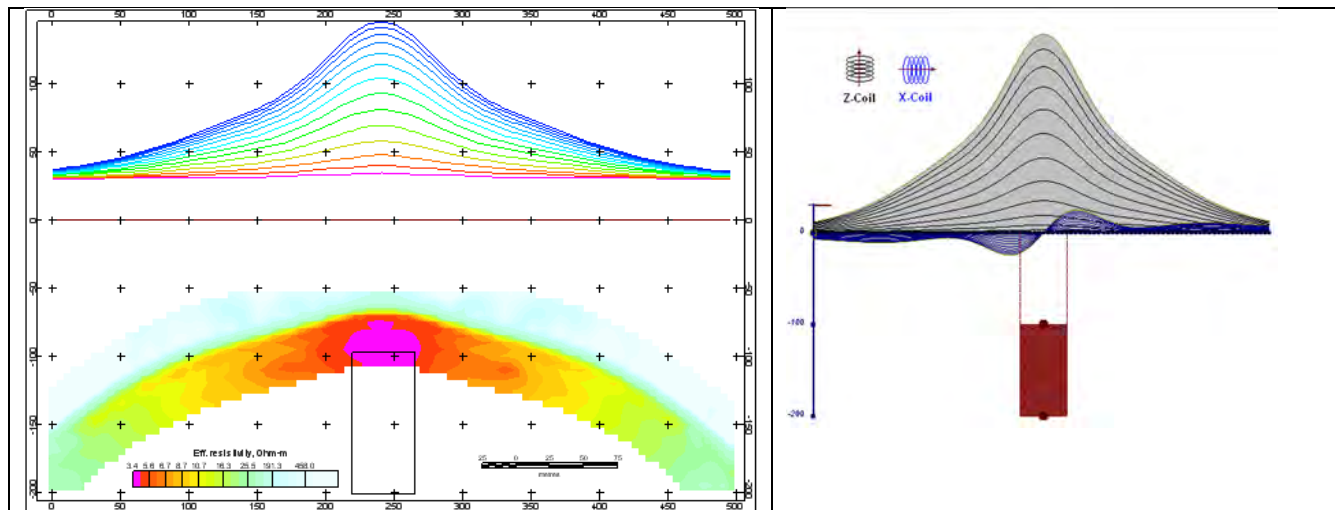


Figure F-4: Maxwell plate model and RDI from the calculated response for "thick" vertical target (depth 100 m, depth extend 100 m). 19-44 chan.

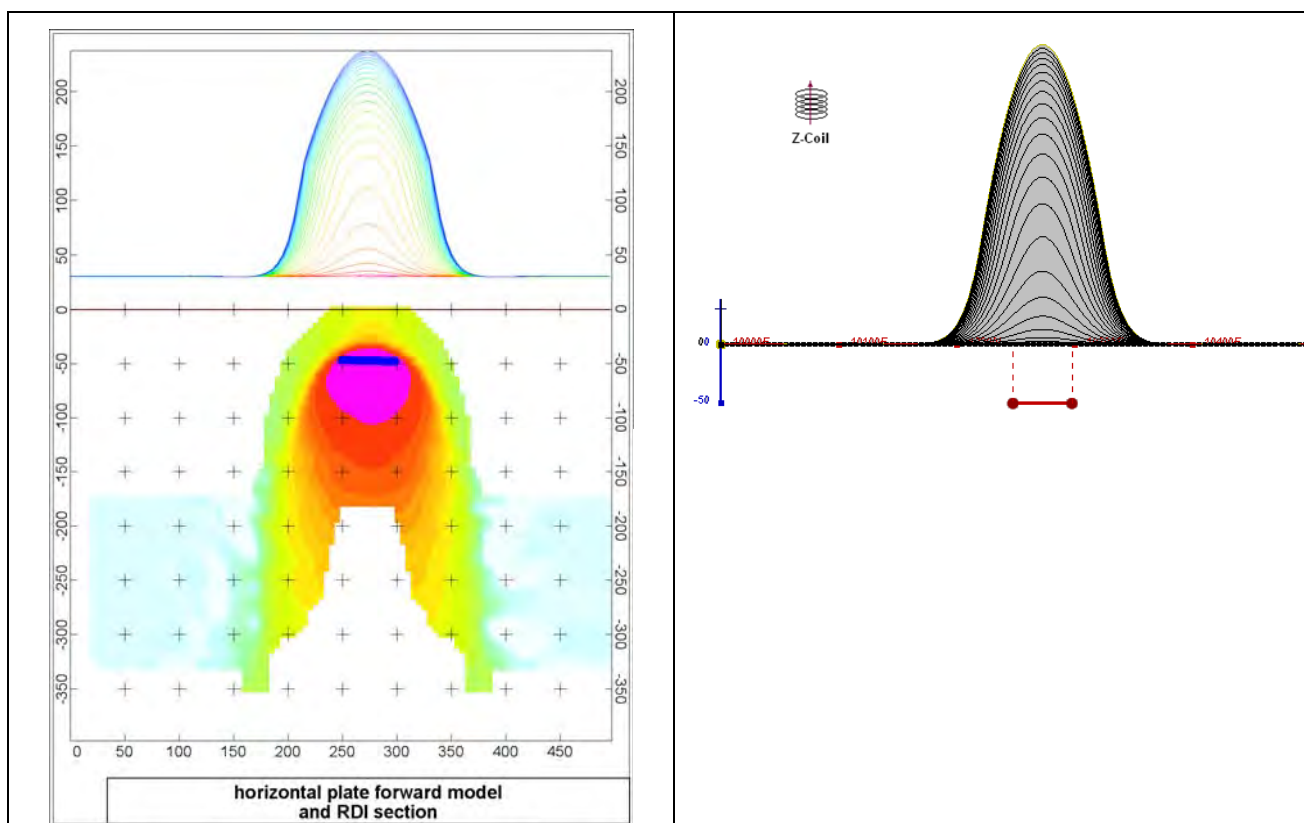


Figure F-5: Maxwell plate model and RDI from the calculated response for horizontal thin plate (depth 50 m, dim 50x100 m). 15-44 chan.

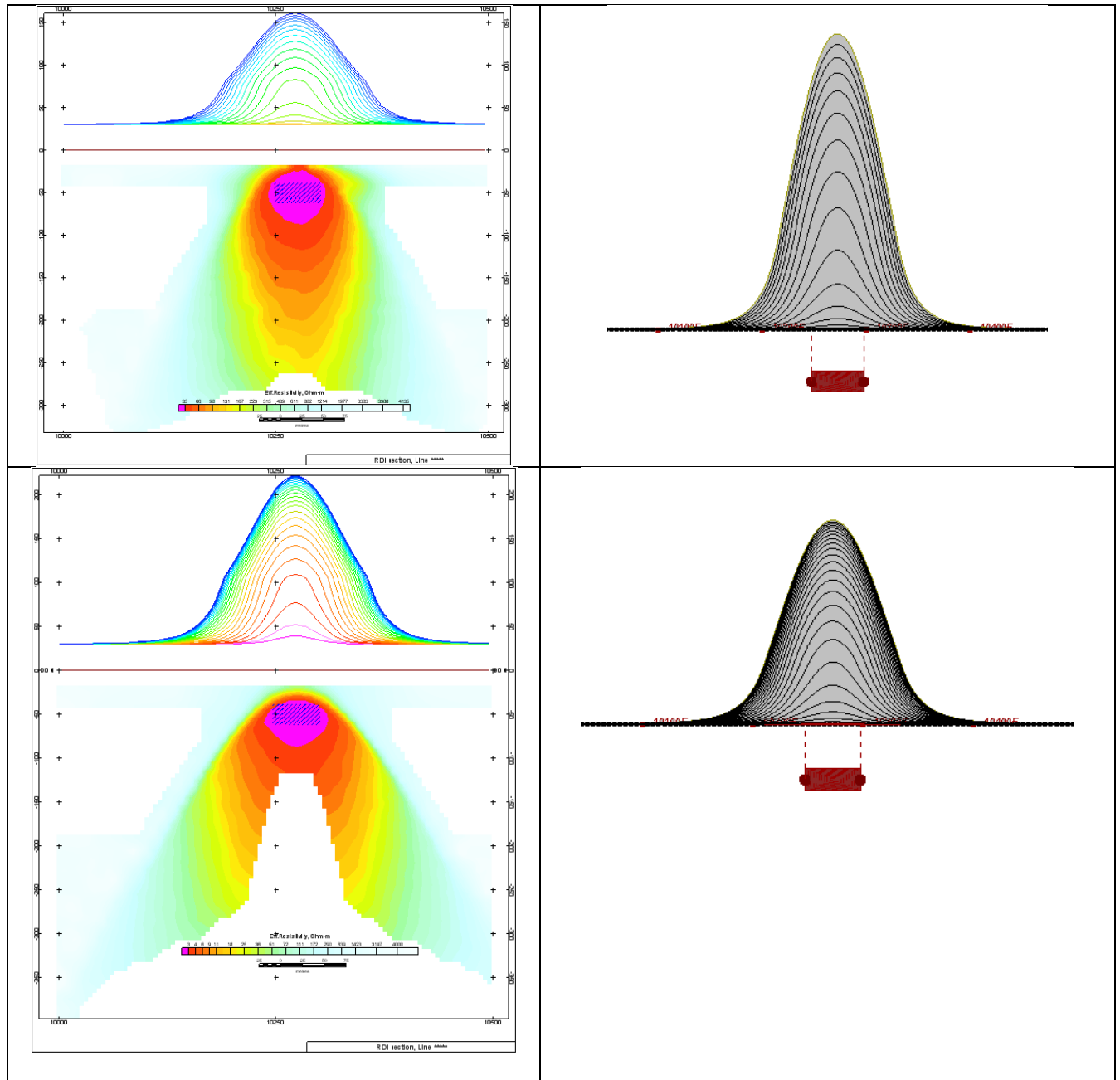


Figure F-6: Maxwell plate model and RDI from the calculated response for horizontal thick (20m) plate – less conductive (on the top), more conductive (below).

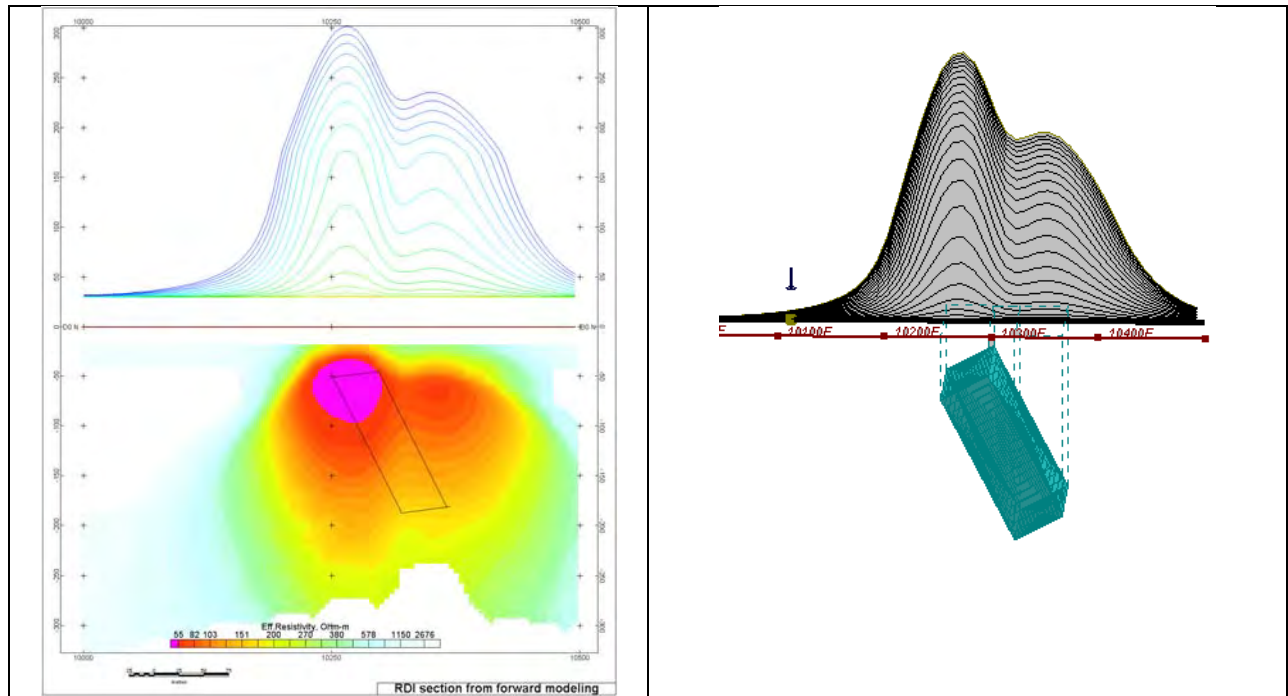


Figure F-7: Maxwell plate model and RDI from the calculated response for inclined thick (50m) plate. Depth extends 150 m, depth to the target 50 m.

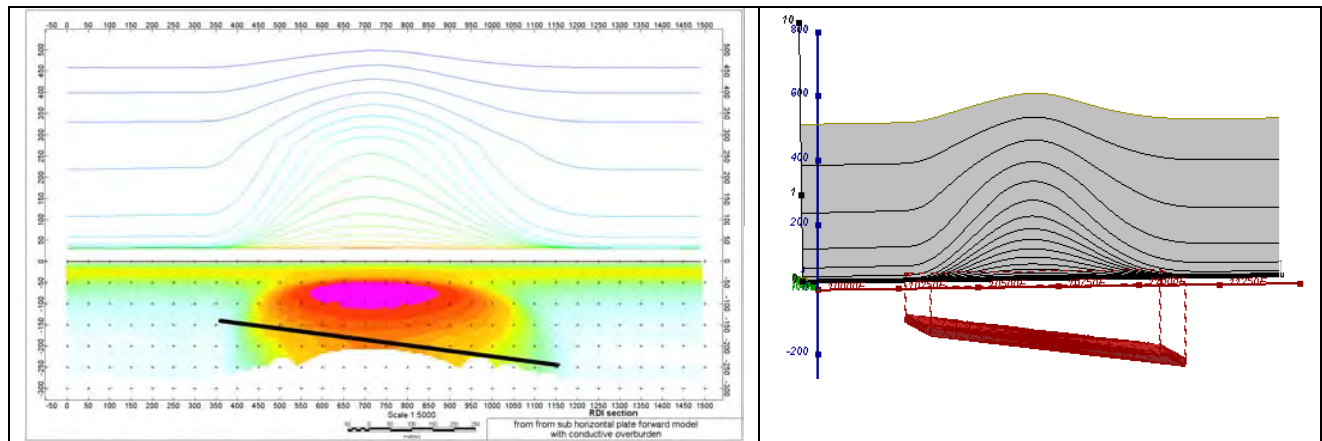


Figure F-8: Maxwell plate model and RDI from the calculated response for the long, wide and deep subhorizontal plate (depth 140 m, dim 25x500x800 m) with conductive overburden.



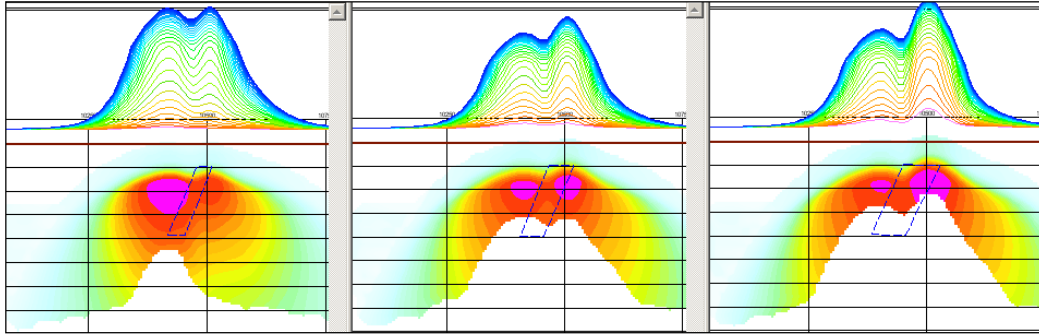


Figure F-9: Maxwell plate models and RDIs from the calculated response for "thick" dipping plates (35, 50, 75 m thickness), depth 50 m, conductivity 2.5 S/m.

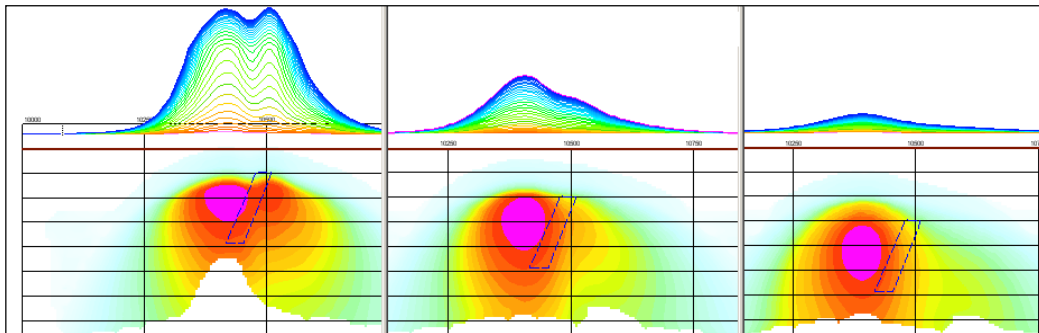


Figure F-10: Maxwell plate models and RDIs from the calculated response for "thick" (35 m thickness) dipping plate on different depth (50, 100, 150 m), conductivity 2.5 S/m.

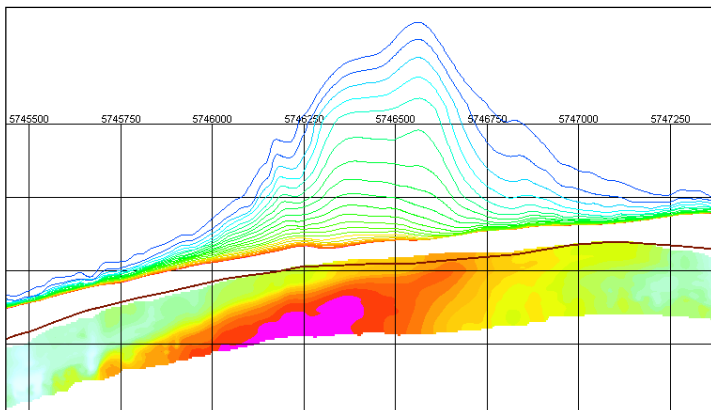
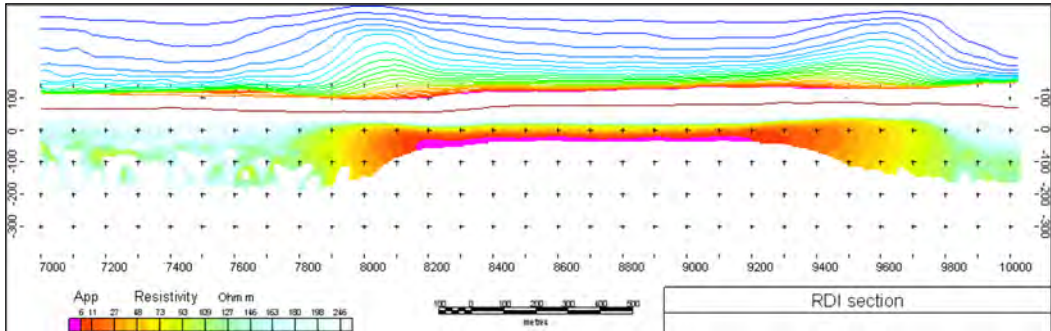
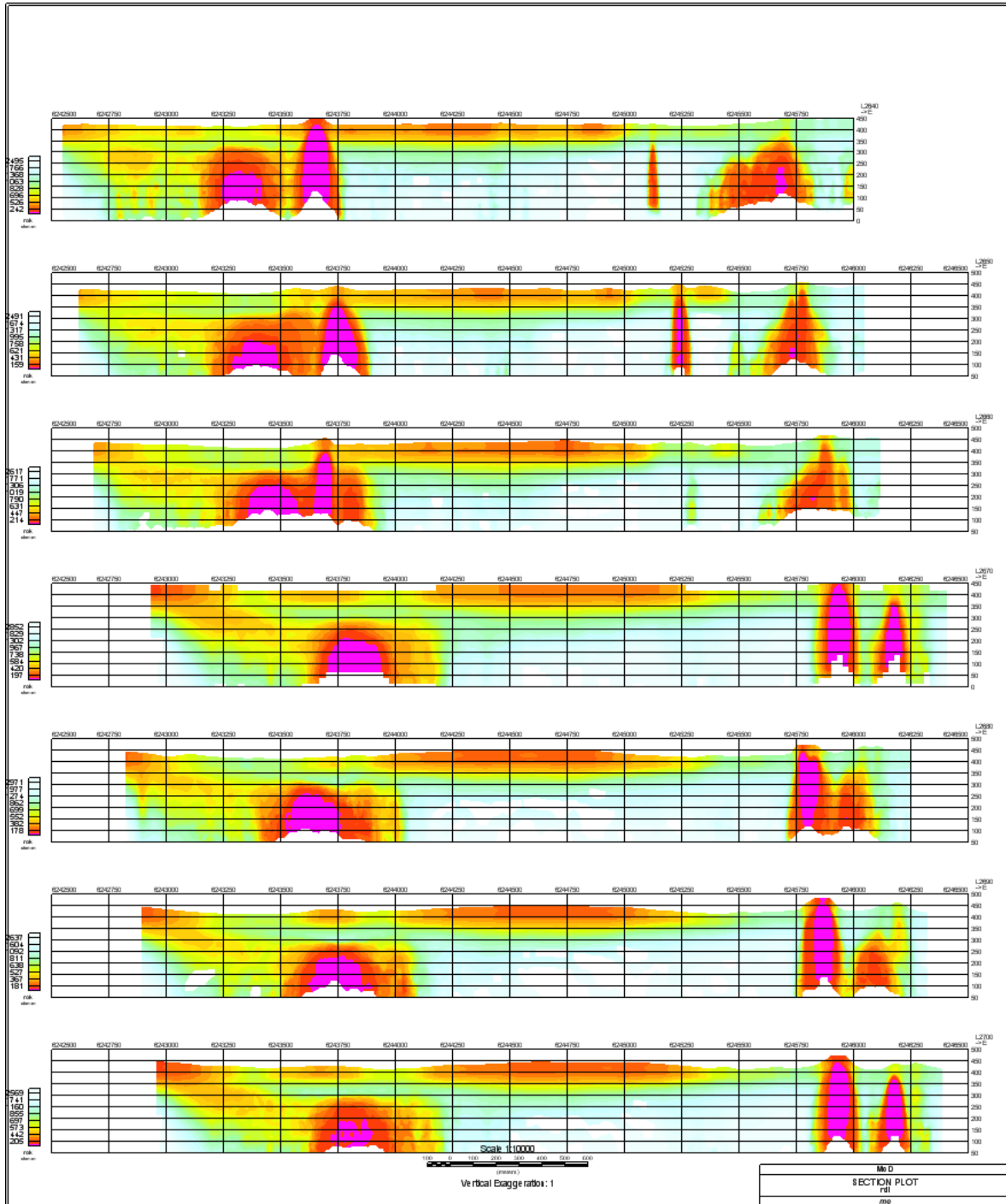


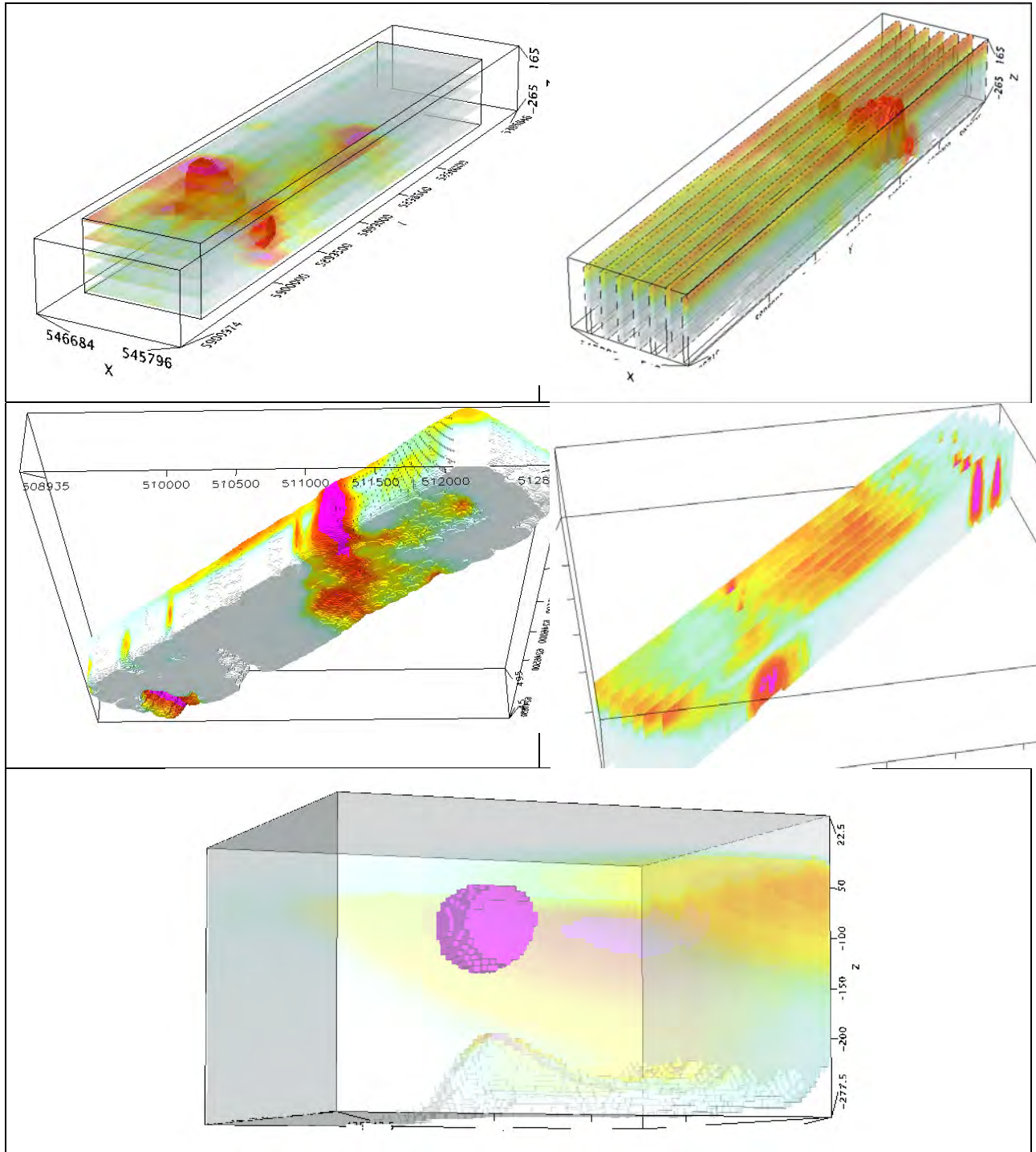
Figure F-11: RDI section for the real horizontal and slightly dipping conductive layers

# FORMS OF RDI PRESENTATION

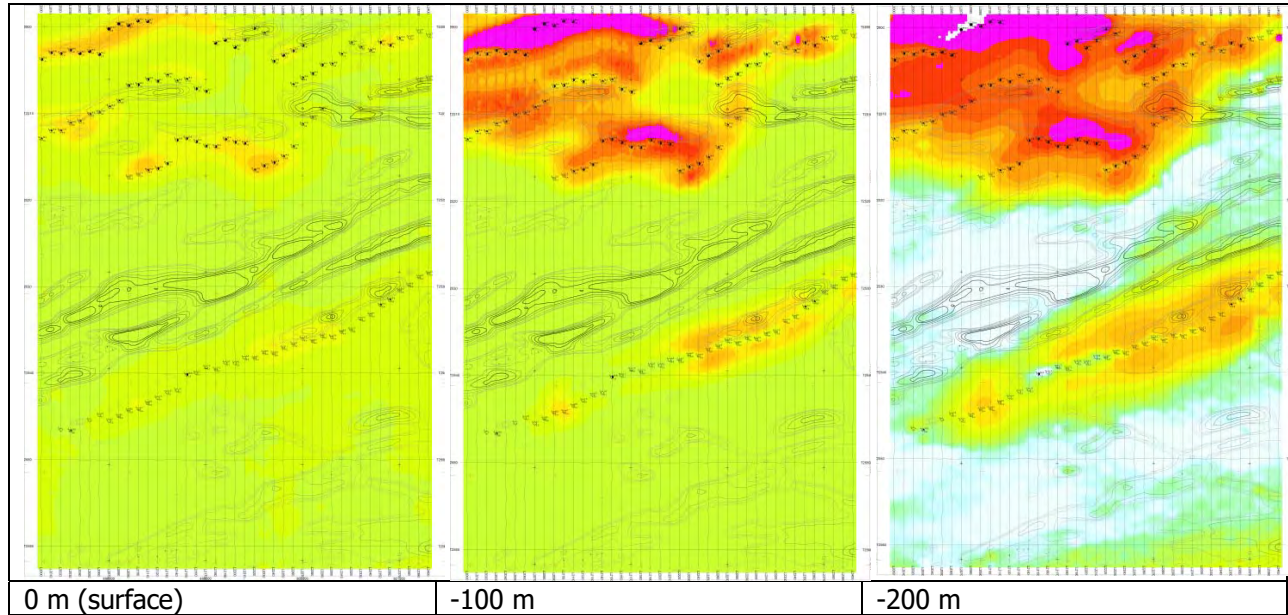
## PRESENTATION OF SERIES OF LINES



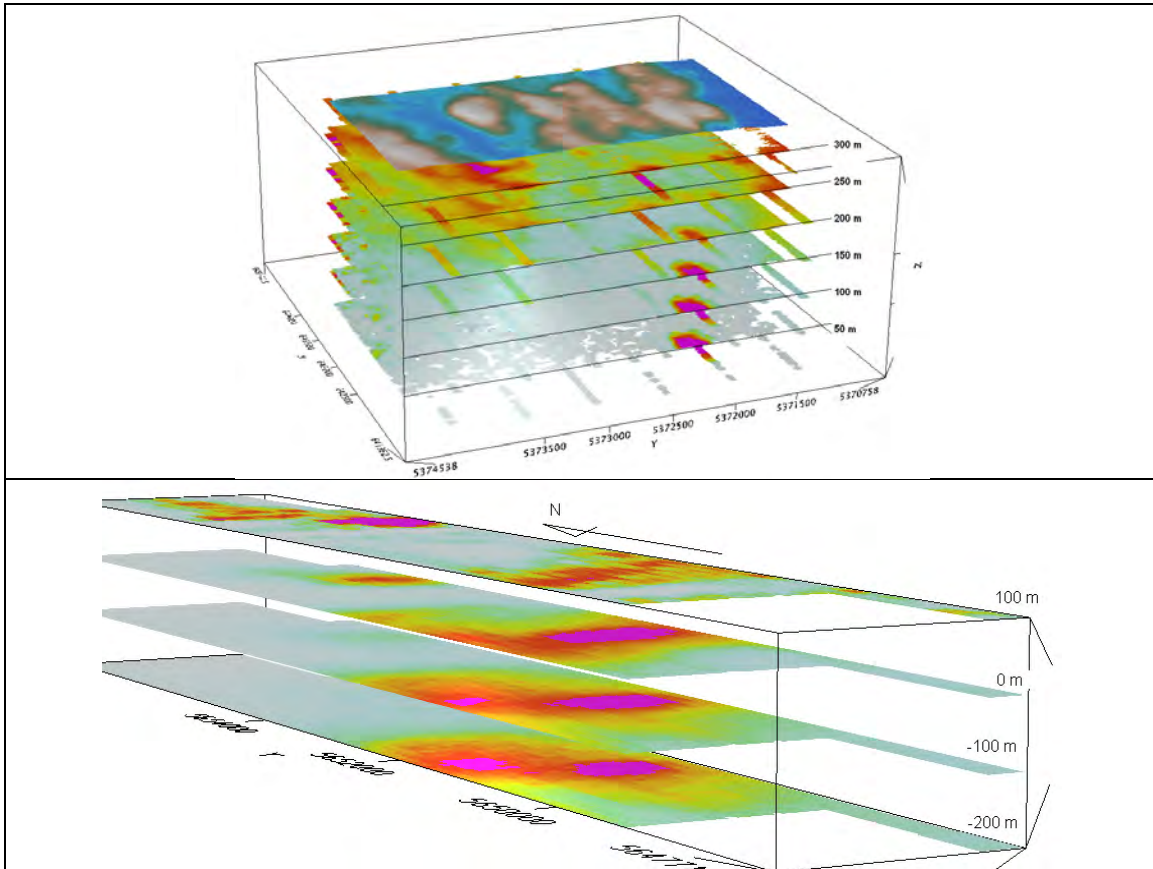
### 3D PRESENTATION OF RDIS



APPARENT RESISTIVITY DEPTH SLICES PLANS:

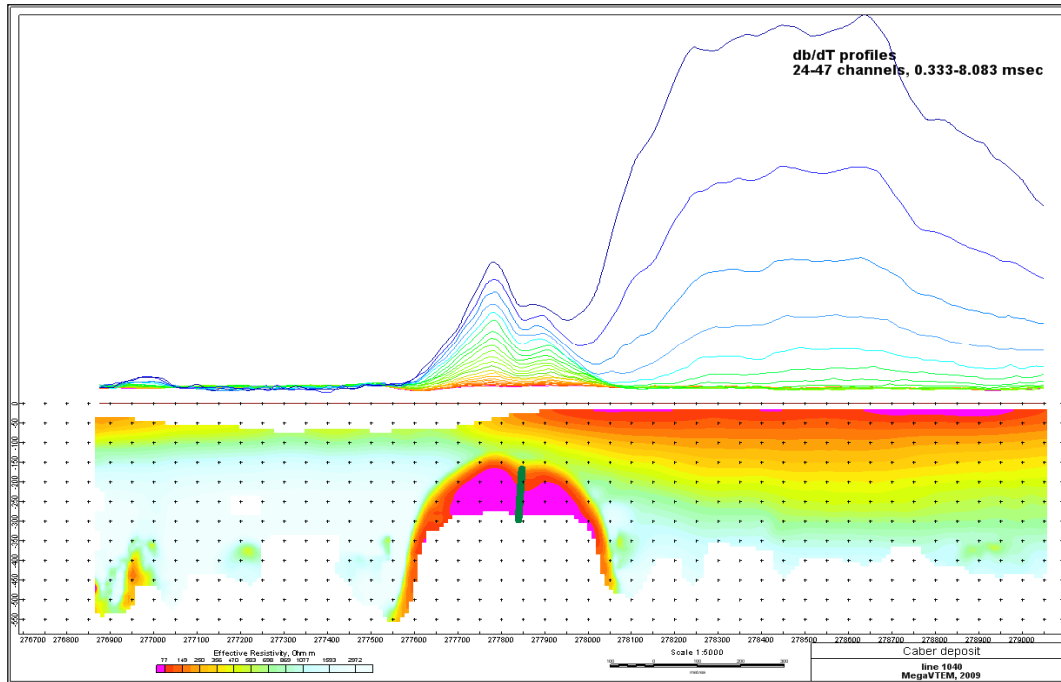


3D VIEWS OF APPARENT RESISTIVITY DEPTH SLICES:

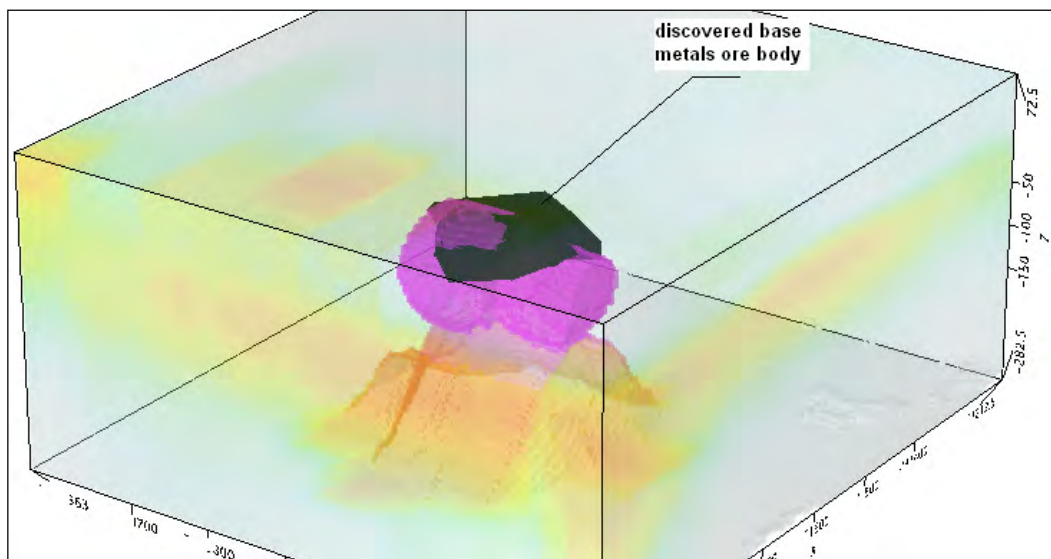


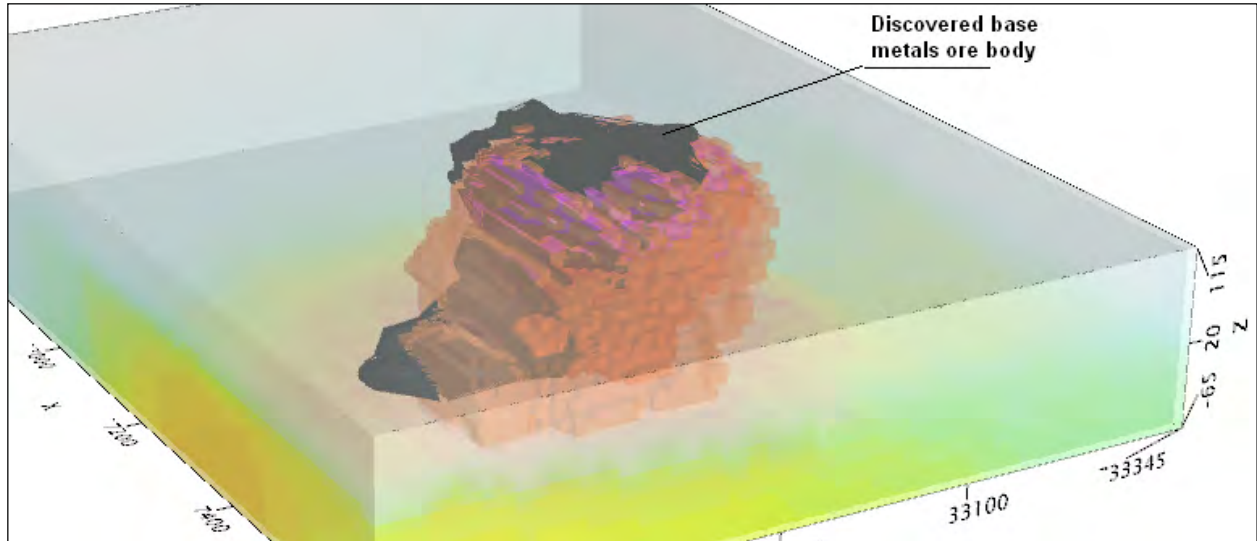
## REAL BASE METAL TARGETS IN COMPARISON WITH RDIS:

RDI section of the line over Caber deposit ("thin" subvertical plate target and conductive overburden).



## 3D RDI VOXELS WITH BASE METALS ORE BODIES (MIDDLE EAST):





Alexander Prikhodko, PhD, P.Ge  
**Geotech Ltd.**  
April 2011